

JOURNAL OF EMERGING INVESTIGATORS

VOLUME 3, ISSUE 3 | MARCH 2020
emerginginvestigators.org

Contraceptives & crops

How the increase in contraceptive chemicals in the environment might impact crop yields

Fighting climate change with algae

Harnessing photosynthesis to reduce atmospheric CO₂

HIV recruitment factors

Investigating the role of a potential new therapeutic target

Can virtual reality help alleviate anxiety?

Treating public speaking anxiety in high schoolers with VR



JOURNAL OF EMERGING INVESTIGATORS

The Journal of Emerging Investigators is an open-access journal that publishes original research in the biological and physical sciences that is written by middle and high school students. JEI provides students, under the guidance of a teacher or advisor, the opportunity to submit and gain feedback on original research and to publish their findings in a peer-reviewed scientific journal. Because grade-school students often lack access to formal research institutions, we expect that the work submitted by students may come from classroom-based projects, science fair projects, or other forms of mentor-supervised research.

JEI is a non-profit group run and operated by graduate students, postdoctoral fellows, and professors across the United States.

EXECUTIVE STAFF

Brandon Sit **EXECUTIVE DIRECTOR**
Michael Mazzola **COO**
Qiyu Zhang **TREASURER**
Caroline Palavacino-Maggio
DIRECTOR OF OUTREACH

BOARD OF DIRECTORS

Sarah Fankhauser, PhD
Katie Maher, PhD
Tom Mueller
Lincoln Pasquina, PhD
Seth Staples

EDITORIAL TEAM

Jamilla Akhund-Zade **EDITOR-IN-CHIEF**
Olivia Ho-Shing **CHIEF LEARNING OFFICER**
Michael Marquis **MANAGING EDITOR**
Laura Doherty **MANAGING EDITOR**
Chris Schwake **MANAGING EDITOR**
Naomi Atkin **HEAD COPY EDITOR**
Eileen Ablondi **HEAD COPY EDITOR**
Lisa Situ **HEAD COPY EDITOR**
Alexandra Was, PhD **PROOFING MANAGER**
Erika J. Davidoff **PUBLICATION MANAGER**

SENIOR EDITORS

Sarah Bier
Kathryn Lee
Nico Wagner
Scott Wieman

**FOUNDING
SPONSORS**



Contents

VOLUME 3, ISSUE 6 | JUNE 2020

- Assessing the Usefulness of a Virtual Environment as a Method of Public Speaking Anxiety Exposure** 4
Sree Poorvika Ramalakshmi Dasari and Seth Hajian
La Salle Academy, Providence, Rhode Island
- The Coagulating Properties of the *M. oleifera* Seed** 7
Aakriti Lakshmanan and Matthew Welch
Ardrey Kell High School, Charlotte, North Carolina
- Conversion of Mesenchymal Stem Cells to Cancer-Associated Fibroblasts in a Tumor Microenvironment** 13
Reshma Ramesh, Ankita Umrao, Jyothsna Rao, and Gururaj Rao
Greenwood High School, Bangalore, India
- Combined Progestin-estrogenic Contraceptive Pills May Promote Growth in Crop-Plants** 17
Sukanta Saha and Barnali Mukhopadhyay
The Heritage School, Kolkata, India
- Investigating the Role of the Novel ESCRT-III Recruitment Factor CCDC11 in HIV Budding: A Potential Target for Antiviral Therapy** 28
Leo Takemaru, Poojan Pandya, Michael W. Lake, Carol A. Carter, and Feng-Qian L, Ward Melville High School, East Setauket, New York, and Half Hollow Hills High School West, Dix Hills, New York
- Herbal Extracts Alter Amyloid Beta Levels in SH-SY5Y Neuroblastoma Cells** 36
Angelina Xu and Margaret Vezza Mitchell
Ridge High School, Basking Ridge, New Jersey
- Temperatures of 20oC Produce Increased Net Primary Production in Chlorella sp.** 42
Kiran Biddinge, Emma Bradley, and Julie Seplaki
Milton Academy, Milton, Massachusetts

An experiment to assess the usefulness of a virtual environment as a method of public speaking anxiety exposure

Sree Poorvika Ramalakshmi Dasari, Seth Hajian
La Salle Academy, Providence, Rhode Island

SUMMARY

This abstract describes an experiment conducted to assess the effectiveness of a virtual environment to act as a method of exposure in the treatment of public speaking anxiety among high school students. In one of the experimental conditions, the participants had to make a presentation to a virtual audience using a Samsung Gear VR headset, which displayed a prerecorded 360-degree video of a classroom full of students. In another experimental condition, the participants had to make a presentation, without the VR headset and an audience. In both conditions, participant's heartbeat rate (response variable) was measured. The results show that the heartbeat during the experimental condition with a VR headset was significantly higher with respect to the heartbeat rate measured to the condition without the headset. This study should be followed up with a treatment study, where a virtual reality device would track a user's vitals during prolonged use and report the user's progress.

INTRODUCTION

In some high school classes, especially those that follow the Socratic style of teaching, students have to speak in front of their peers. Often, participation is mandatory and will count towards the grade for a class. Most high school students find this a challenging task because public speaking anxiety is prevalent among the student population. This apprehension of oral communication, while performing in front of an audience, often leads to poor performance in class, failed learning outcomes, low grades and general demoralization (1).

Currently, public speaking anxiety is treated using three main types of intervention training techniques. First, the cognitive modification technique, which requires support from teachers, family or peers; and involves practice sessions in the company of people a student might feel comfortable making mistakes. Second, the systematic desensitization technique, which involves repeated and frequent practice until a sense of routine replaces a sense of apprehension. Finally, the skills development technique, which focuses on improving specific public speaking skills, such as presentation skills, voice modulation and generating presentation content and order (2).

According to Pribyl et al., a combination of these

intervention techniques could be the most effective way to combat public speaking anxiety (2). A possible route to unification of these techniques is to employ a virtual environment (VE). A virtual environment could be used to create a sense of place illusion. That is, a VE could faithfully reproduce a public speaking environment, such as a podium, audience, auditory input, audience feedback etc., such that a user will feel a sense of being actually there (3). For instance, a virtual environment with a virtual audience (VA) could create a sense of being in a public speaking environment. Based on the effectiveness of modeling a VE, its VA, and the responsiveness of the VA to the user, the VE may seem realistic or plausible to its user (3). It can be used to practice repeatedly without the fear of making mistakes and could be used to focus on specific skills. Therefore, we believe, a VE could unify the benefits of all three interventions techniques.

Currently, there is no empirical evidence to prove that a VE can generate a sense of public speaking anxiety in high school students. This paper discusses an experiment conducted to assess the ability of a VE to expose students to public speaking anxiety, in terms of an increase in heart rate (4). Therefore, the main contribution of this paper is the result of a validation study, which lays the foundation for establishing a VE as a method of exposure to public speaking anxiety with respect to high school students.

The null hypothesis was as follows: there is no significant difference in heart rate of high school students when practicing public speaking alone versus in a virtual environment with a virtual audience. On the other hand, the alternate hypothesis is that there is a significant difference in the heart rate between the two treatment conditions.

Based on a review and synthesis of related literature, we will discuss the principles involved in creating a tangible and immersive virtual public speaking experience (VPSE). We believe that there are three main design principles that govern the development of VPSE, which will evoke public speaking anxiety in its user.

First, a VPSE must be designed to enable private space for an extended practice session. According to Smokowski et al., an effective VE can help a high school student learn by repeated and prolonged practice (5). An effective VE should not only replicate a public speaking environment and audience but also evaluate the user's performance and analyze the results to provide insights about potential areas

to improve (6).

Second, a VPSE must be designed to aid high fidelity interaction and create a sense of being there in an anxiety-inducing environment. For instance, the virtual audience could react to the user of the virtual environment, based on performance. According to Pertaub et al., even a virtual audience can create a sense of public speaking anxiety in a user, and thereby increase the user's sense of being there (7).

Finally, a VPSE must be designed to measure performance and provide feedback. The measure and the instrument used for the measurement has to be reliable and valid. For instance, according to Meehan et al., physiological measures such as heart rate and skin conductance is an objective measure for ascertaining and quantifying anxiety (4, 8).

RESULTS

The percentage change in heart rate of participants in both of the experimental conditions, with respect to their resting heart rate, were analyzed using a paired sample t-test. The results show that participants had a larger change in the heart rate while using a VR headset (mean = 7.115, $SD = 21.792$) when compared the condition where participants did not use the VR headset (mean = 0.304, $SD = 20.725$). The difference found using the t test was significant, $t(14) = 2.662$, $p < 0.05$. The results support the alternate hypothesis by suggesting that speaking to a VA in a VE can significantly increase the heart rate.

DISCUSSION

By conducting this experiment, we learned to use a VPSE as a technique, to expose high school students to public speaking anxiety. As the results of our experiment suggest, there is a significant increase in heart rate of the participant when speaking to a virtual audience. The results provides us evidence against the null hypothesis, and therefore the null hypothesis that there is no significant increase in heart rate has to be rejected. The results do not prove that the increase in heart rate, and therefore the sense of anxiety, is caused by the VPSE. However, it does suggest that there is a strong correlation between the two.

Based on our review of the literature, we have identified three experiments, which support our results, and they are as follows. First, Meehan et al. have proved that heart rate is a reliable and valid measure of presence or sense of being there in a stressful VE (4). Second, according to Jurnet et al., the sense of being there in a stressful VE and the level of anxiety are correlated (9). Finally, a VA can evoke a sense of anxiety in a VE user (10).

From the above evidence and results of our experiment, we contend that a VE has a high likelihood of being an effective method of exposure to public speaking anxiety. However, we believe that this experimental study has two main drawbacks. First, the study was limited to a single factor with two levels. It is likely that other factors that may have confounded the

results. For instance, a participant who is new to VR could be overwhelmed by the technology. Second, the effectiveness of VE has to be established by a longitudinal study, to prove its usefulness in the long term.

We believe that a VE could, in the future, offer a private and immersive environment for prolonged and repeated practice. A VE, which allows repeated practice, and tracks a user's progress while catering to the user's learning pace, will be able to unify all three public speaking intervention techniques (2). To this end, as a first step, we would like to conduct an experiment to establish that a VE can help significantly decrease public speaking anxiety in high school students by conducting a longitudinal study.

MATERIALS AND METHODS

The number of participants who volunteered for the experiment is fifteen. The participants' ages ranged from 16 to 17 years, and the median value was 16.333 years. All fifteen participants were high school students. Nine of the participants were female, and the rest of the participants were male. A Samsung Gear VR was used to display a 360-degree video. An alivecor device (kardia) was used to monitor the heart rate. The alivecor device simply connects with an app on your phone where the user places their fingers on the plates and then the app produces electrocardiograms. The experiment used a single factor repeated measures design. The independent variable had two levels. First, in the without VR level, the participant had to give a short speech without an audience. Second, in the VR level, the participant had to use a VR headset and give a short speech to a virtual audience. The dependent variable was chosen to be the heart rate of the participant.

Upon arrival, the participating students read and signed an informed consent form. Then the participants were given a brief about the tasks they would perform, and about the equipment they would use, without delving too much into the objective of the research to avoid participant bias. After participants acknowledged that they understood the tasks, a Samsung phone displaying the stereoscopic view of a classroom of students was put in the Samsung Gear VR headset. The participants were asked to present a one-minute speech about their favorite animal while wearing the headset that displayed a virtual classroom. During the duration of the speech, the participant held a Kardia Heart Rate Monitor that was connected to an iPhone and recorded their heart rate. The participant was then asked to present the one-minute speech without the headset to just one person in an empty classroom. Heart rate was recorded with the Kardia Heart Rate Monitor during the duration of the speech. Post experiment, participants were interviewed in an unstructured format. The experiment was counterbalanced to avoid order bias.

Received: October 15, 2018

Accepted: August 30, 2019

Published: February 9, 2020

REFERENCES

1. McCroskey, James C. "Classroom Consequences of Communication Apprehension." *Communication Education*, vol. 26, no. 1, 1977, pp. 27-33.
2. Pribyl, Charles B., et al. "The Effectiveness of a Skills-Based Program in Reducing Public Speaking Anxiety." *Japanese Psychological Research*, vol. 43, no. 3, 2001, pp. 148-155.
3. Slater, Mel. "Place Illusion and Plausibility Can Lead to Realistic Behaviour in Immersive Virtual Environments." *Philosophical Transactions of the Royal Society B: Biological Sciences*, vol. 364, no. 1535, 2009, pp. 3549-3557.
4. Meehan, Michael, et al. "Physiological Measures of Presence in Stressful Virtual Environments." *ACM Transactions on Graphics (TOG)*, vol. 21, no. 3., 2002, pp. 645-652.
5. Smokowski, Paul R., and Katie Hartung. "Computer simulation and virtual reality: Enhancing the practice of school social work." *Journal of Technology in Human Services*, vol. 21, no. 1-2, 2003, pp. 5-30.
6. Jarmon, Lelsie, et al., "Virtual World Teaching, Experiential Learning, and Assessment: An Interdisciplinary Communication Course in Second Life." *Computers & Education*, vol. 53, no. 1, 2009, pp. 169-182.
7. Pertaub, David-Paul, et al., "An Experiment on Public Speaking Anxiety in Response to Three Different Types of Virtual Audience." *Presence: Teleoperators & Virtual Environments*, vol. 11, no. 1, 2002, pp. 68-78.
8. Chapman, Diane D. and Sophia J. Stone. "Measurement of Outcomes in Virtual Environments." *Advances in Developing Human Resources*, vol. 12, no. 6, 2010, pp. 665-680.
9. Alsina-Jurnet, Ivan, et al. "The Role of Presence in the Level of Anxiety Experienced in Clinical Virtual Environments." *Computers in Human Behavior*, vol. 27, no. 1, 2011, pp. 504-512.
10. Kelly, Owen, et al. "Psychosocial Stress Evoked by a Virtual Audience: Relation to Neuroendocrine Activity." *CyberPsychology & Behavior*, vol. 10, no. 5, 2007, pp. 655-662.

Copyright: © 2020 Dasari and Hajian. All JEI articles are distributed under the attribution non-commercial, no derivative license (<http://creativecommons.org/licenses/by-nc-nd/3.0/>). This means that anyone is free to share, copy and distribute an unaltered article for non-commercial purposes provided the original author and source is credited.

A Study on the Coagulating Properties of the *M. oleifera* Seed

Aakriti Lakshmanan¹, Matthew Welch¹

¹ Ardrey Kell High School, Charlotte, North Carolina

SUMMARY

Water is an essential part of our lives, but many people struggle to obtain enough clean water to meet their basic needs. However, the solution to this problem may be right in their backyard. *Moringa Oleifera* (*M. oleifera*) seeds contain a coagulating protein that can coagulate and remove particles in water. The purpose of this study was to analyze the coagulating efficiency of the seed and to test a new and innovative way to utilize the seed. When the part of the seed responsible for the coagulating properties was isolated and combined with sand, a new functionalized-sand (f-sand) was created. This research aimed to determine how effectively the *M. oleifera* Cationic Protein (MOCP) functionalized-sand reduces the amount of bacteria compared to other filtration techniques. We accomplished this by testing six different types of contaminated solutions before and after four different filtration techniques: plain sand, f-sand, f-sand with cilantro, and the normal moringa technique, which utilizes only moringa seed powder. We concluded that the MOCP f-sand removed the largest percent of bacteria, and when used in combination with cilantro, it was more efficient than the other techniques. This can have a large impact, especially in developing areas, as it provides a way to have clean water while also helping the economy.

INTRODUCTION

M. oleifera, otherwise known as *Moringa Oleifera*, is a fast growing, highly valued plant found in various parts of the world. It flourishes in tropical climates but can grow anywhere. The *M. oleifera* plant is native to northern India and different parts of Africa (1). The plant is very resilient and produces leaves even during times of drought. This plant has many uses. The whole plant, including the bark, pods, leaves, nuts, seeds, oil, tubers, roots, and flowers, is edible and contains important nutrients essential to our well-being (2). The bark can be used as an appetizer, and it can also be used to treat sores, skin infections, and intestinal spasms. The pods are normally cooked in a broth, and the flesh inside is eaten. The leaves have many medicinal properties, and the whole plant has been said to have anti-inflammatory properties (3). However, the most astonishing capability of this plant is its use as a water filtration system. When the oil is pressed from the seeds of the moringa plant, seed cakes are left over

as a waste product. These seed cakes can be used to filter water (4). Data collected as part of the Global Learning and Observations to Benefit the Environment (GLOBE) initiative funded by NASA shows a steady decrease in the water transparencies in the US over the last few years (5). If this trend exists in a developed country, water quality is likely an even bigger issue for developing countries as they deal with a large population and increased competition for limited natural water resources.

The utility of *M. oleifera* in water filtration may provide a sustainable solution to this issue. Moringa seeds contain a protein, the *Moringa Oleifera* cationic protein (MOCP), which has natural cationic polyelectrolytes that cause coagulation (6). Coagulation has been referred to as the most important step in water filtration, even more so than physical filtration (7). Coagulation is the reduction of electrical potential between particles in the water like microorganisms, colored particles, and clay in a way that agglomerates them to form large structures, referred to as "flocs" which then can be removed by physical filtration (8). The most common coagulants used in wastewater treatment are aluminum salts (alum), ferric and ferrous salts, lime, and cationic, anionic, and non-ionic polymers. While there are many synthetic coagulants, the chemicals found in them are not ideal, and substantial energy is required to produce them. Additionally, wide dispersal of the coagulants to areas in need has proven to be difficult. The ability of a chemical to cause coagulation is based on the charge and size of the coagulant. The coagulant in *M. oleifera*, MOCP, works with negatively charged particles, including most bacteria. Additionally, the MOCP goes a step further than the synthetic coagulants by killing the microorganisms in the water by fusing and damaging the cell membranes during coagulation (9).

M. oleifera grows in the places where people are in the most need of the advantages it offers, making it the perfect substitute for primitive and unsanitary water filtration systems. However, when moringa powder is added to the water by itself, it leaves behind organic matter in the water which encourages the growth of new bacteria, limiting long-term efficiency. This can be fixed by utilizing f-sand. When an anionic sand is mixed with an *M. oleifera* extract then rinsed, the MOCP protein adheres to the sand. The sand now has the same coagulation properties as the seed cake, but it does not leave behind the organic matter that promotes bacteria growth, making it a more efficient solution. Over the past few

decades, most of the research conducted on *M. oleifera* tested its usage on the removal of turbidity (10, 11). However, there has not been a lot of research on the reduction of bacterial load in different sources of drinking water. This is specifically important as many people die due to unsanitary water.

In fact, 289,000 children under 5-years-old die each year due to diarrheal diseases caused by poor water quality and sanitation (12). Specific pathogens, including *Escherichia coli* (*E. coli*), *Salmonella*, *Shigella*, *Campylobacter*, and *Legionella*, can cause different waterborne diseases that may be fatal, especially to people who do not have access to a nearby hospital. Due to the antimicrobial properties of the MOCP, water filtered by the f-sand also contains fewer biological contaminants. Water with fecal contamination is not deadly by itself, but the presence of fecal coliforms can indicate the presence of other pathogenic bacteria. If water contains fecal coliforms, then the water has come into contact with some form of fecal matter, either from a human or an animal. Fecal matter may also contain pathogens or viruses that can cause diseases, such as gastroenteritis, typhoid, and hepatitis A. Thus, it is important that drinking water does not contain fecal contamination because it may be a potential health risk. An additional filtering agent that we tested in this research was cilantro, which is known to have heavy-metal filtering properties. A recent study conducted by researchers in Kenya found that cilantro stems and leaves were capable of removing lead and cadmium ions from water (13). We can create a more efficient filtration system by combining both moringa and cilantro.

Based on the results of the aforementioned research, We hypothesized that the MOCP f-sand and the cilantro filter would more effectively reduce bacteria and other contaminants in water compared to plain sand or the normal-filtration technique. The impact of Moringa in developing countries is very important, as it naturally grows in these areas and can provide an easier way to clean water.

RESULTS

In this study, we gained a greater understanding of the *M. oleifera* seed and its efficiency in different forms on the reduction of bacteria. In order to ensure that the same amount of bacteria was added to each sample, the same serial dilution was conducted on each sample of bacteria. Before filtering, the water samples were thoroughly vortexed in order to ensure that the bacteria were spread evenly in the sample. Then, the same volume of each of the water samples was put through each filtering method. The bacteria strains used include *E. coli*, *Enterobacteria aerogenes*, *Citrobacter freundii*, and *Serratia liquefaciens*. In addition to testing natural water and turbidity, lake water and kaolin clay water were tested respectively. The results support the hypothesis because the MOCP f-sand and cilantro filter technique reduced the growth of the pathogenic bacteria more than any other filtration technique, with a 73.56% average reduction in bacterial colonies when compared to the water samples

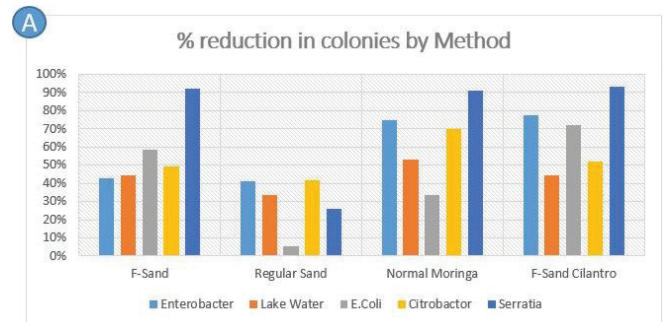


Figure 1. Bacterial Reduction Data. This graph represents the percent reduction of colonies when compared to the original bacteria mixture before it has gone through any treatments. Yellow represents *Citrobacter freundii* bacteria, light blue represents *Enterobacteria aerogenes*, gray represents *E. coli*, dark blue represents *Serratia liquefaciens*, and orange represents lake water. Labels of the x-axis represent the various water treatment methods. The f-sand cilantro technique showed the highest average percentage reduction.

before filtering.

With the plain sand technique, there was a 41.5% reduction of *Citrobacter* cells, 33.33% reduction of lake water bacteria, 25.76% reduction of *Serratia* cells, 41.3% reduction of *Enterobacter* cells, and 5.55% reduction of *E. coli* cells, with an average percent reduction of 34.09%. With the normal moringa technique, there was a 66.5% reduction of *Citrobacter* cells, 53.33% reduction of lake water bacteria, 91.15% reduction of *Serratia* cells, 73.04% reduction of *Enterobacter* cells, and 33.33% reduction of *E. coli* cells, with an average percent reduction of 72.66%. With the f-sand technique, there was a 49.06% reduction of *Citrobacter* cells, 44.44% reduction of lake water bacteria, 92.31% reduction of *Serratia* cells, 42.60% reduction of *Enterobacter* cells, and 38.33% reduction of *E. coli* cells, with an average percent reduction of 61.68%. With the f-sand and cilantro technique, there was a 51.88% reduction of *Citrobacter* cells, 44.44% reduction of lake water bacteria, 93.08% reduction of *Serratia* cells, 77.39% reduction of *Enterobacter* cells, and 72.22% reduction of *E. coli* cells, with an average reduction of 73.56% (Figure 1).

Enterobacter was more efficiently removed using the

Table 1.

Anova: Two-Factor Without Replication

SUMMARY	Count	Sum	Average	Variance
E.Coli	5	61	12.2	130.2
Serratia	5	786	157.2	13315.7
Enterobacter	5	543	108.6	5231.8
Citrobacter	5	450	90	3016
Lake Water	5	79	15.8	88.2
F-Sand	5	483	96.6	8050.8
Regular Sand	5	267	53.4	1807.3
Normal Moringa Technique	5	593	118.6	9511.8
F-Sand Cilantro	5	576	115.2	9267.2
Unfiltered	5	0	0	0

ANOVA

Source of Variation	SS	df	MS	F	P-value	F crit
Rows - Bacteria Type	77718.96	4	19429.74	8.440960275	0.000734	3.006917
Columns - Filter Type	50298.16	4	12574.54	5.462821048	0.005727	3.006917
Error	36829.44	16	2301.84			
Total	164846.56	24				

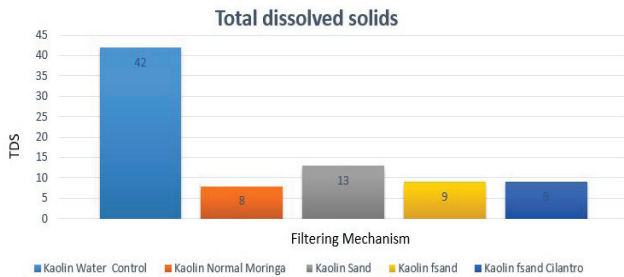


Figure 2. Total Dissolved Solids Data. This graph represents the total dissolved solids (TDS) measured in the kaolin clay water after each treatment. The legend below the graph shows what color each treatment method is correlated to. The normal moringa, f-sand, and f-sand and cilantro techniques all showed a similar reduction in TDS.

normal Moringa technique (172 colonies fewer than the non-filtered control) and f-sand cilantro (178 colonies) compared to the control sand treatment using regular sand (95 colonies), but f-sand alone (98 colonies) did not effectively remove *Enterobacter* compared to the control sand. *Citrobacter* was more efficiently removed using the normal Moringa technique (148 colonies), the f-sand and cilantro technique (110), and f-sand (104 colonies) compared to the control treatment of regular sand (88 colonies). Lake water bacteria were more efficiently removed using the normal Moringa technique (24 colonies) compared to the control treatment of regular sand (15 colonies), but f-sand alone (20 colonies) and f-sand cilantro (20 colonies) were not as effective at removing Lake Water Bacteria compared to the control sand. *E. coli* bacteria were more efficiently removed using the normal Moringa technique (12 colonies), the f-sand and cilantro technique (26 colonies), and f-Sand (21 colonies) compared to the control treatment of regular sand (2 colonies). *Serratia* bacteria were more efficiently removed using the normal Moringa technique (237 colonies), the f-sand and Cilantro Technique (242 colonies), and f-Sand (240 colonies) compared to the control treatment of regular sand (67 colonies). (Table 1) Also, total dissolved solids (TDS) improved across all filtering methods, with f-sand method exhibiting the highest clarity with TDS at eight points (Figure 2).

The data collected from this experiment resulted in a number of interesting findings. First of all, the f-sand and cilantro technique reduced the growth of bacteria better than the other techniques on average, with an average percent reduction of bacterial colonies of 73.56% (Figure 1). However, the normal *M. oleifera* technique performed better on the *Citrobacter* solution specifically. The sand technique removed about 41.5 %, and the f-sand technique removed about 49.06% of the colonies. The f-sand and cilantro method

Table 2.

Colonies Inhibited based on Day 10 Control					
Bacteria	F-Sand	Regular Sand	Normal Moringa Technique	F-Sand Cilantro	Average
E.Coli	21	2	12	26	15
Serratia	240	67	237	242	197
Enterobacter	98	95	172	178	136
Citrobacter	104	88	148	110	113
Lake Water	20	15	24	20	20

and the normal moringa method give similar results on average, showing that the f-sand contains the coagulant, but does not contain any organic material that might contribute to further contamination after some time. Two-factor ANOVA analysis of bacteria types and filtration methods revealed that the bacterial reduction of different bacteria types using different techniques was statistically significant (Table 2). MOCP f-sand does reduce the number of bacteria in water, and when used in combination with cilantro, it was more efficient than the other techniques tested.

DISCUSSION

In this study, we investigated the effectiveness of MOCP f-sand at removing bacteria from water compared to other filtration techniques. We hypothesized that a filtration technique combining MOCP f-sand and cilantro would be the most effective at removing bacteria due to its coagulating and water-softening qualities. The results supported the hypothesis since the MOCP f-sand and cilantro filter technique reduced the growth of the pathogenic bacteria more than any other filtration technique, with an average reduction of bacterial colonies of 115.2. This result was produced because the coagulating properties of the protein was best utilized in the form of f-sand. The same properties that the *M. oleifera* powder contain are also in the f-sand, but without the negative side effect. The regular sand technique did not work as well, due to the absence of the organic coagulant. The normal moringa method performed well; however, it contained raw organic material that may have contributed to the bacterial growth after a certain time period.

For a filter created with the MOCP f-sand to be optimal for use in Third World countries, there are some issues that must be addressed. For example, the f-sand would not be able to function for long periods of time as the MOCP would get washed away. Additionally, bacteria or algae or molds might grow on the filter, especially in warm climates. The water going through the filter contains bacteria, fungi, protozoans, parasites and organic matter which could contaminate the filter, limiting the effectiveness of the filter. This means that the filter would have to go through manual cleaning periodically. However, manual cleaning of the filter would not be an obstacle for implementation in areas where sustainable water filtration is needed.

There were a few limitations experienced during this study. Due to the lack of funding, it was not possible to complete many trials in larger quantities. Additionally, since there was no access to a regulated research laboratory, many of the items required to complete a more in-depth analysis were not accessible. For this reason, the metal content in the water was not tested. Time was another constraint. Since this research was conducted in a high school lab, the only time available was a few hours after school, so it was difficult to run multiple trials. One of the errors encountered had to do with the bacterial culture. The nutrient agar slant was purchased instead of the liquid form, which created a need

Solution Type Label	Solution Description
A	100ml of water collected from Lake. After 48 hours, 0.1 ml of the water was plated on a clean agar plate using a sterile cotton swab. The zig-zag method was utilized while plating as it has been proven to be the most effective plating method. While plating, extra care was taken to ensure that the agar plate is open for the least amount of time possible as to reduce the chance of airborne contaminants landing in the agar
B	The second solution was made with kaolin clay to create a solution with a synthetically produced amount of turbidity. To create the turbidity solution, 0.5 grams of White Kaolin clay powder was added to 100 ml of the deionized water. The solution was stirred for one hour and then allow it to settle for 24 hours. Then, the supernatant was removed, and the TDS of the solution was tested. The final water sources were prepared similarly, each using a different pathogenic bacteria strain listed below
C	Solution developed as outlined in B with <i>E.coli</i>
D	Solution developed as outlined in B with <i>Enterobacteria Aerogene</i>
E	Solution developed as outlined in B with <i>Citrobacter Freundii</i>
F	Solution developed as outlined in B with <i>Serratia Liquefaciens</i>

Figure 3. Total Dissolved Solids Data. This is the list of solutions prepared for testing using different treatment methods and different bacteria types.

for an adjustment of the dilution process. If we repeated this study, a more detailed analysis of the solution, including lead content and the presence of other heavy materials, would be performed. Additionally, it would be valuable to test different types of synthetic coagulants. MOCP f-sand shows great promise for removing pathogenic bacteria from water. As an affordable, effective and natural coagulant, it is suitable for use in developing countries.

METHODS

Four different types of bacteria, *E. coli*, *Enterobacteria aerogenes*, *Citrobacter freundii*, and *Serratia liquefaciens* (Carolina Biological), were diluted and added to water individually to artificially create contaminated solutions. Then, the contaminated water was filtered in four different ways: using plain sand, the normal *M. oleifera* technique, f-sand, and f-sand with cilantro. Additionally, the ability of these filtration methods to reduce turbidity was also tested, by manually adjusting the turbidity of a solution and testing it before and after filtration.

The first step was to prepare the water mixtures. The first water source was lake water. (Figure 3A) 100 mL of water was collected in a sterile container from a nearby water source. After 48 hours, 0.1 mL of the water was plated on a clean agar plate using a sterile cotton swab. The second solution was made with kaolin clay to create a solution with a synthetically produced amount of turbidity (Figure 3B). To create the turbidity solution, 0.5 grams of white kaolin clay powder was added to 100 mL of the deionized water. The solution was stirred for one hour and then allowed to settle for 24 hours. Then the supernatant was removed and the total dissolved solids (TDS) of the solution was measured. The water sources containing bacteria were prepared similarly, each using a different pathogenic bacteria strain: *E. coli* (C),

Enterobacteria aerogene (D), *Citrobacter freundii* (E), and *Serratia liquefaciens* (F). To create these water solutions, a serial dilution was conducted. Using a clean, sterile, and dry pipet, 0.1 mL of the bacteria sample was added to 9.9 mL of distilled water and mixed thoroughly. Using a new pipet, 0.1 mL from Tube 1 was removed and added to Tube 2, which contained 99 mL of distilled water. Each filtration method had a sample size of five for each solution type (Figure 3).

The second step of the study was to design the filter. To create the filter, all of the polyvinyl chloride (PVC) pieces, the muslin cloth and the PVC adhesive were used. First, the 3-inch diameter PVC tube was cut to a length of 4.5 inches (in) using a hacksaw blade using appropriate safety measures such as gloves and goggles. The 1.5-in tube was cut to a length of 2.625 inches (2 5/8 in). Then the 3 in x 1.5 in PVC coupling adapter was added to one end of the 3-in tube using adhesive. Adhesive was used for all following steps to ensure a leakproof design. The 1.5 in female adapter was attached to the other end of the 3 in x 1.5 in PVC coupling adapter with muslin cloth in between and left aside. Then another 1.5 in female adapter was attached with muslin cloth to one side of the 1.5 in tube. On the other side of the 1.5 in tube, a 1.5 in male adapter was attached. A 1.5 in cleanout plug was attached to the male adapter on the 1.5 in tube and the 3 in tube without adhesive. This design included two separate modules. The 3-in module was used for the f-sand tests, and for the f-sand and cilantro test, both modules were attached together (Figure 4).

To prepare the f-sand, whole moringa seeds were crushed using a mortar and pestle. 0.25 grams of the seed powder was added to 10 mL of deionized water. The solution was agitated in a 10 mL centrifuge tube for one hour. At the end of one hour, the solution was set upright for 40 minutes. After letting it settle, the top 6 mL of the solution was removed.

2 mL of solution was added to 2 grams of sand, and the sand was incubated. After incubation at 37°C, the sand was washed 10 times with 10 mL of deionized water. The sand was stored in a sterile container with 10 mL of deionized water.

During the experiments, the different water mixtures were poured through the filter, which was filled with the corresponding agents (regular sand, f-sand, cilantro). For the normal moringa technique, 0.25 grams of the seed powder was added to 10 mL of a bacteria mixture. The mixture was shaken for 15 minutes and allowed to sit for 15 minutes. Using a muslin cloth, any remaining particles in the water were filtered out. (Figure 5) For the f-sand and regular sand, 6.0 grams of the corresponding sand was added to the 3 in water filter module along with 18.0 mL of the water solution. The tube was closed using an end cap. It was mixed by shaking and rolling it for up to 30 minutes then allowed to sit for 1.5 hours. For the f-sand and cilantro technique, 4 cups of cilantro was added to the 1.5 inch module. Then, the 1.5 inch module was attached to the 3 in module filled with sand by opening the cleanout plug of the 3 in module and screwing on the 1.5 in module.

The TDS of the kaolin water solution was tested using a TDS meter (HM Digital), and the reading was recorded for each treatment method. TDS is a measure of the amount of solids in water. A TDS meter measures the conductivity of a solution, and since the conductivity of water is directly related to the amount of total dissolved solids, it can derive the TDS of the water. The TDS was taken once before experimentation and after each treatment.

The petri dishes were self-poured with a nutrient-agar medium (Carolina Biological). In order to count the number of colonies grown in each petri dish, the plates were incubated at 35°C after being plated. Each colony count measurement was taken after five days of incubation. Each petri dish was split into four subsections to make it easier to count. The measurement was first taken by eye, then additional computer software was used to confirm the measurements (Promega Colony Counter). The number of colonies found

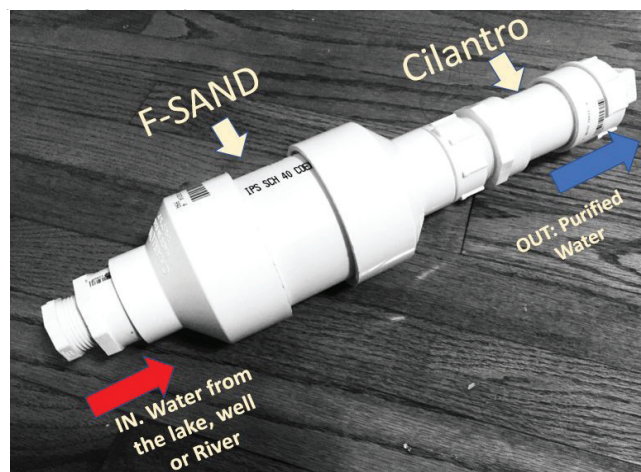


Figure 4. Filter Prototype. This is the filter prototype constructed using PVC materials there are two different components, a larger one for the f-sand and a smaller one for the cilantro.

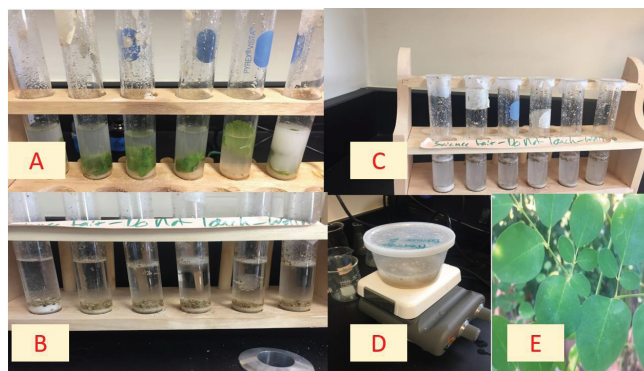


Figure 5. Experimental Images. These are a collection of images taken during experimentation. (a) This is the testing of the f-sand and cilantro method in a test tube. (b-c) This is the testing of the normal moringa technique. (d) This is the creation of the moringa serum to be added to the sand later on. (e) This is a picture of moringa leaves, which can also be eaten for nutritional value.

in one quadrant was then multiplied by four to get the total colony count. 0.1 mL of each bacteria solution was plated on a petri dish using a sterile pipette before treatment to serve as a control, and 0.1 mL of all the bacteria solutions were plated after each treatment. The filter was cleaned in between treatments with antibacterial wipes then allowed to dry.

ACKNOWLEDGEMENTS

I would like to thank Carolina Biological for helping me with questions regarding the bacteria used in this project.

Received: March 31, 2019

Accepted: January 27, 2020

Published: February 14, 2020

REFERENCES

1. Jerri, Huda A., et al. "Antimicrobial Sand via Adsorption of Cationic *Moringa Oleifera* Protein." *Langmuir*, vol. 28, no. 4, 2011, pp. 2262–2268., doi:10.1021/la2038262.
2. Matic, Ivana, et al. "Investigation of Medicinal Plants Traditionally Used as Dietary Supplements: A Review on *Moringa Oleifera*." *J Public Health Afr*, vol. 9, no. 3, Dec. 2018. PAGEPress Publications, doi:10.4081/jphia.2018.841.
3. Minaiyan, Mohsen, et al. "Anti-Inflammatory Effect of Helichrysum Oligocephalum DC Extract on Acetic Acid - Induced Acute Colitis in Rats." *Adv Biomed Res*, vol. 3, no. 1, 2014, p. 87. Medknow, doi:10.4103/2277-9175.128000.
4. Leone, Alessandro, et al. "*Moringa Oleifera* Seeds and Oil: Characteristics and Uses for Human Health." *International Journal of Molecular Sciences*, vol. 17, no. 12, Dec. 2017, p. 2141. MDPI AG, doi:10.3390/ijms17122141.
5. Retrieve Data (ADAT) - GLOBE.Gov. June 2017, <https://web.archive.org/web/20200120203737/https://www.globe.gov/globe-data/retrieve-data>.
6. Vilaseca, Mercè, et al. "Valorization of Waste Obtained

from Oil Extraction in *Moringa Oleifera* Seeds: Coagulation of Reactive Dyes in Textile Effluents.” *Materials*, vol. 7, no. 9, Sept. 2014, pp. 6569–84. MDPI AG, doi:10.3390/ma7096569.

7. “Water Treatment | Public Water Systems | Drinking Water | Healthy Water | CDC.” *Centers for Disease Control and Prevention, Centers for Disease Control and Prevention*, 20 Jan. 2015, www.cdc.gov/healthywater/drinking/public/water_treatment.html.
8. Abebe, Lydia, et al. “Chitosan Coagulation to Improve Microbial and Turbidity Removal by Ceramic Water Filtration for Household Drinking Water Treatment.” *IJERPH*, vol. 13, no. 3, Feb. 2018, p. 269. MDPI AG, doi:10.3390/ijerph13030269.
9. Shebek, Kevin, et al. “The Flocculating Cationic Polypeptide from *Moringa Oleifera* Seeds Damages Bacterial Cell Membranes by Causing Membrane Fusion.” *Langmuir*, vol. 31, no. 15, 2015, pp. 4496–502. American Chemical Society (ACS), doi:10.1021/acs.langmuir.5b00015.
10. Swales, Jennifer. “Researchers Study Inexpensive Process to Clean Water in Developing Nations.” *Penn State News*, 9 June 2015, news.psu.edu/story/358048/2015/06/09/research/researchers-study-inexpensive-process-clean-water-developing.
11. Velegol, Stephanie Butler. “Moringa.” *Stephanie Butler Velegol*, www.svelegol.com/moringa.html.
12. “Facts and Statistics: WaterAid Global.” WaterAid, 2019, www.wateraid.org/facts-and-statistics.
13. Njue, Martin Kivuti. “Using cilantro leaves and stems to remove lead, cadmium and turbidity from contaminated water.” *Diss. Kenyatta University*, 2017.

Copyright: © 2020 Welch and Lakshmanan. All JEI articles are distributed under the attribution non-commercial, no derivative license (<http://creativecommons.org/licenses/by-nc-nd/3.0/>). This means that anyone is free to share, copy and distribute an unaltered article for non-commercial purposes provided the original author and source is credited.

Conversion of mesenchymal stem cells to cancer-associated fibroblasts in a tumor microenvironment: an *In Vitro* study

Reshma Ramesh¹, Ankita Umrao², Jyothsna Rao², Gururaj Rao²

¹Greenwood High School, Bangalore, India

²iCREST-International Stem Cell Services Limited, Bangalore, India

SUMMARY

Carcinomas grow in a complex microenvironment which consists of stromal cells, fibroblasts, immune cells, matrix proteins, and soluble proteins. This microenvironment is critical in providing signals for tumors to proliferate and produce cytokines, which create an area of immune suppression that signals inward migration of mesenchymal stem cells. It also aids in angiogenesis, metastasis and invasion of the tumor, which further enable tumor cells to proliferate and metastasize. Further mesenchymal stem cells are known to migrate into the tumor microenvironment induced cytokines released by the tumor in the microenvironment, further differentiating them to cancer associated fibroblasts (CAF). CAFs are in turn known to promote and aid tumor migration, enabling metastasis. In this study, conditioned media from the MCF7 breast cancer cell line induced a CAF like phenotype in bone marrow mesenchymal stem cells (BMSCs), indicating the potential role of stroma in the progression of cancer. We hypothesize that MCF7-conditioned media induces expression of vimentin and α -smooth muscle actin (α SMA) when co-cultured with (BMSCs), and that this could be involved in aiding cancer metastasis and progression.

INTRODUCTION

Tumor microenvironment includes blood vessels, immune cells, fibroblasts, signaling molecules and the extracellular matrix. The tumor microenvironment is marked by a zone of immune suppression created by tumor cells invaginating across the basement membrane into the interstitial space (1). Invasion of tumor cells into the interstitium enables them to further metastasize and spread in the body. However, this process depends heavily on the stroma of the surrounding area which is comprised of fibroblasts, immune cells, and mesenchymal stem cells. This draws parallels to the “soil and seed theory”, where the cancer cells being the “seeds” and the specific organ microenvironments being the “soil” (2, 3). Tumor cells secrete inflammatory factors, including cytokines, which attract bone marrow mesenchymal stem cells (BMSCs) (4). Tumor cells induce significant changes in the BMSCs and convert them to cancer-associated fibroblasts (CAFs) which further aid in tumor progression (5-7). However, the process of conversion to CAFs is not clear yet.

CAFs are present in the peritumoral area and act in an orchestrated manner, resulting in remodeling of adhesion

molecules and tissue. This is reminiscent of the wound healing process, but with some exceptions, as cancer is viewed as a wound that never heals. Cancer cells are known to “hitch a ride” on CAFs to spread to other parts of the body, through lymphatics and blood vessels (8). CAFs exist in close proximity to the cancer epithelium and constitute the bulk of a tumor’s stroma. They can acquire expression markers associated with metastasis, including vimentin and α -smooth muscle actin (α SMA). Vimentin, a critical prerequisite for metastasis in a number of cancers, is a structural protein that is used to maintain cell integrity and is encoded by the VIM gene (11). In recent studies, vimentin has been shown to regulate the activity between cytoskeletal proteins and cell adhesion molecules by participating in stromal cell adhesion, migration, invasion, and signaling (9). Expression of α SMA allows stromal cells to gain contractile stress fibers for better mobility and stronger capabilities (10), which aid in tumor metastasis.

We hypothesize that cancer cells secrete soluble factors that can induce mesenchymal stem cells to transform into CAFs, which are marked by the expression of α SMA and vimentin. We show that BMSCs cultured in media conditioned by MCF7 cells (a breast cancer cell line) induced expression of vimentin and α SMA. This indicates the presence of soluble factors in MCF7-conditioned medium (MCF7-CM) that convert BMSCs to CAFs. These CAFs in the tumor microenvironment can aid in cancer metastasis and progression.

RESULTS

Increased expression of α SMA and vimentin are some of the characteristic markers of CAF formation. BMSC differentiation was examined during culture in MCF7-CM through semi-quantitative analysis of α SMA and vimentin mRNA expression.

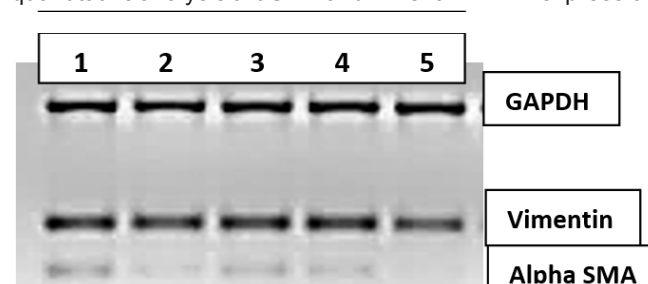


Figure 1. A representative gel electrophoresis picture showing bands for GAPDH (control), vimentin and α SMA. Groups are labeled as 1: BMSC+MCF7-CM, 2: MCF7+BMSC-CM, 3: BMSC+MCF7, 4: MCF7 CONTROL, 5: BMSC control.

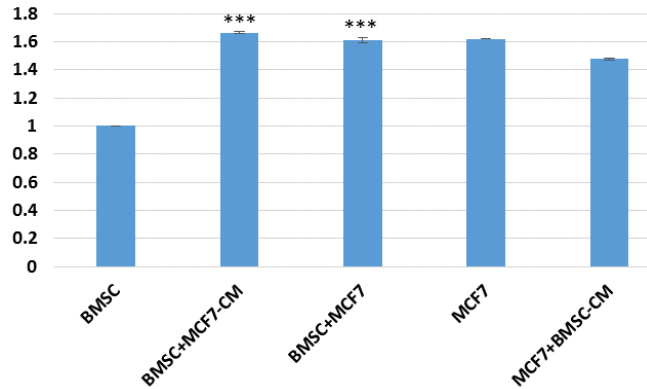


Figure 2. Fold change in mRNA levels of αSMA in the different groups tested. BMSC control, BMSC+MCF7-CM (BMSCs cultured in MCF7-CM), BMSC+MCF7 (MSCs co-cultured with MCF7), MCF7 control, MCF7+BMSC-CM (MCF7 cultured in BMSCs conditioned medium). The data was normalized to BMSC control levels. Statistical significance was denoted as *** with p -value <0.001. Error bars represent standard error of the mean (n=3).

Untreated BMSC and MCF7 were considered control groups (BMSC and MCF7, respectively) and were compared with BMSCs co-cultured with MCF7 (BMSC+MCF7), BMSCs cultured in MCF7-CM (BMSC+MCF7-CM), and MCF7 cells cultured in BMSC-conditioned media (MCF7+BMSC-CM). The BMSC control expressed the lowest levels of αSMA and vimentin (**Figures 1-3**). BMSC+MCF7-CM showed the highest expression levels ($p < 0.001$) of αSMA and vimentin, indicating that the MCF7-CM induced BMSCs to acquire a CAF-like phenotype. Vimentin levels in both BMSC+MCF7 and BMSC+MCF7-CM were statistically significant ($p < 0.001$) when compared with BMSCs control group (**Figure 3**). The αSMA expression level was significantly higher ($p < 0.001$) in BMSC+MCF7-CM and BMSC+MCF7 when compared with the MCF7 and BMSC controls, whereas there was no significant difference observed between MCF7+BMSC-CM and the controls (**Figure 2**).

DISCUSSION

Tumor progression is a series of orchestrated events that take place around the interstitial space, which is heavily populated by endothelial cells, immune cells, and fibroblasts. A definite step in tumor progression is the invasion of cancer cells through the basement membrane (stroma) into the interstitial tissue. Fibroblasts form a significant proportion of the tumor microenvironment, and play a crucial role in aiding tumor progression. Tumor activity, due to cell-cell interaction or due to soluble factors released by the cancer cells, leads to changes in the extracellular adhesion molecules, which lead to molecular and architectural remodeling of the stroma. The result is the transformation of fibroblasts into CAFs, which are basic components of periglandular sheaths and play a pivotal role in wound healing and chronic inflammation (1).

These CAFs aggregate in the peritumoral area and surround the carcinoma cells which themselves surround the normal cells. In addition, progenitor cells like BMSCs

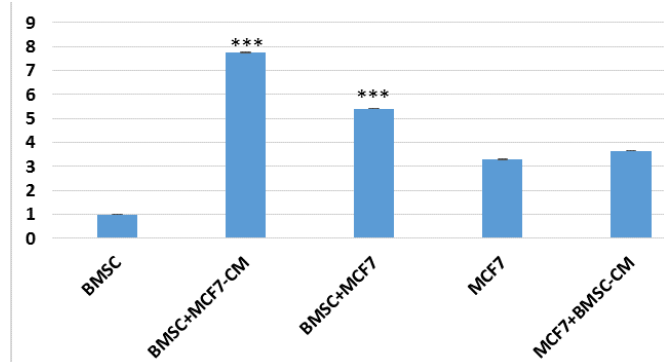


Figure 3. Fold change in mRNA levels of vimentin in the different groups tested. BMSC control, BMSC+MCF7-CM (BMSCs cultured in MCF7-CM), BMSC+MCF7 (MSCs co-cultured with MCF7), MCF7 control, MCF7+BMSC-CM (MCF7 cultured in BMSCs conditioned medium). Statistical significance was denoted as *** with p -value <0.001. Error bars represent standard error of the mean (n=3).

are recruited into the area and get converted to CAFs, which comprise the major cell type in a desmoplastic response in a tumor area. This conversion also contributes to angiogenesis, which is a major step towards tumor metastasis (12,13). Another significant phenotypic change in the tumor which indicates definite tumor progression is the endothelial to mesenchymal transition (EMT), induced by TGFβ present in the microenvironment (14).

A remarkable sequence of events mediated by tumor cells results in the EMT leading to extracellular matrix remodeling, which results in a permissive microenvironment which aids in tumor migration and immunosuppression. Transdifferentiation of cancer cells into myoepithelial cells leads to the transformation of the surrounding stroma to a CAF phenotype (15,16). Although myofibroblasts are very crucial in wound healing, they contribute to the chronic inflammation and desmoplasia that leads to chronic fibrosis seen in cancers (17).

Results from this study showed that the predicted mechanism of action is mediated by tumor-derived soluble factors that induce transition of BMSCs to CAFs, which overexpress vimentin and αSMA (18,19). The experiment clearly shows that MCF7 cells conditioned medium are crucial for BMSCs transition to CAFs (5,10) as compared to cell-cell interaction as seen in co-culture (BMSC+MCF7). This could also induce CAFs to produce inflammatory, angiogenic factors including TGFβ and VEGF which could be responsible for an immuno-suppressed tumor microenvironment and also for inducing neoangiogenesis, which is vital for tumor angiogenesis (2,10).

We would like to follow up on our findings by exploring other markers for CAFs, as well measure the levels of TGFβ and VEGF in these groups. This will help in understanding the tumor microenvironment and interaction of stem cells with tumor via different cytokines.

METHODS

Cell lines

The breast cancer cell line MCF7 was obtained from NCCS, Pune and BMSCs were obtained from Lonza. The cells were maintained in Dulbecco's Modified Eagle's Medium (DMEM) (Invitrogen) supplemented with 10% Fetal Bovine Serum (FBS) (Invitrogen). Passage number ranging from 5-7 was used for MCF7 and 2-3 for BMSCs. All the cultures were maintained at 37°C in a 5% CO₂ humidified incubator.

BMSCs were grown on a 3D collagen scaffold that provides optimal factors required for BMSCs and offers the "niche" for its growth. The collagen scaffold also helps in mimicking the 3D environment as in vivo.

Preparation of Conditioned Medium (CM)

MCF7 cells were cultured in DMEM with 10% FBS. At 70-80% confluency, media was replaced with serum-free media, and collected after 18 hours of incubation. The collected medium was centrifuged at 1500 rpm for 10 minutes. Supernatant was aliquoted and stored at -80°C. Conditioned media from BMSCs was prepared and stored in a similar manner. Conditioned media obtained from MCF7 cells and BMSCs were named as MCF7-CM and BMSC-CM, respectively.

Cell treatment with CM

To observe the effect of CM on cells, different groups of cells were cultured in a 3D scaffold (in-house technology, under patent application number: 201841037897) for 48 hours and were harvested for RNA isolation:

1. BMSC control
2. BMSC+ 50%MCF7-CM
3. MCF7+BMSC
4. MCF7 control
5. MCF7+ 50%BMSC-CM

Semi-quantitative Polymerase Chain Reaction (RT-PCR)

Total RNA was isolated from the cells of each group using a Qiagen RNA Isolation kit. RNA was quantified and purity was checked at 260 nm and 280 nm using a spectrophotometer. cDNA was prepared using a Genei RT PCR kit and stored at -80°C.

PCR was carried out with 200 ng cDNA for 50 µL PCR reaction. The forward and reverse primers used were as follows: αSMA, 5'-ACTGAGCGTGGCTATTCCTCCGTT-3' and 5'-GCAGTGGCCATCTCATTTTCA-3'; vimentin, 5'-CCAGGCAAAGCAGGAGTC-3' and 5'-CGAAGGTGACGAGCCATT-3'; GAPDH (internal control), 5'-GGTCGGAGTCAACGGATTTGGTCG-3' and 5'-CCTCCGACGCTGCTTACCAC-3'. PCR was set up using Jumpstart mix (Sigma), 20 pmol each of forward and reverse primer (Europhins) and the volume was attained using molecular grade water. PCR was carried out for 5 minutes at 95°C (initial denaturation), followed by 30 cycles of 95°C for 1 minute, 61.15°C (αSMA), 57.1°C (Vimentin), 66°C (GAPDH) for 30 seconds, 72°C for 1 minute, and a final extension at 72°C for 10 minutes. PCR products along with 100 bp ladder

(Sigma) were run on a 3% agarose gel and were observed under a UV-transilluminator. The target gene expression was analyzed using ImageJ software and was normalized to that of GAPDH. Three independent experiments were performed.

Statistical analysis

Quantitative data is shown as mean ± standard error of the mean (SEM). Analysis of variance (ANOVA) followed by Tukey's test was performed and statistical significance was obtained using GraphPad Prism software. $p < 0.05$ was considered as significant.

Received: September 16, 2019

Accepted: January 1, 2020

Published: February 18, 2020

REFERENCES

1. Ruoslahti, E. "How cancer spreads." *Scientific American*, vol. 275, no. 3, 72-77, 1996. doi:10.1038/scientificamerican0996-72.
2. Langley, Robert R, and Isaiah J Fidler. "The Seed and Soil Hypothesis Revisited-The Role of Tumor-Stroma Interactions in Metastasis to Different Organs." *International Journal of Cancer*, vol. 128, no. 11, 2011. doi:10.1002/ijc.26031.
3. Chao-Nan Qian. "Encyclopedia of Cancer: "Seed and Soil" theory of Metastasis." *Journal of Clinical Medicine.*, vol. 8, no. 5, 2012. <https://doi.org/10.3390/jcm8050747>
4. Dominici, M *et al.* "Minimal criteria for defining multipotent mesenchymal stromal cells." *Cytotherapy*, vol. 8, no. 4, 2006. doi:10.1080/14653240600855905
5. Mishra, P J *et al.* "Carcinoma-associated fibroblast-like differentiation of human mesenchymal stem cells." *Cancer Research*, vol. 68, no. 11, 2008. doi:10.1158/0008-5472.CAN-08-0943.
6. Au, P, *et al.* "Bone marrow-derived mesenchymal stem cells facilitate engineering of long-lasting functional vasculature." *Blood*, vol. 111, no. 9, 2008. doi:10.1182/blood-2007-10-118273.
7. Bexell, D, *et al.* "Bone marrow multipotent mesenchymal stroma cells act as pericyte-like migratory vehicles in experimental gliomas." *Molecular Therapy*, vol. 17, no. 1, 2009. doi:10.1038/mt.2008.229.
8. Karagiannis, G. S, *et al.* "Cancer-Associated Fibroblasts Drive the Progression of Metastasis through both Paracrine and Mechanical Pressure on Cancer Tissue." *Molecular Cancer Research*, vol. 10, no. 11, 2012. doi:10.1158/1541-7786.MCR-12-0307.
9. Danielsson, F, *et al.* "Vimentin diversity in health and disease." *Cells*, vol. 7, no. 10, 2018. doi:10.3390/cells7100147.
10. Wen, S, *et al.* "BM-MSCs promote prostate cancer progression via the conversion of normal fibroblasts to cancer-associated fibroblasts." *International Journal of Oncology*, vol. 47, no. 2, 2015. doi:10.3892/ijo.2015.3060.

11. Tianyi, L, *et al.* "Cancer-Associated Fibroblasts Build and Secure the Tumor Microenvironment." *Frontiers in Cell and Development Biology*, vol. 7, no. 60, 2019. doi:10.3389/fcell.2019.00060.
12. Hanahan, D and Weinberg, R. A. "Hallmarks of cancer: the next generation." *Cell*, vol. 144, no. 5, 2011. doi:10.1016/j.cell.2011.02.013.
13. Russo, F P, *et al.* "The bone marrow functionally contributes to liver fibrosis." *Gastroenterology*, vol. 130, no. 6, 2006. doi:10.1053/j.gastro.2006.01.036
14. Direkze, N C, *et al.* "Bone marrow contribution to tumor-associated myofibroblasts and fibroblasts." *Cancer Research*, vol. 64, no. 23, 2004. doi:10.1158/0008-5472.CAN-04-1708
15. Potenta, S, Zeisberg, E, and Kalluri, R. "The role of endothelial-to-mesenchymal transition in cancer progression." *British Journal of Cancer*, vol. 99, no. 9, 2008. doi:10.1038/sj.bjc.6604662.
16. Petersen, O W, *et al.* "The plasticity of human breast carcinoma cells is more than epithelial to mesenchymal conversion." *Breast Cancer Research*, vol. 3, no. 4, 2001. doi:10.1186/bcr298.
17. Petersen, O W, *et al.* "Epithelial to mesenchymal transition in human breast cancer can provide a nonmalignant stroma." *The American Journal of Pathology*, vol. 162, no. 2, 2003. doi:10.1016/S0002-9440(10)63834-5.
18. Yin, *et al.* "Heterogeneity of cancer-associated fibroblasts and roles in the progression, prognosis, and therapy of hepatocellular carcinoma." *Journal of Hematology & Oncology*, vol. 12, no. 1 2019. doi:10.1186/s13045-019-0782-x.
19. Kucerova, L, *et al.* "Tumor-driven Molecular Changes in Human Mesenchymal Stromal Cells." *Cancer Microenvironment*, vol. 8, no. 1, 2015. doi:10.1007/s12307-014-0151-9.

Copyright: © 2019 Ramesh, Umrao. Rao, and Rao. All JEI articles are distributed under the attribution non-commercial, no derivative license (<http://creativecommons.org/licenses/by-nc-nd/3.0/>). This means that anyone is free to share, copy and distribute an unaltered article for non-commercial purposes provided the original author and source is credited.

Combined progestin-estrogenic contraceptive pills may promote growth in crop-plants

Sukanta Saha¹, Barnali Mukhopadhyay¹

¹ The Heritage School, Kolkata, India

SUMMARY

Recently, there has been an increase in abundance of chemicals in the environment, especially from therapeutic usages. The effects of these deposited chemicals on the environment and human functions such as the endocrine system are of growing concern. A comparative study was conducted of the combined-effects of ethinyl estradiol and the progestin norgestrel commonly present in contraceptive tablets on the growth of flowering plants. The dicotyledon *Vigna radiata* (mung bean) and monocotyledon *Triticum aestivum* (winter wheat) were treated with progestin-estrogenic contraceptive tablets at 0.150%, 0.300%, 0.450%, 0.600% w/v using distilled water as a control over a period of 6 days. Morphological growth (percentage germination, embryonic and adventitious tissue proliferation, root length, and shoot length) was measured and chlorophyll concentrations were calculated using Arnon's equation for each group. Morphological growth was highest in *V. radiata* treated with the 0.150% solution and in *T. aestivum* treated with the 0.450% solution. Maximal inhibition of morphological growth was observed at 0.600% in *V. radiata*. Progestin-estrogenic contraceptive tablets enhanced morphological growth of *T. aestivum* at all experimental groups compared to the control. Calculated chlorophyll concentrations were higher than the control group at all experimental conditions for both the crop-plants. Maximum chlorophyll concentrations were also found in *V. radiata* and *T. aestivum* treated with 0.150% and 0.450% w/v solutions. While the impact of these chemicals on human health remains unclear, removing these chemicals from the environment is currently not cost-efficient and may either augment or diminish crop yields.

INTRODUCTION

The growth of the pharmaceutical industry and rising population has resulted in increasing amounts of chemicals and their metabolites being deposited in the environment (1-4), contaminating even our drinking water (5). The effects of these pharmaceutical compounds on the environment were seen in 2004 after the mass death of vultures in the Indian subcontinent caused by the anti-inflammatory drug, diclofenac (6). One such class of compounds that has garnered special attention in recent times is gonadal-steroid hormone, i.e. estrogen, progestogen, and androgen.

These hormones are also part of a broader class of compounds called endocrine-disrupting chemicals (EDCs). EDCs are chemicals produced exogenously, which interfere with naturally produced hormones responsible for reproduction, homeostasis, growth, development, and behavior. These EDCs mimic natural hormones and bind to their receptors, interfering in various biological activities such as synthesis, elimination, secretion or transportation of biomolecules (7). Most hormonal EDCs in water bodies exist in the scales of ng/L or µg/L (8, 9). Numerous studies have detected hormones in the sewage, groundwater, and surface water (10-13). Animal livestock feed designed to promote growth are major sources of these hormones (14-16). Another common source of these hormones is the discharge of chemical metabolites from therapeutic usages like contraception and menopausal-hormone therapy after usage by humans. Estrogen and progestin are well-known EDCs (17, 18). Both can be found in contraceptive tablets (19, 20), and feed for animal livestock (21, 22). Every year 30,700kg of natural and synthetic estrogen is discharged from use of contraceptive tablets alone while a further 83,000kg is discharged from livestock globally (23). No such quantifications for progestin have been done to date. When present in water bodies, both ethinyl estradiol and norgestrel reportedly disrupt the hormonal balance of fishes and specifically impede their reproductive system (24, 25). Water from rivers and streams are often directly used for irrigation. In both underdeveloped and well-developed countries, the instruments to detect and remove many of these chemicals are not sustainable (26, 27). Hence, studying the effects of these hormones on crop-plants is crucial.

Ethinyl estradiol is a semisynthetic form of estradiol, which is an estrogen. It binds to the same estrogen-receptor complex and activates similar transcription of genes as natural estrogen (28). It has greater resistance to metabolism than estradiol (29) and therefore, is more susceptible to be egested directly into sewage and not as its metabolites. It is structurally similar to its plant-based counterpart phytoestrogen and binds to the same receptors (30). It is anti-androgenic (31-33). In lower vertebrates like fishes, ethinyl estradiol is heavily involved in feminization (34, 35), and can even affect their trans-generational population sustainability by compromising embryonic survival rate (36). It is usually metabolized by CYP3A4 and CYP2C9 along with a few other isoforms of cytochrome P450 of the electron-transport chain

(37). It's predicted no-effect concentration (PNEC) is derived to be 0.1 ng/L (38). Even though sewage-water is usually passed through sewage treatment plants (STP), removal of ethinyl estradiol is not efficient and often the STP effluent has higher concentrations of ethinyl estradiol than the PNEC (39, 40). It is one of the most common estrogens used in combined oral contraceptives (41). It is almost exclusively used with norgestrel in combined-contraceptive tablets. While the adverse effects of both natural and synthetic estrogens have been studied extensively, studies on the effects of progestin are far less common. Norgestrel specifically has been one of the lesser studied progestins.

Norgestrel is a synthetic (progestin) form of progestogen, containing equal quantities of levonorgestrel which is the active enantiomer, and the inactive isomer dextro-norgestrel, making it identical in its biological activity to that of levonorgestrel, but only half as potent (29). However, neither norgestrel nor levonorgestrel has been studied extensively. Most synthetic progestins are structurally similar to progesterone and testosterone (42). Plant-based counterpart of progestins, phytoprogestin is very rare. Progestin, including norgestrel are mediated by nuclear progestin receptors. Levonorgestrel can bind to their androgen receptors in fishes (43). Metabolites of levonorgestrel can exhibit estrogenic activity (44, 45). Progestins are also involved in feminization of fishes (46-48), but a lack of suitable technology to detect the extremely small concentrations of progestin accurately has posed a challenge to detect and derive their PNEC, although concentrations of up to 50 ng/L could be detected in STP effluents (49). A previous study by Fent *et al.* in 2015 compiles the lowest observed effect concentration ranging from 0.8 ng/L to 750 ng/L, on various fishes such as the fathead minnow, zebrafish, roach, etc. These are likely to be true for norgestrel as well since norgestrel has also been suggested to be an active EDC (50). Fates of progestins are not known, but the few studies carried out suggest that they get deposited into sediments and nearby agricultural lands (51). With the possible introduction of progestin-based male birth-control tablets in the future (52), a considerable increase of concentrations in the sewage is likely to be foreseen at this point.

Ethinyl estradiol and progestin work together to inhibit folliculogenesis and ovulation by hindering the mid-cycle surge of luteinizing hormone and the follicle-stimulating hormone (53). These also make the endometrium unsuitable for implantation and thickens the mucus at the cervix (54). The result is contraception.

Ethinyl estradiol and progestins are also responsible for disruptions in plant metabolism (55) although their effects are quite varied. Traces of progesterone were found in mung beans (*Vigna radiata*) (56). In winter wheat (*Triticum aestivum*), estrogen promoted root and leaf growth (57). In wheat, progesterone can promote generative development and induce flowering (58). However, β -estradiol did not cause any significant difference in its seed germination (59). But it decreased the germination rate of *Lactuca sativa*, *Daucus*

carota, and *Lycopersicon esculentum* in a separate study (60). Germinated seedlings were measured for their root length and *Daucus carota* exhibited an 11% increase while the other two species had decreased root lengths compared to the control groups.

In another study, 17β -estradiol enhanced shoot growth in *Helianthus annuus* (61). The use of sewage water rather than fresh water for irrigation resulted in better growth in many other plants (62, 63). *Medicago sativa* irrigated with sewage water specifically containing 0.3 $\mu\text{g/L}$ estrogen showed increased vegetative growth (64). Ethinyl estradiol can affect growth and photosynthetic rates in green algae, cyanobacteria (65) and *Arabidopsis thaliana* (66). Progesterone stimulated germination and pollen tube growth in tobacco pollen (67). In chickpea, both progesterone and estradiol enhanced germination velocity, morphological growth and biochemical processes like alpha-amylase, peroxidase and catalase activities among others (68).

V. radiata is a green, dicotyledonous (flowering plant with a pair of leaves, or cotyledons, in the embryo of the seed), leguminous crop-plant, and considered as staple food throughout Southern and Eastern Asia, one of the most densely populated regions. In most other parts of the world it is still a very common food source. Protein is the major form of nutrition found in mung beans (20.97% to 31.32%) (69) with 43.5% of which are essential amino acids (70). These crops are usually planted and harvested before and after cereal crops. Since mung beans are legumes, they can increase the biomass and nitrogen content of soil, acting as green manure (71-73) Mung beans are also well known for their detoxifying bioactivities (74).

T. aestivum is green or brown, monocotyledonous (flowering plant with one leaf, or cotyledon, in the embryo of the seed), grass-like crop-plant, and considered a staple around the world; widely used for cereal production around the world among other major uses. It is vernalized (induction of flowering due to a prolonged period of growth at low temperatures) in the winter. Nutritional benefits include high quantities of carbohydrate, proteins and dietary fiber. Approximately 749 million tons of wheat were produced in 2016 worldwide, second only to maize in terms of the highest production of cereal (75, 76). Although the 13% protein content of *T. aestivum* is relatively low compared to its carbohydrate content (52.4% to 90%) (77), the majority of the protein is in the form of gluten. Lately gluten has been in high demand for its adhesivity and viscoelasticity, which can facilitate the production of processed food (78). In agronomic plants such as wheat, adventitious roots play a significant role in its growth and development (79).

With farmlands and livestock being situated just outside cities, it is possible that the water used to irrigate these farms contain estrogen and progestins. Studying their effects on common crops like wheat and mung beans could be crucial to better farming choices while use of these hormones as potential growth-regulators in these crops to

sustain the growing population is another area of interest. A comparative study could also help understand how the effects vary between different species and seed types (mono/dicotyledonous) which have not been studied extensively yet. While effects of individual gonadal-steroid hormones have been studied extensively, studies on the combined effects of these compounds are uncommon but could be of greater significance (80). Hence progestin-estrogenic tablets were chosen as potential growth regulators in this study. The limited scope of the study resulted in selecting tablets containing other accessory substances like their coatings instead of the synthetic hormones in their pure forms. A pilot experiment with two different concentrations of sample solution and distilled water was done on *V. radiata*, which showed varied root and shoot growth over three days. A possible research question including the effect of different concentrations on the growth of plants seemed imminent.

To better understand the combined effects of ethinyl estradiol and norgestrel on morphological growth, root length, shoot length, percentage germination and embryonic leaf and adventitious root proliferation were observed along with changes in chlorophyll concentration, in two different species, one being a monocotyledon (*T. aestivum*) and the other a dicotyledon (*V. radiata*) over six days. In *T. aestivum*, the roots proliferate early on in the germination process before the shoot while in *V. radiata*, it is the opposite. During photosynthesis, chlorophyll b is responsible for the absorption of light and chlorophyll a donates electrons in the electron transport chain. Total chlorophyll concentration can hence be an indirect measurement of the rate of photosynthesis (81), and therefore rate of growth.

Consequently, the scope of this study was to determine the extent to which contraceptive tablets containing the synthetic hormones, ethinyl estradiol and norgestrel (at 0.000%, 0.150%, 0.300%, 0.450% and 0.600% w/v), affect the growth of *V. radiata* and *T. aestivum*. The results suggested that 0.150% w/v sample stimulated the greatest growth in *V. radiata* while 0.450% w/v sample was best for growth in *T. aestivum*. It is important to consider these effects before removing them in sewage water treatment plants.

RESULTS

The growth medium consisted of distilled water and four different concentrations of contraceptive pills containing ethinyl estradiol and norgestrel. For 6 days, 20 seeds were exposed to these solutions in petri-dishes in a lab with a single non-LED yellow light source directly above (Figure 1). The number of germinated seeds was recorded on Day 1. On Day 2, the number of *V. radiata* seedlings with visible embryonic leaves and number of *T. aestivum* seedlings with at least two adventitious roots were recorded. Shoot and root lengths were measured using strings and ruler on Day 6. On Day 7, chlorophyll were extracted, centrifuged and analyzed in a spectrophotometer. Absorbance values were used in Arnon's equations to determine the exact chlorophyll a and



Figure 1: Experimental Setup of *V. radiata*.

b concentrations. The procedure to determine chlorophyll concentrations was repeated with five extracts from each solution to attain a mean value.

Qualitatively, it was observed that the 0.600% w/v sample of *V. radiata* had almost no root growth compared to the other concentrations. These seedlings did not stand upright towards the light source. Growth of very thin layers of mold was also observed in the 0.600% w/v samples of both of the species. The leaf-blades of *T. aestivum* in the 0.450% w/v sample were greener in colour when compared to the other two concentrations. The mung bean sprouts in the 0.150% w/v sample seemed healthier than the rest; the leaves were slightly larger, and the stems were considerably thicker.

The percentage of seeds germinated varied across the five treatment conditions (Figure 2). 95% of *V. radiata* seeds and 70% of *T. aestivum* seeds germinated in the 0.150% and 0.450% w/v samples respectively. These were the highest percentages of germination out of the 20 seeds that were initially set up. The lowest percentage of germinated seeds were in 0.600% w/v of *V. radiata* at 55% and in 0.150% w/v

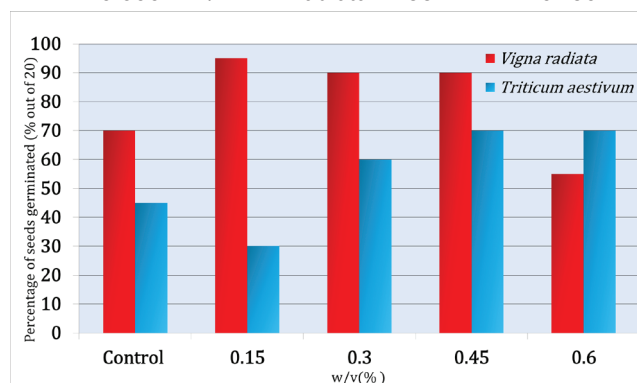


Figure 2: Percentage germination of *V. radiata* and *T. aestivum* on Day 1. We counted the number of seedlings that germinated on Day 1 in each and converted them to percentages out of the initial number of 20 seeds.

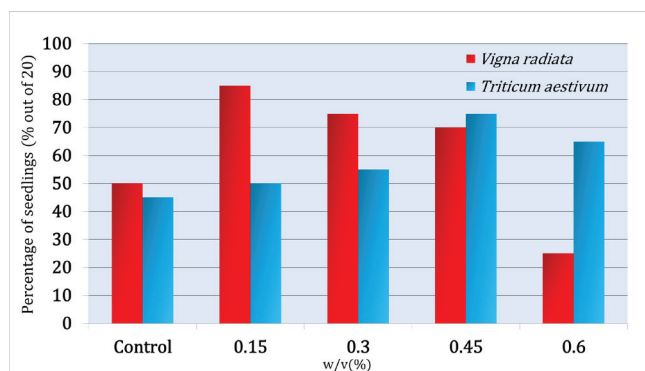


Figure 3: Embryonic leaf proliferation of *V. radiata* and adventitious root proliferation of *T. aestivum* on Day 2. The number of *V. radiata* seedlings with embryonic leaves and the number of *T. aestivum* seedlings that had at least two adventitious roots was counted for each of the different concentrations. This percentage was considered out of the number of seedlings that were germinated on Day 2.

of *T. aestivum* at 30%. The control groups exhibited 70% and 45% germination respectively.

Embryonic leaves sprouted the most in the 0.150% w/v sample of *V. radiata* (85%) and the least from the 0.600% w/v sample (25%) on Day 2 (Figure 3). Only 50% of the seeds had the embryonic leaves in the control group. Concentrations of 0.150%, 0.300% and 0.450% w/v exhibited higher leaf proliferation than the control group, but 0.600% w/v concentration exhibited a lower proliferation. The highest percentage of seedlings with two adventitious roots in *T. aestivum* was from the 0.450% w/v sample (75%) and the least was from the control group, which was 45% (Figure 3). All concentrations showed higher root tissue proliferation than the control, but after the peak at 0.450% w/v, root proliferation decreased in 0.600% w/v condition.

Highest mean shoot length of *V. radiata* was observed in 0.150% w/v to be 13.81 cm and the lowest mean in 0.600% w/v to be 4.09 cm (Figure 4). This was 2.89 cm (26.47%) higher and 6.83 cm (62.55%) lower than the control (10.92 cm). Other than the 0.150% w/v sample, only the 0.300% w/v

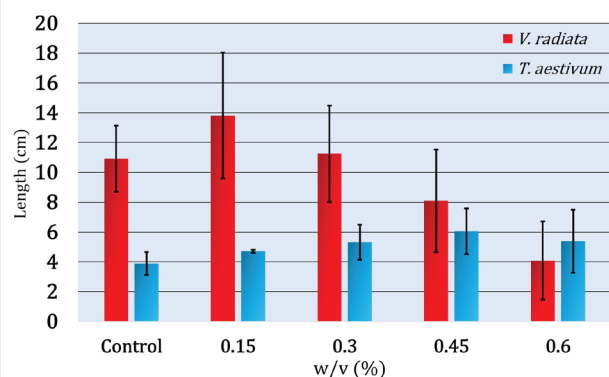


Figure 4: Shoot lengths of *V. radiata* and *T. aestivum* on Day 6. The lengths of shoots of each seedling were measured using strings and rulers. The mean (n=20) was calculated for each concentration and plotted. One-way ANOVA test was conducted to determine statistically significant (*V. radiata*: $p < 0.00001$ and *T. aestivum*: $p < 0.001321$) differences between the five treatment conditions.

sample exhibited a marginal increase of mean shoot length from the control, while the other concentrations exhibited lower means. These results were statistically significantly different ($p < 0.05$, one-way ANOVA, f-ratio value of 21.30, greater than f-critical value of 2.48).

Highest mean shoot length of *T. aestivum* was observed in the 0.450% w/v sample (6.05 cm) and the lowest in the control (3.89 cm) (Figure 4). There was an increase of 2.16 cm (55.53%) from the control. These results were statistically significantly different ($p < 0.05$, one-way ANOVA, f-ratio value of 5.01, greater than f-critical value of 2.51).

Mean root length was the highest in 0.150% w/v sample (4.77 cm) while the lowest was in the 0.600% w/v sample (1.3 cm) for *V. radiata* (Figure 5). This showed an increase of 0.11 cm (2.36%) and a decrease of 3.36 cm (72.10%) from the mean length of the control (4.66 cm). The other three concentrations showed decreased lengths of root from the control. These results were statistically significantly different ($p < 0.05$, one-way ANOVA, f-ratio value of 13.92, greater than f-critical value of 2.48).

T. aestivum had the highest mean root length in 0.450% w/v sample at 2.13 cm and the lowest in the control at 1.00 cm (Figure 5). An increase of 1.13 cm (113.00%) from the control was observed. All concentrations of sample solution increased the length of root of *T. aestivum* compared to the control. The control had a wider variety of mean root lengths per seedling than the others. These results were statistically significantly different ($p < 0.05$, one-way ANOVA, f-ratio value of 7.66, greater than f-critical value of 2.51).

Chlorophyll concentrations fluctuated across the five different conditions for both species of crop-plants. However, highest total chlorophyll concentrations were observed in the 0.150% w/v sample as 10.45 mg/mL and the 0.600% w/v sample as 10.63 mg/mL concentrations of *V. radiata* and *T. aestivum*, respectively, while lowest was observed in both controls, which were 2.28 mg/mL and 5.13 mg/mL respectively (Figure 6). This was an increase of 8.17 mg/mL

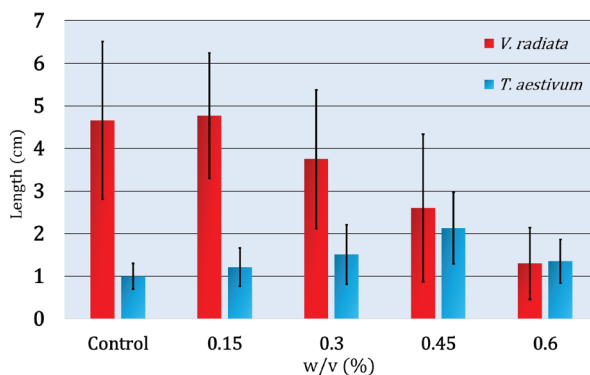


Figure 5: Root lengths of *V. radiata* and *T. aestivum* on Day 6. The lengths of roots of each seedling were measured using strings and rulers. For *T. aestivum*, all the adventitious roots in each seedling were measured, and the mean (n=20) was calculated for every concentration. One-way ANOVA test was conducted to determine statistically significant (*V. radiata*: $p < 0.00001$ and *T. aestivum*: $p < 0.000036$) differences between the five treatment conditions.

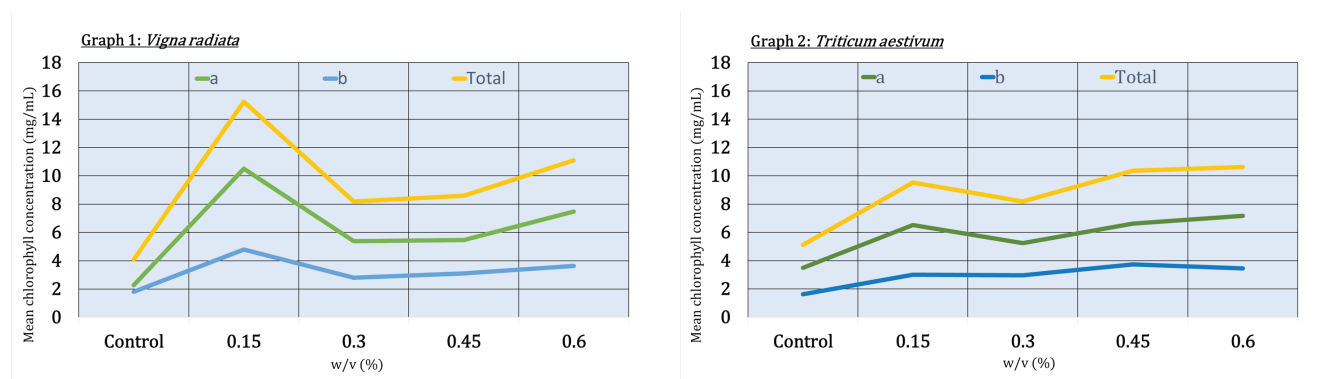


Figure 6: Chlorophyll concentrations *Vigna radiata* and *Triticum aestivum* on Day 6. Mean (n=5) chlorophyll concentrations a, b and total were plotted for both the species. One-way ANOVA test was conducted to determine statistically significant ($p < 0.00001$) differences between the five treatment conditions. Standard deviations were far too insignificant to be visible on the graphical representation and were thus omitted.

(358.33%) and 5.5 mg/mL (107.21%) from the control groups. It should also be noted that the second highest chlorophyll concentration was found in the 0.450% w/v sample in *T. aestivum* leaves. This was 10.36 mg/mL, a decrease of only 0.27 mg/mL from the highest. Even though a correlation was difficult to identify between chlorophyll concentration and sample solutions, a similar trend was observed in both the species (increased after 0.000%, decreased after 0.150%, increased after 0.450% and continued to increase up to 0.600%). One-way ANOVA tests were carried out for both datasets at $p < 0.05$ (f-ratio of *V. radiata* 281195.04 > 2.87, f-ratio of *T. aestivum* 40109.09 > 2.87), suggesting statistically significant differences between each obtained data.

DISCUSSION

Progestin-estrogenic tablets affected the growth of both *V. radiata* and *T. aestivum* similarly. The 0.150% w/v condition consistently promoted maximum morphological growth in *V. radiata* while 0.600% w/v condition consistently inhibited it the most. Similarly, *T. aestivum* had maximum morphological growth in the 0.450% w/v sample and the lowest in the control group, except percent germination, which was the lowest in the 0.150% w/v sample.

Variation of chlorophyll concentration was ambiguous, although the highest total chlorophyll concentration was found in the 0.150% w/v sample in *V. radiata*. In *T. aestivum*, the higher concentrations were found in the 0.450% and 0.600% w/v conditions. The fluctuating nature of both the graphs portraying chlorophyll concentrations of the two plants does suggest that a more extensive study of the effects of progestin-estrogenic tablets on chlorophyll concentration is essential to draw a more reliable conclusion. However, the similar pattern in which they vary suggests that the exposure of varied concentrations of progestin-estrogenic contraceptive tablets could have similar effects on plants regardless of the species and the number of cotyledons present in the seeds.

Studies on phytoestrogens and phytoprogestins are not very common. However, one study on the former did suggest their involvement in the initiation of hypersensitive cell death and defense competency in soybean, which leads

us to consider its possible effects on the growth of these crops (82). Both Graham's study and Turner *et al.* (2007) suggests some overlap between plant and animal nuclear receptor or other steroidal hormone signaling pathways (82, 30). Phytoestrogens also differ in their binding affinities to different estrogen receptors and modulate the efficacy of receptor binding to the estrogen response element (83), which is a short DNA sequence within the promoter of a gene that regulates transcription (84). Hence, it may be reasonable to speculate that certain concentrations of these hormones improve cell proliferation while other concentrations, perhaps when in excess, diminish cell proliferation by prohibiting enzymatic actions.

Chlorophyll b concentration of *T. aestivum* in the 0.600% w/v sample decreased compared to the 0.450% w/v sample which is unlikely because chlorophyll a concentration increased. Either of these data points may be anomalous. Maximum morphological growth and chlorophyll concentration was consistently found in the 0.150% and 0.450% w/v samples for *V. radiata* and *T. aestivum*, respectively. The only inconsistent result could be the maximum chlorophyll concentration found in the 0.600% w/v sample of *T. aestivum*.

This experimental design could be modified to be carried out in pots of soil instead of petri-dishes, which would be a more accurate model of the actual environmental conditions. Now that we are aware of the potential effects, possibly at a magnified scale, a concentration range in the scale of ng/L or $\mu\text{g/L}$ could be considered in future studies, as it may be more representative of the natural concentration levels. Only 20 seeds were used for each concentration, which could be expanded in the future to broaden the impact of the conclusions. Crop-plants even within the same species can be incredibly varied in terms of growth. A larger sample size would therefore be more representative of the target population, provide stronger results from statistical analysis, and help overcome random errors, assuming that no systematic error is prevalent within the design of the experiment. Additionally, a wider range of concentrations with smaller intervals could be considered for more accuracy and reliability. Incubators should have been used to better control

the environmental conditions during the experiment.

Furthermore, this experiment lacked a negative control. Contraceptive pills contain excipient (and inactive) substances like cornstarch and lactose and bulking agents. It is possible that these may have influenced the growth of the seedlings, and it is not clear if the observed effects are solely due to the ethinyl estradiol and norgestrel present in the tablets. But this negative control could not be included as the specific brand of contraceptives used do not contain inert tablets, although many other brands do. The used tablets are monophasic; all tablets contain equal amounts of active and inactive substances and are sold in packs of 21. Future studies should consider using a 28-days pill package so that the inert tablets could be utilized in designing the negative control.

The findings of this study imply that the prevalence of progestin-estrogenic tablets may alter optimum conditions required for cultivation of crops, while at some concentrations the growth may in fact be enhanced. Hence, appropriate regulation of the concentrations of progestins and estrogen may be necessary for sustainable agriculture. One important step in regulating the chemicals could be the improvements of technology in STPs to detect and remove EDCs in the long term. Since installation of such STPs could be very expensive and not inefficient currently (85), sewage pathways should be planned so that only specific streams and rivers are dedicated for disposal of EDCs and installed with STPs, enabling the rest of the water bodies to be safer. Therefore, another implication of this study could be the urgent development of accessible sensors so that EDCs including ethinyl estradiol and norgestrel can be studied more extensively.

If future studies confirm that steroid hormones improve crop growth, then farmers may be able to easily detect and utilize these chemicals available in river-waters to their advantage. This experiment was done over only 6 days and it could be interesting to observe the effects over a longer period, such as 12 weeks, or even the full lifecycle of the crops. One important question that arises is whether traces of these hormones could be found in the wheat and mung bean harvests if they are used as growth-promoters, and could be considered for further studies.

Ethinyl estradiol and norgestrel could potentially also be used as fertilizers directly for irrigation if regulated appropriately. However, the effects of these two chemicals when ingested in humans must be considered as well. Similar studies that delve into the combined effects as well as the individual effects of common EDCs can be pivotal in accurately predicting the fate and effects of these chemicals in the environment. Furthermore, these studies must be done on various other crop species and types to better understand the wide array of effects these could have as suggested by the comparison between the effects on *V. radiata* and *T. aestivum*.

METHODS

The procedure was primarily based on Bowlin (2014) (86), with alterations made to match the availability of equipment and the scope of this study.

Preparation of Stock Solutions of Progestin-estrogenic Tablets

Contraceptive pills were powdered using a mortar and pestle. 0.300 ± 0.001 g weighed using an electronic balance of powder was mixed in 200 ± 0.5 mL of distilled water to make a 0.150% sample solution. Similar method was followed using 0.600 g, 0.900 g and 1.20 g of powdered tablets and 200 mL of distilled water to make 0.300%, 0.450% and 0.600% w/v solutions. Every tablet weighed 0.067 g and contained 0.050 mg ethinyl estradiol and 0.500 mg norgestrel. These were stored at room temperature for use over the duration of the experiment.

Setting-up Seeds with the Apparatus (Figure 1)

A filter paper was kept on the base of a petri-dish. 20 seeds (taken from the same vendor at a local market) of both the species were chosen and rinsed in a 10% bleaching powder solution (10 g in 100 mL of distilled water) for 10-15 minutes. These were spread over the filter paper in each petri-dish. There were 5 petri-dishes for both species, each with 20 seeds, for every concentration of sample solution. All petri-dishes were placed around a hanging non-LED light source, which was turned on every 12 hours throughout the experiment. 25 ± 0.5 mL of sample solution was poured into each petri-dish using 50 mL measuring cylinder every 48 hours for 6 days. Volume of solution in the petri dish did not remain constant throughout the 6 days as it was being used up by the seedlings while some of it also evaporated due to the heat from the non-LED light.

Recording Morphological Growth

Percentage germination i.e. number of seeds germinated, was recorded for all the set-ups (out of 20) on Day 1. A seed was considered to be germinated if the coleoptile had emerged from the seed. On Day 2, the numbers of *V. radiata* seedlings whose embryonic leaves had sprout and the numbers of *T. aestivum* seedlings that had two adventitious roots were counted. Steps 4 to 6 were repeated for all germinated seedlings on Day 3 and Day 6. A string was used to trace the length of the shoot from the bottom of the shoot up to the tip of the apical meristem of *V. radiata* and up to the tip of the leaf blade of *T. aestivum*. The string was then cut at the tips to be measured on a ruler for its length. The same method was repeated for the root length. Strings were used to measure the length from the origin of the primary root of *V. radiata* up to the tip. For *T. aestivum*, the lengths of each adventitious root were measured and the total root lengths per seedling were found.

Determining Chlorophyll Concentration

On Day 6, 2 mg of leaves were measured from each condition of each species using a digital balance. The leaves were pat dried on tissue papers and weighed using a digital balance. The leaves were taken in the mortar and to it 4 mL of 80% acetone was added and crushed with the pestle to soften the cellulose. The crushed suspension was transferred into separate centrifuge tubes. Another 8 mL of acetone was added to make the volume up to 13 mL in each tube and centrifuged at 3500 RPM for 5 minutes. The supernatant for each set of sample solution (0.000%, 0.150%, 0.300%, and 0.600%) was decanted into test tubes. The spectrophotometer was calibrated to zero using 80% acetone as a blank. The absorbance of the supernatant from each sample solution was recorded at wavelengths of 645 nm and 663 nm. Chlorophyll a and b and total chlorophyll content (mg/mL) were determined using the Arnon's equations:

$$\text{Chlorophyll a: } 12.7A_{663} - 2.69A_{645}$$

$$\text{Chlorophyll b: } 22.9 A_{645} - 4.68 A_{663}$$

$$\text{Total Chlorophyll: Chlorophyll a + Chlorophyll b}$$

...where A_{663} and A_{645} are absorbances at 663 nm and 645 nm.

Sample calculations:

Total chlorophyll concentration of *V. radiata* (at 0.150%):

Chlorophyll a:

$$12.7A_{663} - 2.69A_{645} = 12.7(0.906) - 2.69(0.395) \\ = 10.44 \text{ mg/mL}$$

Chlorophyll b:

$$22.9 A_{645} - 4.68 A_{663} = 22.9(0.395) - 4.68(0.906) \\ = 4.81 \text{ mg/mL}$$

Total Chlorophyll:

$$\text{Chlorophyll a + Chlorophyll b} = 10.44 + 4.81 = 15.25 \text{ mg/mL}$$

Statistical Analysis

One-way ANOVA tests were done using Microsoft Excel to determine the significance of variance between the mean root and shoot lengths and chlorophyll concentration of five independent groups. There is only one independent variable in an ordered range (0.150% to 0.600%). F-ratio values were greater than the respective f-critical values when $p < 0.05$. Significant differences in mean lengths of root and shoot and mean total chlorophyll concentrations were observed. The null hypotheses were thus rejected and the experimental hypotheses stating that, root length, shoot length and total chlorophyll concentrations are affected by exposure to varied concentrations of progestin-estrogenic tablet solution, were accepted.

Received: September 24, 2019

Accepted: February 10, 2020

Published: February 21, 2020

REFERENCES

- Batt, Angela L., *et al.* "Evaluating the Vulnerability of Surface Waters to Antibiotic Contamination from Varying Wastewater Treatment Plant Discharges." *Environmental Pollution*, vol. 142, no. 2, 2006, pp. 295–302., doi:10.1016/j.envpol.2005.10.010.

- Gaw, Sally, *et al.* "Sources, Impacts and Trends of Pharmaceuticals in the Marine and Coastal Environment." *Philosophical Transactions of the Royal Society B: Biological Sciences*, vol. 369, no. 1656, 2014, p. 20130572., doi:10.1098/rstb.2013.0572.
- Glassmeyer, Susan T., *et al.* "Transport of Chemical and Microbial Compounds from Known Wastewater Discharges: Potential for Use as Indicators of Human Fecal Contamination." *Environmental Science & Technology*, vol. 39, no. 14, 2005, pp. 5157–5169., doi:10.1021/es048120k.
- Hummel, Daniela, *et al.* "Simultaneous Determination of Psychoactive Drugs and Their Metabolites in Aqueous Matrices by Liquid Chromatography Mass Spectrometry†." *Environmental Science & Technology*, vol. 40, no. 23, 2006, pp. 7321–7328., doi:10.1021/es061740w.
- Pharmaceuticals in Drinking Water. WHO Press, https://www.who.int/water_sanitation_health/publications/2011/pharmaceuticals_20110601.pdf.
- Oaks, J. Lindsay, *et al.* "Diclofenac Residues as the Cause of Vulture Population Decline in Pakistan." *Nature*, vol. 427, no. 6975, 2004, pp. 630–633., doi:10.1038/nature02317.
- Crisp, Thomas M., *et al.* Special Report on Environmental Endocrine Disruption: An Effects Assessment Analysis. USEPA, <https://archive.epa.gov/raf/web/pdf/endocrine.pdf>.
- Ingerslev, Flemming, and Bent Halling-Sørensen. Evaluation of Analytical Chemical Methods for Detection of Estrogens in the Environment. Danish Environmental Protection Agency, 2003, https://pdfs.semanticscholar.org/4bdb/226151b93f236f3bbff22bb87823c070c9df.pdf?_ga=2.133698126.1516064087.1581290267-64757373.1581290267.
- Kinnberg, Karin. Evaluation of in Vitro Assays for Determination of Estrogenic Activity in the Environment. Danish Environmental Protection Agency, 2003, https://pdfs.semanticscholar.org/13e2/907c526739a46d2c9fd9442a3835dd9c1536.pdf?_ga=2.134027086.1516064087.1581290267-64757373.1581290267.
- Bradley, Paul M., *et al.* "Biodegradation of 17β-Estradiol, Estrone and Testosterone in Stream Sediments." *Environmental Science & Technology*, vol. 43, no. 6, 2009, pp. 1902–1910., doi:10.1021/es802797j.
- Fernandez, Marc P., *et al.* "An Assessment of Estrogenic Organic Contaminants in Canadian Wastewaters." *Science of The Total Environment*, vol. 373, no. 1, 2007, pp. 250–269., doi:10.1016/j.scitotenv.2006.11.018.
- Fick, Jerker, *et al.* "Therapeutic Levels of Levonorgestrel Detected in Blood Plasma of Fish: Results from Screening

- Rainbow Trout Exposed to Treated Sewage Effluents.” *Environmental Science & Technology*, vol. 44, no. 7, 2010, pp. 2661–2666., doi:10.1021/es903440m.
13. Hutchins, Stephen R., *et al.* “Analysis of Lagoon Samples from Different Concentrated Animal Feeding Operations for Estrogens and Estrogen Conjugates.” *Environmental Science & Technology*, vol. 41, no. 3, 2007, pp. 738–744., doi:10.1021/es062234.
 14. Duckett, S. K., and J. G. Andrae. “Implant Strategies in an Integrated Beef Production System.” *Journal of Animal Science*, vol. 79, no. E-Suppl, 2001, doi:10.2527/jas2001.79e-supple110x.
 15. Preston, R.I. “Hormone Containing Growth Promoting Implants in Farmed Livestock.” *Advanced Drug Delivery Reviews*, vol. 38, no. 2, 1999, pp. 123–138., doi:10.1016/s0169-409x(99)00012-5.
 16. Bartelt-Hunt, Shannon L., *et al.* “Effect of Growth Promotants on the Occurrence of Endogenous and Synthetic Steroid Hormones on Feedlot Soils and in Runoff from Beef Cattle Feeding Operations.” *Environmental Science & Technology*, vol. 46, no. 3, 2012, pp. 1352–1360., doi:10.1021/es202680q.
 17. Blair, R. M. “The Estrogen Receptor Relative Binding Affinities of 188 Natural and Xenochemicals: Structural Diversity of Ligands.” *Toxicological Sciences*, vol. 54, no. 1, Jan. 2000, pp. 138–153., doi:10.1093/toxsci/54.1.138.
 18. Bauer, E. R. S., *et al.* “Characterisation of the Affinity of Different Anabolics and Synthetic Hormones to the Human Androgen Receptor, Human Sex Hormone Binding Globulin and to the Bovine Progesterin Receptor.” *Apmis*, vol. 108, no. 12, 2000, pp. 838–846., doi:10.1111/j.1600-0463.2000.tb00007.x.
 19. Combined Estrogen-Progestogen Contraceptives and Combined Estrogen-Progestogen Menopausal Therapy. *IARC*, 2007, <https://www.ncbi.nlm.nih.gov/books/NBK321672/>.
 20. “NCI Thesaurus.” National Institutes of Health, U.S. Department of Health and Human Services, ncit.nci.nih.gov/ncitbrowser/ConceptReport.jsp?dictionary=NCI_Thesaurus&code=C703.
 21. Regal, Patricia, *et al.* “Natural Hormones in Food-Producing Animals: Legal Measurements and Analytical Implications.” *Food Production - Approaches, Challenges and Tasks*, 2012, doi:10.5772/26789.
 22. Schiffer, B, *et al.* “The Fate of Trenbolone Acetate and Melengestrol Acetate after Application as Growth Promoters in Cattle: Environmental Studies.” *Environmental Health Perspectives*, vol. 109, no. 11, 2001, pp. 1145–1151., doi:10.1289/ehp.011091145.
 23. Adeel, Muhammad, *et al.* “Environmental Impact of Estrogens on Human, Animal and Plant Life: A Critical Review.” *Environment International*, vol. 99, 2017, pp. 107–119., doi:10.1016/j.envint.2016.12.010.
 24. Durhan, Elizabeth J., *et al.* “Identification of Metabolites of Trenbolone Acetate in Androgenic Runoff from a Beef Feedlot.” *Environmental Health Perspectives*, vol. 114, no. Suppl 1, 2006, pp. 65–68., doi:10.1289/ehp.8055.
 25. Orlando, Edward F, *et al.* “Endocrine-Disrupting Effects of Cattle Feedlot Effluent on an Aquatic Sentinel Species, the Fathead Minnow.” *Environmental Health Perspectives*, vol. 112, no. 3, 2004, pp. 353–358., doi:10.1289/ehp.6591.
 26. Koh, Y.k.k., *et al.* “Treatment And Removal Strategies For Estrogens From Wastewater.” *Environmental Technology*, vol. 29, no. 3, 2008, pp. 245–267., doi:10.1080/09593330802099122.
 27. Snyder, S., *et al.* “Analytical Methods Used to Measure Endocrine Disrupting Compounds in Water.” *Practice Periodical of Hazardous, Toxic, and Radioactive Waste Management*, vol. 7, no. 4, 2003, pp. 224–234., doi:10.1061/(asce)1090-025x(2003)7:4(224).
 28. “NCI Thesaurus.” National Institutes of Health, U.S. Department of Health and Human Services, ncit.nci.nih.gov/ncitbrowser/ConceptReport.jsp?dictionary=NCI_Thesaurus&code=C486.
 29. Kuhl, H. “Pharmacology of Estrogens and Progestogens: Influence of Different Routes of Administration.” *Climacteric*, vol. 8, no. sup1, 2005, pp. 3–63., doi:10.1080/13697130500148875.
 30. Turner, Joseph V., *et al.* “Molecular Aspects of Phytoestrogen Selective Binding at Estrogen Receptors.” *Journal of Pharmaceutical Sciences*, vol. 96, no. 8, 2007, pp. 1879–1885., doi:10.1002/jps.20987.
 31. Coss, Christopher C., *et al.* “Preclinical Characterization of a Novel Diphenyl Benzamide Selective ER α Agonist for Hormone Therapy in Prostate Cancer.” *Endocrinology*, vol. 153, no. 3, 2012, pp. 1070–1081., doi:10.1210/en.2011-1608.
 32. Mp, Ekback. “Hirsutism, What to Do?” *International Journal of Endocrinology and Metabolic Disorders*, vol. 3, no. 3, 2017, doi:10.16966/2380-548x.140.
 33. Nieschlag, E., *et al.* *Testosterone: Action, Deficiency, Substitution.* Cambridge University Press, 2012.
 34. Christiansen, Lisette Bachmann, *et al.* *The Effect of Estrogenic Compounds and Their Fate in Sewage Treatment Plants and Nature.* Danish Environmental Protection Agency, <https://www.yumpu.com/en/document/read/14087592/feminisation-of-fish-miljstyrelsen>.
 35. Jobling, Susan, *et al.* “Widespread Sexual Disruption in Wild Fish.” *Environmental Science & Technology*, vol. 32, no. 17, 1998, pp. 2498–2506., doi:10.1021/es9710870.
 36. Bhandari, Ramji K., *et al.* “Transgenerational Effects from Early Developmental Exposures to Bisphenol A or 17 α -Ethinylestradiol in Medaka, *Oryzias Latipes*.” *Scientific Reports*, vol. 5, no. 1, 2015, doi:10.1038/srep09303.
 37. Wang, Bonnie, *et al.* “The involvement of CYP3A4 and CYP2C9 in the metabolism of 17 alpha-ethinyl estradiol.” *Drug Metabolism and Disposition*, vol. 32, no. 11, Oct.

- 2004, pp. 1209–1212., doi:10.1124/dmd.104.000182.
38. Caldwell, Daniel J., *et al.* “Predicted-No-Effect Concentrations for the Steroid Estrogens Estrone, 17 β -Estradiol, Estriol, and 17 α -Ethinylestradiol.” *Environmental Toxicology and Chemistry*, vol. 31, no. 6, 27 Apr. 2012, pp. 1396–1406., doi:10.1002/etc.1825.
 39. Baronti, Chiara, *et al.* “Monitoring Natural and Synthetic Estrogens at Activated Sludge Sewage Treatment Plants and in a Receiving River Water.” *Environmental Science & Technology*, vol. 34, no. 24, Dec. 2000, pp. 5059–5066., doi:10.1021/es001359q.
 40. Ifelebuegu, A. O. “Removal of Endocrine Disrupting Chemicals in Wastewater Treatment Applications.” Coventry University, 2013.
 41. Evans, Ginger, and Eliza L. Sutton. “Oral Contraception.” *Medical Clinics of North America*, vol. 99, no. 3, 2015, pp. 479–503., doi:10.1016/j.mcna.2015.01.004.
 42. Sitruk-Ware, Regine, and Anita Nath. “The Use of Newer Progestins for Contraception.” *Contraception*, vol. 82, no. 5, 2010, pp. 410–417., doi:10.1016/j.contraception.2010.04.004.
 43. Ellestad, Laura E., *et al.* “Environmental Gestagens Activate Fathead Minnow (*Pimephales Promelas*) Nuclear Progesterone and Androgen Receptors in Vitro.” *Environmental Science & Technology*, vol. 48, no. 14, 2014, pp. 8179–8187., doi:10.1021/es501428u.
 44. Schoonen, W.g.e.j., *et al.* “Contraceptive Progestins. Various 11-Substituents Combined with Four 17-Substituents: 17 α -Ethinyl, Five- and Six-Membered Spiromethylene Ethers or Six-Membered Spiromethylene Lactones.” *The Journal of Steroid Biochemistry and Molecular Biology*, vol. 74, no. 3, 2000, pp. 109–123., doi:10.1016/s0960-0760(00)00094-7.
 45. García-Becerra Rocio, *et al.* “The Intrinsic Transcriptional Estrogenic Activity of a Non-Phenolic Derivative of Levonorgestrel Is Mediated via the Estrogen Receptor- α .” *The Journal of Steroid Biochemistry and Molecular Biology*, vol. 82, no. 4-5, 2002, pp. 333–341., doi:10.1016/s0960-0760(02)00192-9.
 46. Runnalls, Tamsin J., *et al.* “Several Synthetic Progestins with Different Potencies Adversely Affect Reproduction of Fish.” *Environmental Science & Technology*, vol. 47, no. 4, Aug. 2013, pp. 2077–2084., doi:10.1021/es3048834.
 47. Zucchi, Sara, *et al.* “Progestins and Antiprogestins Affect Gene Expression in Early Development in Zebrafish (*Danio Rerio*) at Environmental Concentrations.” *Environmental Science & Technology*, vol. 46, no. 9, 2012, pp. 5183–5192., doi:10.1021/es300231y.
 48. Zeilinger, Jana, *et al.* “Effects Of Synthetic Gestagens On Fish Reproduction.” *Environmental Toxicology and Chemistry*, vol. 28, no. 12, 2009, p. 2663-2670., doi:10.1897/08-485.1.
 49. Fent, Karl. “Progestins as Endocrine Disrupters in Aquatic Ecosystems: Concentrations, Effects and Risk Assessment.” *Environment International*, vol. 84, 2015, pp. 115–130., doi:10.1016/j.envint.2015.06.012.
 50. Jenkins, R. L. “Androstenedione and Progesterone in the Sediment of a River Receiving Paper Mill Effluent.” *Toxicological Sciences*, vol. 73, no. 1, 2003, pp. 53–59., doi:10.1093/toxsci/kfg042.
 51. Liu, Shan, *et al.* “Steroids in Marine Aquaculture Farms Surrounding Hailing Island, South China: Occurrence, Bioconcentration, and Human Dietary Exposure.” *Science of The Total Environment*, vol. 502, 2015a, pp. 400–407., doi:10.1016/j.scitotenv.2014.09.039.
 52. J.K., Amory. “Testosterone/Progestin Regimens: a Realistic Option for Male Contraception?” *Current Opinion in Investigational Drugs*, vol. 5, no. 10, 2004, pp. 1025–1030., <https://www.ncbi.nlm.nih.gov/pubmed/15535423>.
 53. Craig, Charles R., and Robert E. Stitzel. *Modern Pharmacology with Clinical Applications*. Lippincott, 2004.
 54. “Estrogen and Progestin (Oral Contraceptives): MedlinePlus Drug Information.” MedlinePlus, U.S. National Library of Medicine, medlineplus.gov/druginfo/meds/a601050.html.
 55. Dodgen, Laurel K., *et al.* “Effect of Transpiration on Plant Accumulation and Translocation of PPCP/EDCs.” *Environmental Pollution*, vol. 198, 2015, pp. 144–153., doi:10.1016/j.envpol.2015.01.002.
 56. Iino, Mayumi, *et al.* “Progesterone: Its Occurrence in Plants and Involvement in Plant Growth.” *Phytochemistry*, vol. 68, no. 12, 2007, pp. 1664–1673., doi:10.1016/j.phytochem.2007.04.002.
 57. Janeczko A. Influence of Selected Steroids on Plant Physiological Processes—Especially Flowering Induction. Krakow: Ph.D. Dissertation, Agriculture University, 2000.
 58. Janeczko, Anna, and Władysław Filek. “Stimulation of Generative Development in Partly Vernalized Winter Wheat by Animal Sex Hormones.” *Acta Physiologiae Plantarum*, vol. 24, no. 3, 2002, pp. 291–295., doi:10.1007/s11738-002-0054-0.
 59. Nirmala, G.C., *et al.* “Effect of Estrogen and Progesterone on Seed Germination.” *Veterinary World*, vol. 1, no. 8, 2008, pp. 241–242., <http://www.veterinaryworld.org/2008/August/Effect%20of%20Estrogen%20and%20Progesterone%20on%20seed%20germination.pdf>
 60. Dabrosca, Brigida, *et al.* “Phytotoxicity Evaluation of Five Pharmaceutical Pollutants Detected in Surface Water on Germination and Growth of Cultivated and Spontaneous Plants.” *Journal of Environmental Science and Health, Part A*, vol. 43, no. 3, 2008, pp. 285–294., doi:10.1080/10934520701792803.
 61. Bhattacharya, B., and K. Gupta. “Steroid Hormone Effects on Growth and Apical Dominance of Sunflower.” *Phytochemistry*, vol. 20, no. 5, 1981, pp. 989–991., doi:10.1016/0031-9422(81)83014-2.
 62. Vaisman, I., *et al.* “Reducing Ground Water Pollution from Municipal Waste Water Irrigation of Rhodes Grass Grown on Sand Dunes.” *Journal of Environmental*

- Quality, vol. 10, no. 4, 1981, pp. 434–439., doi:10.2134/jeq1981.00472425001000040002x.
63. Bielorai, H., *et al.* "Drip Irrigation of Cotton with Treated Municipal Effluents: I. Yield Response." *Journal of Environmental Quality*, vol. 13, no. 2, 1984, pp. 231–234., doi:10.2134/jeq1984.00472425001300020011x.
64. Shore, Laurence S., *et al.* "Effects of Estrone and 17 Beta-Estradiol on Vegetative Growth of Medicago Sativa." *Physiologia Plantarum*, vol. 84, no. 2, 1992, pp. 217–222., doi:10.1111/j.1399-3054.1992.tb04656.x.
65. Perron, Marie-Claude, and Philippe Juneau. "Effect of Endocrine Disrupters on Photosystem II Energy Fluxes of Green Algae and Cyanobacteria." *Environmental Research*, vol. 111, no. 4, 2011, pp. 520–529., doi:10.1016/j.envres.2011.02.013.
66. Upadhyay, Pallavi, and Camelia Maier. "Effects of 17 β -Estradiol on Growth, Primary Metabolism, Phenylpropanoid-Flavonoid Pathways and Pathogen Resistance in Arabidopsis Thaliana" *American Journal of Plant Sciences*, vol. 07, no. 13, 2016, pp. 1693–1710., doi:10.4236/ajps.2016.713160.
67. Ylstra, B., *et al.* "Steroid Hormones Stimulate Germination and Tube Growth of in Vitro Matured Tobacco Pollen." *Plant Physiology*, vol. 107, no. 2, Jan. 1995, pp. 639–643., doi:10.1104/pp.107.2.639.
68. Erdal, Serkan, and Rahmi Dumlupinar. "Progesterone and β -Estradiol Stimulate Seed Germination in Chickpea by Causing Important Changes in Biochemical Parameters." *Zeitschrift Für Naturforschung C*, vol. 65, no. 3-4, Jan. 2010, pp. 239–244., doi:10.1515/znc-2010-3-412.
69. Anwar, F., *et al.* "Chemical Composition and Antioxidant Activity of Seeds of Different Cultivars of Mungbean." *Journal of Food Science*, vol. 72, no. 7, 2007, doi:10.1111/j.1750-3841.2007.00462.x.
70. Kudre, Tanaji G, *et al.* "Comparative Study on Chemical Compositions and Properties of Protein Isolates from Mung Bean, Black Bean and Bambara Groundnut." *Journal of the Science of Food and Agriculture*, vol. 93, no. 10, Dec. 2013, pp. 2429–2436., doi:10.1002/jsfa.6052..
71. Meelu, O.P. *et al.* "Grain Yield Responses in Rice to Eight Tropical Green Manures." *Tropical Agriculture*, vol. 69, no. 2, 1992, pp. 133–136.
72. Devendra, C., *et al.* "Food-Feed Systems in Asia - Review -." Asian-Australasian *Journal of Animal Sciences*, vol. 14, no. 5, Jan. 2001, pp. 733–745., doi:10.5713/ajas.2001.733.
73. Sustainable Crop Rotations with Cover Crops. The Ohio State University, 2009, https://pdfs.semanticscholar.org/bd8a/0a36820baf18110e83835117a4545cdcd3d2.pdf?_ga=2.173349731.1516064087.1581290267-64757373.1581290267.
74. Tang, Dongyan, *et al.* "A Review of Phytochemistry, Metabolite Changes, and Medicinal Uses of the Common Food Mung Bean and Its Sprouts (*Vigna radiata*)." *Chemistry Central Journal*, vol. 8, no. 1, 2014, doi:10.1186/1752-153x-8-4.
75. United Nations, Food and Agriculture Organization. World food situation: FAO cereal supply and demand brief. Rome, Italy, 2016.
76. United Nations, Food and Agriculture Organization, Statistics Division. "Crops/World Total/Wheat/Production Quantity/2014 (pick list)." 2015.
77. "Wheat." FoodData Central, US Department of Agriculture, fdc.nal.usda.gov/fdc-app.html#/food-details/339623/nutrients.
78. Day, L., *et al.* "Wheat-Gluten Uses and Industry Needs." *Trends in Food Science & Technology*, vol. 17, no. 2, 2006, pp. 82–90., doi:10.1016/j.tifs.2005.10.003.
79. Davis, Tim D., and Bruce E. Haissig. Biology of Adventitious Root Formation. Plenum, 1994, <https://link.springer.com/content/pdf/10.1007/978-1-4757-9492-2.pdf>.
80. Wise, Amber, *et al.* "Are Oral Contraceptives a Significant Contributor to the Estrogenicity of Drinking Water?" *Environmental Science & Technology*, vol. 45, no. 1, 2011, pp. 51–60., doi:10.1021/es1014482.
81. Fleischer, Walter E. "The Relation Between Chlorophyll Content And Rate Of Photosynthesis." *The Journal of General Physiology*, vol. 18, no. 4, 1935, pp. 573–597., doi:10.1085/jgp.18.4.573.
82. Graham, T.L. "Biosynthesis and Distribution of Phytoestrogens and Their Roles in Plant Defense, Signal Transduction, and Cell-to-Cell Signaling." *Journal of Medicinal Food*, vol. 2, no. 3-4, 1999, pp. 93–97., doi:10.1089/jmf.1999.2.93.
83. Kostelac, Drazen, *et al.* "Phytoestrogens Modulate Binding Response of Estrogen Receptors α and β to the Estrogen Response Element." *Journal of Agricultural and Food Chemistry*, vol. 51, no. 26, 2003, pp. 7632–7635., doi:10.1021/jf034427b.
84. Gruber, Christian J, *et al.* "Anatomy of the Estrogen Response Element." *Trends in Endocrinology & Metabolism*, vol. 15, no. 2, 2004, pp. 73–78., doi:10.1016/j.tem.2004.01.008.
85. Liu, Ze-Hua, *et al.* "Removal Mechanisms for Endocrine Disrupting Compounds (EDCs) in Wastewater Treatment — Physical Means, Biodegradation, and Chemical Advanced Oxidation: A Review." *Science of The Total Environment*, vol. 407, no. 2, 2009, pp. 731–748., doi:10.1016/j.scitotenv.2008.08.039.
86. Bowlin, Kelsey Marie. "Effects of β -Estradiol on the Germination and Growth in Zea Mays." Northwest Missouri State University, 2014, <https://www.nwmissouri.edu/library/theses/2014/BowlinKelseyM.pdf>

Copyright: © 2020 Saha and Mukhopadhyay. All JEI articles are distributed under the attribution non-commercial, no derivative license (<http://creativecommons.org/licenses/>)

by-nc-nd/3.0/). This means that anyone is free to share, copy and distribute an unaltered article for non-commercial purposes provided the original author and source is credited.

Investigating the role of the novel ESCRT-III recruitment factor CCDC11 in HIV budding: a potential target for antiviral therapy

Leo Takemaru^{1*}, Poojan Pandya^{2*}, Michael W. Lake³, Carol A. Carter⁴, Feng-Qian Li^{5‡}

¹Ward Melville High School, East Setauket, New York

²Half Hollow Hills High School West, Dix Hills, New York

³Department of Biochemistry and Cell Biology, Stony Brook University, Stony Brook, New York

⁴Department of Microbiology and Immunology, Stony Brook University, Stony Brook, New York

⁵Department of Pharmacological Sciences, Stony Brook University, Stony Brook, New York

*These authors contributed equally to this work.

‡Correspondence to: feng-qian.li@stonybrook.edu

SUMMARY

Acquired immunodeficiency syndrome (AIDS) is a life-threatening condition caused by the human immunodeficiency virus (HIV). By damaging the immune system, HIV compromises the body's ability to fight infectious and non-infectious diseases. To discover potential targets for antiviral therapies, we explored the role of Coiled-Coil Domain-Containing 11 (CCDC11) in HIV-1 budding. CCDC11 serves an important role in cytokinesis by recruiting Endosomal Sorting Complex Required for Transport III (ESCRT-III) membrane scission machinery to the midbody of the cell in preparation for the separation into two daughter cells. ESCRT-III has also been implicated in the budding process of HIV and other enveloped viruses. Therefore, we hypothesized that CCDC11 is required for viral budding. To investigate this, we performed ELISAs (enzyme-linked immunosorbent assays) to detect the HIV-1 Gag capsid protein p24 as a measure of viral particle release. We found that ectopic expression of CCDC11 in human embryonic kidney (HEK) 293T cells significantly increased the production of HIV-1 particles in culture media. To rigorously test our hypothesis, we established CCDC11-knockout HEK293T cells using CRISPR-Cas9 technology. CCDC11 knockout was verified by DNA sequencing, western blotting, and immunofluorescence staining. We found that knockout of CCDC11 markedly decreased the production of HIV-1 particles. The defective viral production in CCDC11-knockout cells was partially restored when wild-type CCDC11 was re-expressed. Collectively, our data suggested that CCDC11 is critical for efficient HIV-1 budding. Considering that CCDC11 expression is generally low in the majority of adult human tissues, CCDC11 might be a viable target for antiviral therapeutics without major side effects.

INTRODUCTION

Coiled-Coil Domain-Containing 11 (CCDC11) was initially discovered as a gene mutated in human laterality disorder patients suffering from heterotaxy and *situs inversus* (1). Made up of 514 amino acids, CCDC11 harbors three coiled-coil domains. Four unique human CCDC11 mutations have been reported to date (1-4). Further studies showed that CCDC11 plays an important role in the establishment of left-right lateral asymmetry (2-5). Interestingly, in animals, the left-right asymmetry of internal organs is determined during early embryogenesis through the function of cilia, small hair-like structures that are present on the surface of many cell types (6-7). Cilia are evolutionarily conserved microtubule-based organelles that protrude from the apical cell surface to perform diverse biological functions (7-9). They are present on most cells of the human body and play crucial roles in mechanosensation, photoreception, intracellular signaling, and fluid movement. Cilia in the embryonic node break left-right symmetry by rotating clockwise to generate leftward fluid flow. Genetic defects in the structure and function of cilia are associated with a range of disorders termed ciliopathies including organ laterality defects, polydactyly (extra digits), and polycystic kidney disease (7-9).

Consistent with CCDC11's role as an essential factor for ciliogenesis, CCDC11 localizes to centrosomes, centriolar satellites, and cilia (2,4). Depletion of CCDC11 from mammalian cultured cells or zebrafish and frog embryos leads to abnormal cilia, resulting in left-right patterning defects (2-5). Surprisingly, more recently, it was reported that CCDC11 is also important for cell division (10). CCDC11 has been shown to localize to the middle region between two dividing daughter cells, called the midbody, in different human cell lines. Knockdown of CCDC11 protein in human cultured cells using small interfering RNA (siRNA) blocks cell division, resulting in abnormal cells with two or more nuclei. Multinucleation is a hallmark of cell division defects due to the failure of cytokinesis, the final phase of mitosis (10). The Endosomal Sorting Com-

plex Required for Transport III (ESCRT-III) machinery acts in membrane deformation and scission in different biological processes (11-13). At the end of cytokinesis, ESCRT-III is recruited to the midbody to cleave the intercellular membrane bridge between nascent daughter cells in a process known as abscission (11-13). Importantly, CCDC11 facilitates the midbody recruitment of Charged Multivesicular Body Protein 2A (CHMP2A), a core subunit of the ESCRT-III complex (10). At present, the precise molecular roles of CCDC11 in ciliogenesis and cytokinesis are largely unknown.

ESCRT-III has been shown to play an important role for the budding of viral particles from the cell surface (14-17). Viral buds, small protrusions at the plasma membrane, are initially induced by the assembly of the major HIV-1 structural polyprotein Gag. During final stages of membrane remodeling, the ESCRT machinery is recruited to the sites of viral budding to complete membrane scission and release of mature viral particles from the host cell. ESCRT consists of four distinct subcomplexes (ESCRT-0, -I, -II, and -III) and associated proteins such as Vacuolar Protein Sorting 4 (Vps4) and the ALG2-Interacting protein X (ALIX) (14,17-18). These ESCRTs are recruited sequentially and transiently to Gag assembly sites. At the final step of viral budding, ESCRT-III, which is composed of CHMP family members, forms spiral filaments that facilitate the constriction of membrane necks to promote viral release. In addition to cytokinetic abscission and viral budding, ESCRTs are implicated in a variety of cellular processes requiring an internal membrane fission event including the formation of multivesicular bodies (MVBs), plasma and nuclear membrane repair, neuronal pruning, and autophagy (19-20).

CCDC11 has been reported to be involved in ciliogenesis and cytokinesis, but its potential role in other biological processes is currently unknown. Intriguingly, T cells, the physiological hosts for HIV-1, lack cilia but have been suggested to repurpose components of the ciliary machinery for the assembly and function of the immunological synapse even in the absence of a primary cilium (21-22). Since the ESCRT-III machinery functions in viral budding, we set out to test our hypothesis that CCDC11 is necessary for the recruitment of ESCRT-III to the sites of viral budding at the plasma membrane, thereby promoting the release of viral particles from the cell surface.

RESULTS

Ectopic expression of CCDC11 robustly promotes the production of HIV particles

Since ESCRT-III directly participates in the budding process of several different enveloped viruses, and because CCDC11 is required for ESCRT-III recruitment to the midbody, we explored the possibility that CCDC11 promotes the release of HIV particles from cells. To test this possibility, we first investigated the effect of CCDC11 overexpression on the production of HIV-1 particles. We transiently transfected wild-type (WT) HEK293T cells with a plasmid encoding the

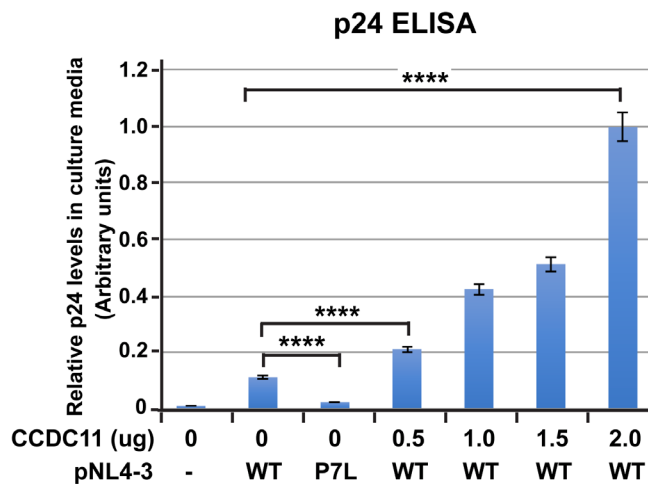


Figure 1. Forced expression of CCDC11 in HEK293T cells robustly enhances the production of HIV-1 particles. Wild-type (WT) HEK293T cells were transfected in triplicate with 2 μ g of a HIV-1 pNL4-3- Δ Env plasmid bearing WT- or P7L-Gag with or without increasing amounts of CCDC11 as indicated. An expression plasmid for Renilla luciferase (50 ng) was cotransfected to normalize transfection frequency. After 30 hours of transfection, the culture media were harvested, clarified by centrifugation to remove cellular debris, and used for p24 ELISA assays. Data are presented as means \pm standard deviations. Statistical analysis was performed using one-way analysis of variance (ANOVA), and $p < 0.05$ was considered statistically significant. ****, $p < 0.0001$.

entire HIV-1 genome except for the envelope (HIV-1 pNL4-3- Δ Env) and increasing amounts of DNA encoding CCDC11. The pNL4-3- Δ Env plasmid lacks the envelope protein and thus produces noninfectious HIV-1 particles. As a control, we transfected cells with pNL4-3- Δ Env harboring a proline-to-leucine substitution in the *gag* gene that impairs Gag binding to Tsg101 (23). Tsg101 is a component of ESCRT-I that directly binds the P₇TAP motif in Gag to promote the recruitment of the ESCRT-III complex. Twenty-four hours after transfection, we harvested culture media and performed an enzyme-linked immunosorbent assay (ELISA) for HIV-1 Gag-related capsid protein p24 to evaluate viral particle release. We detected a significant level of p24 antigen in the media from cells transfected with WT pNL4-3 (**Figure 1**). In contrast, we found much lower p24 levels in the media of P7L-pNL4-3-expressing cells, as expected, due to defective recruitment of Tsg101 to the viral budding sites (4.6-fold decrease, $p < 0.0001$). Intriguingly, coexpression of WT-pNL4-3 with increasing amounts of CCDC11 robustly enhanced p24 antigen levels in a dose-dependent fashion (8.9-fold increase from 0 to 2 μ g of the CCDC11 plasmid, $p < 0.00001$). These results suggested that CCDC11 promotes the budding of HIV-1 particles from the cell surface into the culture media in HEK293T cells.

Characterization of CCDC11-knockout HEK293T cells

To generate CCDC11-knockout cells using the CRISPR/Cas9 system (24-25), we chose human embryonic kidney (HEK) 293T cells since these cells are widely used, show

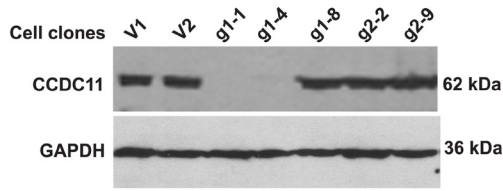


Figure 2. Western blot analysis of control empty vector and CCDC11-knockout candidate cell clones. Total cell lysates from the following cell clones were subjected to western blot analysis using anti-CCDC11 antibody: control vector clones (V1 and V2) and CCDC11-knockout candidate cell clones (g1-1, g1-4, and g1-8 from gRNA-1-transfected cells and g2-2 and g2-9 from gRNA-2 transfected cells). GAPDH served as a loading control.

high transfection efficiency, and have the ability to form cilia, albeit at low efficiency. We designed two short guide RNAs (gRNAs) against the 5' region of the human CCDC11 coding sequence (gRNA-1 and -2) as described in Materials and Methods. gRNAs escort Cas9 nucleases to specific target genomic sites and generate double-strand breaks, which are repaired by error-prone non-homologous end joining (NHEJ), thereby inducing short insertions and deletions (indels). The pSpCas9(BB)-2A-Puro (PX459) V2.0 expression vector (24) containing CCDC11 gRNA-1 or -2 was transiently transfected into HEK293T cells and grown in the presence of puromycin. Multiple single colonies were selected and further expanded. The empty vector was also transfected to establish negative control cell clones.

To validate CCDC11 knockout, we prepared total cell lysates from two control (V1 and V2) and five CCDC11-knockout candidate clones (g1-1, g1-4, g1-8, g2-2, and g2-9) and subjected these samples to western blot analysis using an antibody against CCDC11 (Figure 2). As expected, a single band at the size of about 62 kDa for CCDC11 in control V1 and V2 lanes. Although g1-8 from gRNA-1-transfected cells and g2-2 and g2-9 from gRNA-2-transfected cells retained significant CCDC11 expression, no CCDC11 expression was detected in cells transfected with g1-1 and g1-4. This indicates that the pool of endogenous CCDC11 protein was significantly diminished in the latter cells and that the knockout was successful.

To determine the exact nature of insertion and deletion (indel) mutations in the CCDC11 gene, we purified genomic DNA from V1, g1-1, g1-4, and g2-9 cell clones and amplified by PCR a 403-bp CCDC11 genomic region encompassing the gRNA sequences (Figure 3A). We then subcloned the PCR products into pGEM-T Easy TA vector, followed by restriction digest to verify the presence of an insert (Figure 3B). Subsequently, we sequenced multiple plasmids that carry inserts of the correct size (Figure 3C). The CCDC11 gene is located on chromosome 18, and HEK293T cells contain three copies of the CCDC11 gene (<http://hek293genome.org/v2/>). Consistent with the lack of the endogenous protein by western blotting (Figure 2), the g1-1 cell line harbored three different

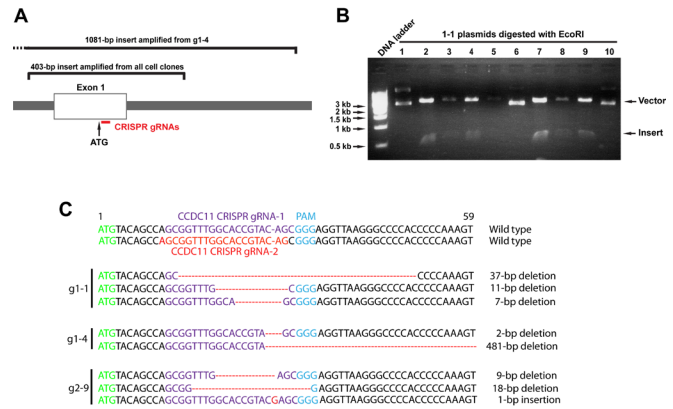


Figure 3. CRISPR/Cas9-mediated knockout of the CCDC11 gene in HEK293T cells. A) Location of two CCDC11 gRNAs and DNA fragments that were amplified by PCR for sequencing analysis. The start codon ATG and exon 1 of the CCDC11 gene are indicated. B) Example of agarose gel electrophoresis for restriction enzyme digests of plasmid DNAs. PCR-amplified 403-bp fragments from the genomic DNA of the CCDC11-knockout cell line g1-1 were subcloned into pGEM-T Easy TA vector, and, after minipreps, plasmid DNAs were digested with EcoRI to verify the presence of insert DNAs at the correct size. C) Sequencing analysis and alignment of the CCDC11 gRNA targeting region from 1-1, 1-4, and 2-9 CCDC11-knockout candidate clones.

frameshift mutations, causing truncations in the N-terminal region. In contrast, we initially found only a 2-bp deletion in g1-4 cell clone, even though this clone showed no CCDC11 expression. We reasoned that g1-4 cells might contain a deletion or insertion larger than the 403-bp CCDC11 genomic region that we analyzed. We therefore attempted to sequence a longer PCR product (1081 bp) and found a 481-bp deletion (Figure 3C). It is largely possible that a third mutation could be an even larger deletion or insertion. As expected from the presence of the endogenous protein (Figure 2), the g2-9 cell line contained two in-frame deletions in addition to one frameshift deletion. Based on these results, we selected g1-1 and g1-4 for further studies below.

To further confirm that g1-1 and g1-4 CCDC11-knockout cells lacked the endogenous protein, we performed immunofluorescence staining. In control V1 cells, CCDC11 localized to acetylated α -tubulin (A-tub)-marked centrioles (arrows), whereas CCDC11 was undetectable at centrioles in g1-1 and g1-4 cells (Figure 4A). In control V1 cells undergoing cytokinesis, clear CCDC11 fluorescence signals were detected at the midbody between the A-tub-positive microtubule bundles, while CCDC11 signals were missing in CCDC11-knockout cells (Figure 4B). In agreement with its critical role in cytokinesis (10), CCDC11-knockout HEK293T cells exhibited a moderate growth defect with the appearance of some multinucleated cells (data not shown). These data demonstrate that these CCDC11-knockout cells are indeed devoid of the endogenous protein.

CCDC11 has been reported to function in ciliogenesis, and knockdown of CCDC11 using siRNA in cultured cells or

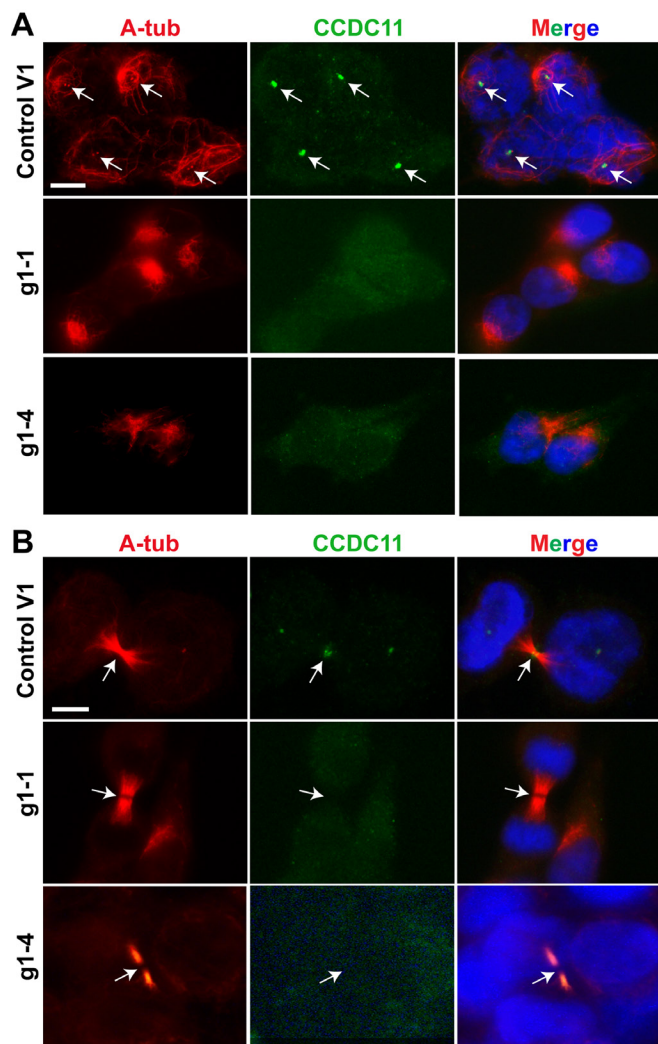


Figure 4. Validation of CCDC11 knockout using immunofluorescence staining. A) Lack of CCDC11 protein at centrioles in g1-1 and g1-4 CCDC11-knockout cells. V1 control and CCDC11-knockout HEK293T cells were immunostained for CCDC11 and the centriolar marker A-tub. Nuclei were detected by DAPI. Arrows point to centrioles. Scale bar, 10 μ m. B) Lack of CCDC11 protein at the midbody in CCDC11-knockout cells undergoing cytokinesis. V1 control and CCDC11-knockout cells were immunostained for CCDC11 and A-tub that marks midbody microtubules. Nuclei were visualized by DAPI. Arrows denote the midbody. Scale bar, 10 μ m.

morpholino oligos in zebrafish embryos results in a significant reduction in the number of cilia (2). A significant decrease in ciliary numbers was also observed in skin fibroblasts from a CCDC11 mutant patient with *situs inversus totalis* (5). To investigate whether a complete loss of CCDC11 is associated with defective ciliogenesis in HEK293T cells, we cultured control V1 and g1-1 and g1-4 CCDC11-knockout cell lines to confluence and serum-starved for 24 hours to induce ciliogenesis. We then performed immunofluorescence staining for CCDC11 and the ciliary marker A-tub. Many control V1 cells possessed fully elongated cilia (arrows), and CCDC11 was clearly detectable at the base of each cilium

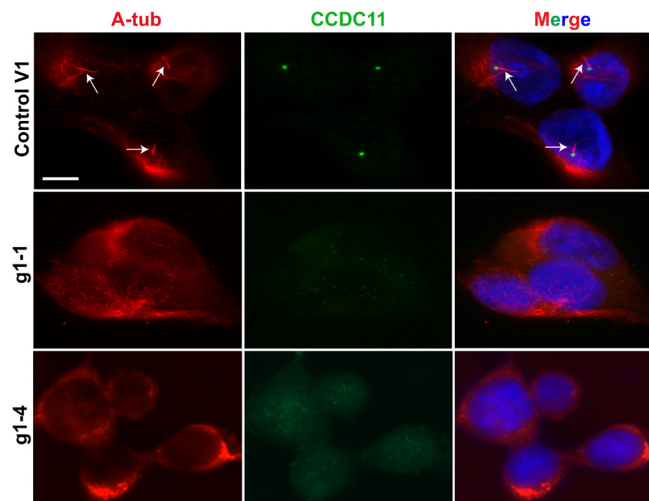


Figure 5. Loss of cilia in CCDC11-knockout HEK293T cells. A) V1 control and g1-1 and g1-4 CCDC11-knockout cells were immunostained for CCDC11 and the ciliary marker A-tub. Arrows indicate elongated cilia. Nuclei were visualized by DAPI. Scale bar, 10 μ m.

(Figure 5). However, neither cilia nor CCDC11 were observed in g1-1 or g1-4 CCDC11-knockout cells. Taken together, these data confirm that the CCDC11-knockout cells lack endogenous CCDC11 and further support the important role of CCDC11 in ciliogenesis.

CCDC11 is required for efficient HIV particle production

Having established CCDC11-knockout cell lines, we asked if loss of CCDC11 influences the production of HIV-1 particles. Transfection of the WT pNL4-3- Δ Env plasmid into control V1 cells increased p24 antigen levels in the culture media 11.0-fold compared to untransfected V1 background levels (Figure 6A). Expression of the P7L-pNL4-3- Δ Env plasmid again resulted in lower p24 levels in the media. Significantly, transfection of the WT plasmid into g1-1 and g1-4 CCDC11-knockout cells yielded low p24 antigen levels near the background level (g1-1, 9.2-fold decrease, $p < 0.0001$; g1-4, 13.8-fold decrease, $p < 0.0001$ compared to the V1 control). Consistent with expression of endogenous CCDC11 protein, g2-9 cells transfected with the WT plasmid produced a p24 level comparable to that of control V1 cells transfected with the WT plasmid. These findings supported our hypothesis that CCDC11 is required for the efficient production of HIV-1 particles.

Next, we performed a rescue experiment by re-introducing CCDC11 into the CCDC11-knockout cells. Transient transfection of a CCDC11 expression plasmid into g1-1 and g1-4 CCDC11-knockout cells effectively increased p24 antigen levels in the culture media in a dose-dependent manner (g1-1, 11.1-fold increase from 0 to 2 μ g of the CCDC11 plasmid, $p < 0.0001$; g1-4, 12.0-fold increase, $p < 0.0001$) (Figure 6B). Taken together, these results demonstrate

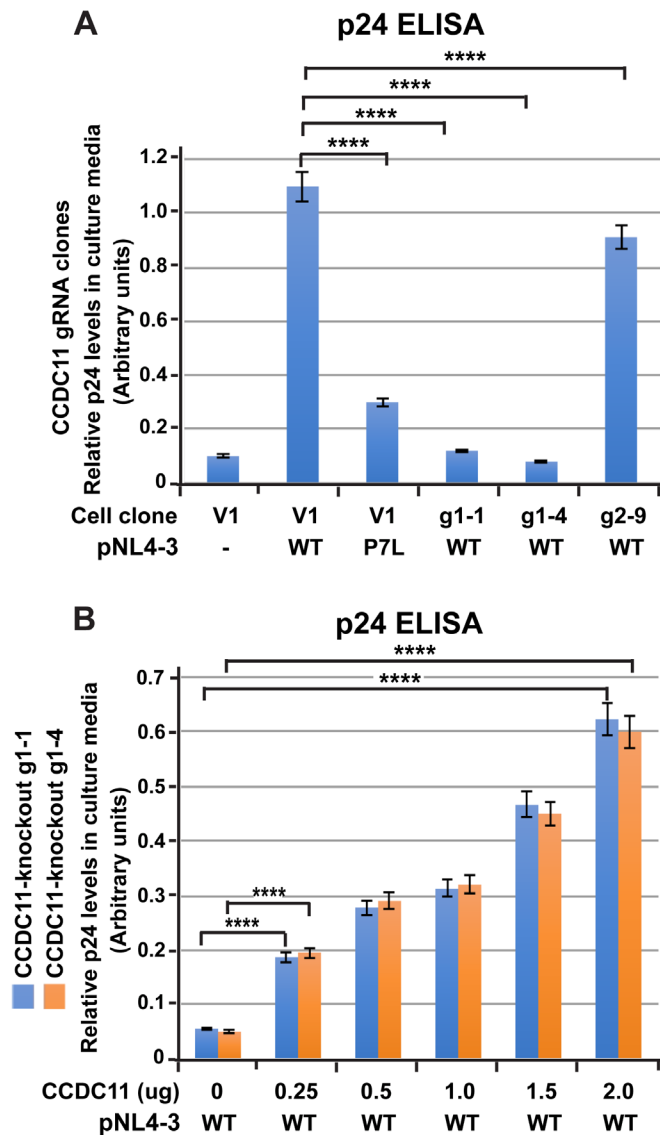


Figure 6. CCDC11 plays an important role in the generation of HIV-1 particles. A) CCDC11-knockout cells exhibit a significant reduction in HIV-1 production. Control (V1 and g2-9) and CCDC11-knockout (g1-1 and g1-4) HEK293T clones were transfected in triplicate with 1 μ g of a HIV-1 pNL4-3- Δ Env plasmid bearing WT- or P7L-Gag as indicated. (B) Re-introduction of CCDC11 rescues the efficient production of HIV-1 particles in CCDC11-knockout cells. g1-1 and g1-4 CCDC11-knockout HEK293T clones were transfected with 1 μ g of HIV-1 pNL4-3- Δ Env plasmid bearing WT-Gag with or without increasing amounts of CCDC11 as indicated. Samples were treated as described in Figure 1.

that CCDC11 plays a crucial role in the production of HIV-1 particles, most likely by acting during the viral assembly and/or budding process.

Discussion

During cell division, CCDC11 is required for the efficient midbody recruitment of CHMP2A, a core component of the ESCRT-III membrane scission complex, at the terminal stage

of cytokinesis (10). Since ESCRT-III has also been shown to function in viral budding (14-17), we hypothesized that CCDC11 also plays a critical role in this process. To examine this possibility, we established CCDC11-knockout HEK293T cells. We chose HEK293T cells since these cells are widely used, show high transfection efficiency, and have the ability to form cilia, albeit at low efficiency. To our knowledge, our study is the first report of CCDC11-knockout mammalian cell culture models. We demonstrated that the CCDC11-knockout cell lines completely lack the endogenous protein when examined by western blotting, immunofluorescence staining, or sequencing analysis. This protein had not been previously linked to HIV-1 replication but, remarkably, appeared to play a crucial role in production of HIV-1 particles in HEK293T cells, as CCDC11-knockout cells failed to produce viral particles. The defect was rescued by ectopic CCDC11 expression, providing direct evidence, for the first time, that the protein is required for productive assembly (Figure 6). Moreover, expression of exogenous CCDC11 robustly augmented HIV-1 particle production (Figure 1). This finding suggested that CCDC11 might be a limiting factor in the viral assembly and/or budding process.

Based on our findings, we proposed the following model for the potential role of CCDC11 in HIV-1 budding: We hypothesized that, in wild-type cells, CCDC11 is initially recruited to sites of viral budding at the plasma membrane (Figure 7). By analogy to its role in cytokinesis, CCDC11 then engages in the recruitment of the ESCRT-III complex, thereby promoting membrane deformation, bud scission and viral release. In contrast, in the absence of CCDC11, the targeting of ESCRT-III is diminished, leading to inefficient viral release.

CCDC11 has been shown to localize to centrioles, centriolar satellites, and cilia, and CCDC11 is required for ciliogenesis in multiple different experimental systems (2,5). However, a conflicting report demonstrated that CCDC11 does not overtly influence ciliary numbers or morphology (4). All of these previous studies employed either gene knockdown approaches or skin fibroblasts from a patient with *situs inversus totalis* harboring a CCDC11 mutation that expresses a truncated protein (amino acids 1-349) (2,4-5). Using our CCDC11-knockout HEK293T cells, which completely lack the protein, we found that CCDC11 was indeed necessary for ciliogenesis (Figure 5). Whether the viral function of CCDC11 is related to its role in ciliogenesis is currently unknown.

What is the underlying molecular mechanism of CCDC11 function in the production of HIV-1 particles? Although several possibilities exist, we favored the idea that CCDC11 facilitates the recruitment of ESCRT-III components to the site of viral budding, possibly via direct protein-protein interactions. At least two candidate interacting partners exist: During virion formation at the plasma membrane, Tsg101 is recruited to the PTAP motif in the HIV-1 Gag p6 protein, where it facilitates recruitment of the ESCRT-III complex (14,26). The ESCRT adaptor protein ALIX, although typically considered auxiliary, could play an important role in egress from cell types that

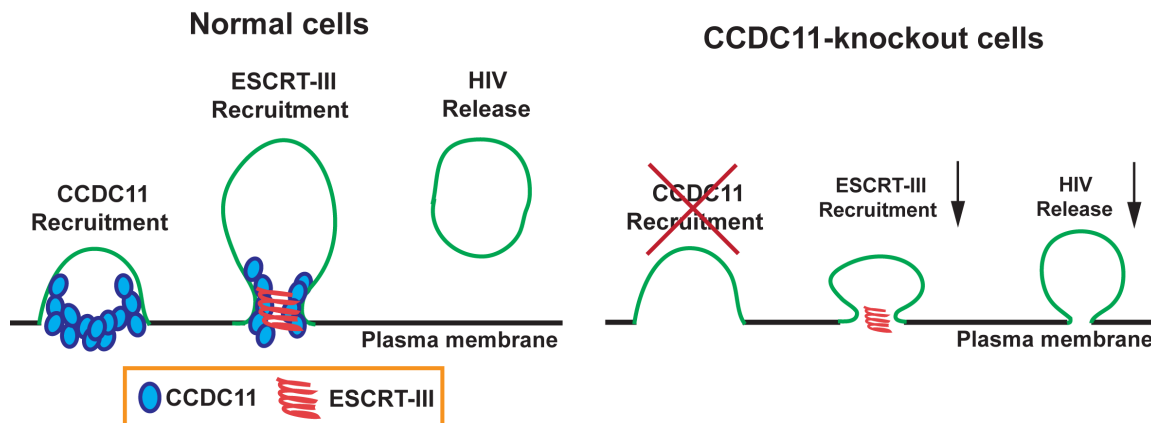


Figure 7. Proposed molecular mechanisms for CCDC11 functions during HIV-1 budding. Left: In wild-type cells, CCDC11 facilitates the recruitment of the ESCRT-III membrane scission complex to the sites of viral budding at the plasma membrane, thereby promoting viral release. Right: In CCDC11-knockout cells, the recruitment of ESCRT-III is diminished, leading to inefficient viral release.

exhibit weak PTAP-dependence (27). ALIX physically binds to the LYPXnL motif of Gag p6, as well as to the nucleocapsid domain in Gag. ALIX then recruits CHMP4B, a component of ESCRT-III, to virus assembly sites (28-29). Since we observed that CCDC11-knockout cells exhibited dramatically reduced viral production (Figure 6A), it is possible that CCDC11 is involved in the Tsg101 pathway or in both Tsg101 and ALIX pathways. At this point, however, we cannot rule out the possibility that CCDC11 regulates other aspects of viral production, for instance, the stability and intracellular trafficking of viral proteins. Future investigations will examine CCDC11 localization and colocalization with ESCRT components at viral budding sites, as well as protein-protein interactions between CCDC11 and various ESCRT components. Future experiments could also test for non-ESCRT interactors through proteomic analysis. Additionally, it would be particularly important to assess if CCDC11 is expressed in T cells or induced upon HIV infection as T lymphocytes are the primary target for HIV.

In summary, we have established the first CCDC11-knockout mammalian cell models. Our results demonstrated that CCDC11 is crucial for ciliogenesis and, notably, HIV-1 production. We envision that CCDC11-knockout cells will be a useful tool for studies of CCDC11 functions in various biological processes such as ciliogenesis, cytokinesis, and viral budding. Interestingly, CCDC11 expression is generally low in the majority of adult human tissues in comparison to the abundant expression of Tsg101 and ALIX (Human Protein Atlas, <http://www.proteinatlas.org>). Possibly, due to its restricted expression, targeted inhibition of CCDC11 function by small molecules may be beneficial as an anti-HIV therapy without major side effects and could be used in conjunction with existing anti-HIV medications.

MATERIALS AND METHODS

Plasmids and bacterial transformation

Expression plasmids for flag-tagged human CCDC11 and for HIV-1 pNL4-3-ΔEnv have been described previously (15). All plasmids were transformed into DH5α *E. coli* competent

cells (New England Biolabs), and a Plasmid Plus Midi Kit (Qiagen) was used to purify the plasmid DNAs.

Cell culture and transfection

Human embryonic kidney (HEK) 293T cells were purchased from American Type Culture Collection (ATCC, CRL-3216) and grown in Dulbecco's Modified Eagle Medium (DMEM) and 10% fetal bovine serum with 100 U/ml penicillin-streptomycin at 37 °C in a 5% CO₂ incubator. Cells were transfected with Lipofectamine 3000 (Thermo Fisher Scientific) according to the manufacturer's instructions.

Generation of CCDC11-knockout HEK293T cells using the CRISPR/Cas9 system

To generate CCDC11-knockout cells using the CRISPR/Cas9 system (24-25), two short guide RNAs (gRNAs) against the 5' region of the human CCDC11 coding sequence (gRNA-1 and -2) were designed using the CRISPR design tool (<http://crispr.mit.edu/>): gRNA-1, 5'-GCGGTTTGGCACCGTACAGC-3'; gRNA-2, 5'-AGCGTTTGGCACCGTACAG-3'. HEK293T cells were transfected with pSpCas9(BB)-2A-Puro (PX459) V2.0 (24) (Addgene plasmid 62988) containing a human CCDC11 gRNA using Lipofectamine 3000. The empty vector was transfected as a negative control. Transfected cells were selected in the presence of puromycin (2.5 ug/ml). Following 1-2 weeks of culture, multiple single colonies were isolated and further grown for experiments.

To determine CCDC11-knockout mutations, genomic DNA was isolated from the cell colonies, and PCR fragments encompassing the gRNA sequence were generated using GoTaq DNA polymerase (Promega) and used for sequencing at the Genomics Core Facility at the Stony Brook University. The primers used to amplify CCDC11 genomic fragments were: 5'-ATGGTGACCAGACCGACTTC-3' and 5'-GGTGAGCGACCTTATCTTCC-3' (403-bp amplicon);, 5'-GACAGAGCGAGACCTGTCT-3' and 5'-GGTGAGCGACCTTATCTTCC-3' (1081-bp amplicon).

Western blotting

WT and CCDC11-knockout HEK293T cells were harvested and lysed in radioimmunoprecipitation assay (RIPA) buffer (20 mM Tris-HCl [pH 7.5], 150 mM NaCl, 1 mM EDTA, 1 mM EGTA, 1% Nonidet P-40 [NP-40], 0.5% sodium deoxycholate, and 0.1% SDS) with protease cocktail inhibitors (Roche) added before use, followed by sonication. The lysates were centrifuged at 13,000 rpm, and supernatant was collected and mixed with 5x SDS sample buffer, followed by denaturing the proteins at 95 °C for 3 minutes. The samples were loaded onto a 10% SDS-polyacrylamide gel and the gel was run for 2 hours at 90 V. Proteins were transferred from the gel onto a nitrocellulose membrane (0.45 µm) (Bio-Rad) with a power supply running for 14 hours at 16 V. The membrane was then washed with Tris-buffered saline with 0.1% Tween 20 (TBST) and blocked in 5% skim milk for 1 hour at room temperature. Rabbit anti-CCDC11 primary antibody (Sigma-Aldrich, HPA040595, 1:500) or mouse anti-GAPDH antibody (Proteintech, 60004-1-Ig, 1:5,000) was added, followed by incubation for 1 hour. The membrane was washed 3 times for 15 minutes each with TBST. Secondary antibodies conjugated with horseradish peroxidase were added and incubated for 1 hour at room temperature. Antibodies were then removed, and the membrane was washed with TBST 3 times for 15 minutes each. SuperSignal™ West Pico Chemiluminescent Substrate (Thermo Fisher Scientific) was used to detect the proteins of interest on X-ray films.

Immunofluorescence staining

HEK293T cells were grown on glass coverslips in a 12-well plate for 24-48 hours. The cells were then washed and fixed with cold 50% methanol/50% acetone. The fixed cells were incubated for 1 hour in 300 µl of blocking buffer containing 5% goat serum in diluent solution (2% bovine serum albumin and 0.2% Triton X-100 in PBS). The blocking buffer was discarded, and the cells were incubated at 4 °C overnight in 300 µl of the diluent solution containing the following primary antibodies: rabbit anti-CCDC11 (Sigma-Aldrich, HPA040595, 1:300) and mouse anti-acetylated α -tubulin (Sigma-Aldrich, T7451, 1:300). Subsequently, the cells were washed and incubated for 1 hour with appropriate anti-rabbit or anti-mouse IgG secondary antibodies conjugated with DyLight 488 and DyLight 549 (Vector Laboratories). The cells were washed, counterstained with 4',6-diamidino-2-phenylindole (DAPI), used as a nuclear counterstain, for two minutes at room temperature, washed again, and mounted onto a glass slide using Fluoromount-G (Southern Biotech) for microscopic analyses.

Quantification of HIV particle release using p24 ELISA

The day before transfection, cells were trypsinized and split in triplicate into 6-well plates with 2 ml DMEM culture media. After 18-24 hours, when cells reached 70-90% confluency, either 3 µg total DNA (**Figures 1 and 6B**) or 2 µg total DNA (**Figure 6A**) were transfected into each well

using Lipofectamine 3000 following the manufacturer's protocol. The total amount of plasmid DNA was adjusted using an empty vector if appropriate. An expression plasmid for Renilla luciferase (pRL-TK) (50 ng/well) was cotransfected to normalize transfection efficiency.

After 30 hours of transfection, culture media were harvested and clarified by centrifugation to remove cellular debris. We utilized the HIV-1 p24 Capture ELISA kit (ImmunoDX, LLC) to measure the levels of Gag p24 in the culture media by reading the optical densities (OD) at a wavelength of 450 nm using a microplate reader. The cells were lysed using 1X passive lysis buffer (Promega) with sonication and used to measure Renilla luciferase activities by the Dual-Luciferase Reporter Assay System (Promega) and a Berthold luminometer (Berthold Technologies). For normalization, the ELISA OD values of Gag p24 were divided by the values of Renilla luciferase activities to account for transfection efficiency.

Acknowledgements

We would like to thank Dr. Susan Watanabe for her help throughout the study and Dr. Ken Takemaru for critically reading the manuscript.

Received: September 23, 2019

Accepted: February 2, 2020

Published: February 24, 2020

REFERENCES

1. Perles, Z., *et al.* "A Human Laterality Disorder Associated with Recessive Ccdc11 Mutation." *J Med Genet*, vol. 49, no. 6, 2012, pp. 386-390, doi:10.1136/jmedgenet-2011-100457.
2. Silva, E., *et al.* "Ccdc11 Is a Novel Centriolar Satellite Protein Essential for Ciliogenesis and Establishment of Left-Right Asymmetry." *Mol Biol Cell*, vol. 27, no. 1, 2016, pp. 48-63, doi:10.1091/mbc.E15-07-0474.
3. Noel, E. S., *et al.* "A Zebrafish Loss-of-Function Model for Human Cfap53 Mutations Reveals Its Specific Role in Laterality Organ Function." *Hum Mutat*, vol. 37, no. 2, 2016, pp. 194-200, doi:10.1002/humu.22928.
4. Narasimhan, V., *et al.* "Mutations in Ccdc11, Which Encodes a Coiled-Coil Containing Ciliary Protein, Causes Situs Inversus Due to Dysmotility of Monocilia in the Left-Right Organizer." *Hum Mutat*, vol. 36, no. 3, 2015, pp. 307-318, doi:10.1002/humu.22738.
5. Gur, M., *et al.* "Roles of the Cilium-Associated Gene Ccdc11 in Left-Right Patterning and in Laterality Disorders in Humans." *Int J Dev Biol*, vol. 61, no. 3-4-5, 2017, pp. 267-276, doi:10.1387/ijdb.160442yc.
6. Nonaka, S., *et al.* "Determination of Left-Right Patterning of the Mouse Embryo by Artificial Nodal Flow." *Nature*, vol. 418, no. 6893, 2002, pp. 96-99, doi:10.1038/nature00849.
7. Goetz, S. C., and K. V. Anderson. "The Primary Cilium: A

- Signalling Centre During Vertebrate Development.” *Nat Rev Genet*, vol. 11, no. 5, 2010, pp. 331-344, doi:10.1038/nrg2774.
8. Nigg, E. A., and J. W. Raff. “Centrioles, Centrosomes, and Cilia in Health and Disease.” *Cell*, vol. 139, no. 4, 2009, pp. 663-678, doi:10.1016/j.cell.2009.10.036.
9. Hildebrandt, F., T. Benzing, and N. Katsanis. “Ciliopathies.” *N Engl J Med*, vol. 364, no. 16, 2011, pp. 1533-1543, doi:10.1056/NEJMra1010172.
10. Ahmed, A., et al. “The Cilium- and Centrosome-Associated Protein Ccdc11 Is Required for Cytokinesis Via Midbody Recruitment of the Escrt-iii Membrane Scission Complex Subunit Chmp2a.” *J Emerging Investigators*, 2018.
11. Mierzwa, B., and D. W. Gerlich. “Cytokinetic Abscission: Molecular Mechanisms and Temporal Control.” *Dev Cell*, vol. 31, no. 5, 2014, pp. 525-538, doi:10.1016/j.devcel.2014.11.006.
12. Nahse, V., et al. “The Abscission Checkpoint: Making It to the Final Cut.” *Trends Cell Biol*, vol. 27, no. 1, 2017, pp. 1-11, doi:10.1016/j.tcb.2016.10.001.
13. Olmos, Y., and J. G. Carlton. “The Escrt Machinery: New Roles at New Holes.” *Curr Opin Cell Biol*, vol. 38, 2016, pp. 1-11, doi:10.1016/j.ceb.2015.12.001.
14. Hurley, J. H., and A. K. Cada. “Inside Job: How the Escrts Release Hiv-1 from Infected Cells.” *Biochem Soc Trans*, vol. 46, no. 5, 2018, pp. 1029-1036, doi:10.1042/BST20180019.
15. Strickland, M., et al. “Tsg101 Chaperone Function Revealed by Hiv-1 Assembly Inhibitors.” *Nat Commun*, vol. 8, no. 1, 2017, p. 1391, doi:10.1038/s41467-017-01426-2.
16. Usami, Y., et al. “The Escrt Pathway and Hiv-1 Budding.” *Biochem Soc Trans*, vol. 37, no. Pt 1, 2009, pp. 181-184, doi:10.1042/BST0370181.
17. Martin-Serrano, J., and S. J. Neil. “Host Factors Involved in Retroviral Budding and Release.” *Nat Rev Microbiol*, vol. 9, no. 7, 2011, pp. 519-531, doi:10.1038/nrmicro2596.
18. Henne, W. M., N. J. Buchkovich, and S. D. Emr. “The Escrt Pathway.” *Dev Cell*, vol. 21, no. 1, 2011, pp. 77-91, doi:10.1016/j.devcel.2011.05.015.
19. Christ, L., et al. “Cellular Functions and Molecular Mechanisms of the Escrt Membrane-Scission Machinery.” *Trends Biochem Sci*, vol. 42, no. 1, 2017, pp. 42-56, doi:10.1016/j.tibs.2016.08.016.
20. Alfred, V., and T. Vaccari. “When Membranes Need an Escrt: Endosomal Sorting and Membrane Remodelling in Health and Disease.” *Swiss Med Wkly*, vol. 146, 2016, p. w14347, doi:10.4414/smw.2016.14347.
21. Stephen, L. A., et al. “The Ciliary Machinery Is Repurposed for T Cell Immune Synapse Trafficking of Lck.” *Dev Cell*, vol. 47, no. 1, 2018, pp. 122-132 e124, doi:10.1016/j.devcel.2018.08.012.
22. Cassioli, C., and C. T. Baldari. “A Ciliary View of the Immunological Synapse.” *Cells*, vol. 8, no. 8, 2019, doi:10.3390/cells8080789.
23. Medina, G., et al. “Tsg101 Can Replace Nedd4 Function in Asv Gag Release but Not Membrane Targeting.” *Virology*, vol. 377, no. 1, 2008, pp. 30-38, doi:10.1016/j.virol.2008.04.024.
24. Ran, F. A., et al. “Genome Engineering Using the Crispr-Cas9 System.” *Nat Protoc*, vol. 8, no. 11, 2013, pp. 2281-2308, doi:10.1038/nprot.2013.143.
25. Yan, Q., et al. “Multiplex Crispr/Cas9-Based Genome Engineering Enhanced by Drosha-Mediated Sgrna-Shrna Structure.” *Sci Rep*, vol. 6, 2016, p. 38970, doi:10.1038/srep38970.
26. VerPlank, L., et al. “Tsg101, a Homologue of Ubiquitin-Conjugating (E2) Enzymes, Binds the L Domain in Hiv Type 1 Pr55(Gag).” *Proc Natl Acad Sci U S A*, vol. 98, no. 14, 2001, pp. 7724-7729, doi:10.1073/pnas.131059198.
27. Fujii, K., J. H. Hurley, and E. O. Freed. “Beyond Tsg101: The Role of Alix in ‘Escrting’ Hiv-1.” *Nat Rev Microbiol*, vol. 5, no. 12, 2007, pp. 912-916, doi:10.1038/nrmicro1790.
28. Dussupt, V., et al. “The Nucleocapsid Region of Hiv-1 Gag Cooperates with the Ptap and Lypxnl Late Domains to Recruit the Cellular Machinery Necessary for Viral Budding.” *PLoS Pathog*, vol. 5, no. 3, 2009, p. e1000339, doi:10.1371/journal.ppat.1000339.
29. Popov, S., et al. “Divergent Bro1 Domains Share the Capacity to Bind Human Immunodeficiency Virus Type 1 Nucleocapsid and to Enhance Virus-Like Particle Production.” *J Virol*, vol. 83, no. 14, 2009, pp. 7185-7193, doi:10.1128/JVI.00198-09.

Copyright: © 2020 Takemaru et al. All JEI articles are distributed under the attribution non-commercial, no derivative license (<http://creativecommons.org/licenses/by-nc-nd/3.0/>). This means that anyone is free to share, copy and distribute an unaltered article for non-commercial purposes provided the original author and source is credited.

Herbal extracts alter amyloid beta levels in SH-SY5Y neuroblastoma cells

Angelina Xu, Margaret Veza Mitchell

Ridge High School, Basking Ridge, New Jersey

SUMMARY

Alzheimer's disease (AD) is a type of dementia that affects more than 5.5 million Americans. It is characterized by progressive memory loss and impairment of other cognitive abilities that affect daily life. Unfortunately, there are no approved treatments that can delay the advancement of the disease. However, it is known that factors such as amyloid beta ($A\beta$) plaques and tau neurofibrillary tangles disrupt connections between neurons, leading to the eventual death of neurons that are responsible for memory. For this investigation, we focused on the neurotoxic $A\beta_{1-40}$ peptide, which is formed by the amyloidogenic cleavage and processing of amyloid precursor protein (APP), a crucial component in the development of AD. Neuroinflammatory cytokines have also been shown to reduce the efflux transport of $A\beta$ from the brain, leading to increased $A\beta$ concentrations. The objective of the experiment was to test the effects of various herbal extracts (bugleweed, hops, saffras, and white camphor) on $A\beta_{1-40}$ peptide levels in human neuroblastoma cells that were transfected to overexpress APP. Due to the herbal extracts' common anti-inflammatory property, the experiment determined whether or not this property had the potential to change $A\beta_{1-40}$ concentrations. Prior to the quantification of $A\beta_{1-40}$ peptide with an enzyme-linked immunosorbent assay (ELISA), we determined the cytotoxicity of the extracts using an MTT, 3-(4,5-dimethylthiazol-2-yl)-2,5-diphenyltetrazolium bromide, assay to discern whether decreases in $A\beta_{1-40}$ concentrations were the result of cell death. The results indicated that white camphor was toxic to neuroblastoma cells and resulted in decreased $A\beta_{1-40}$ levels; saffras was not toxic and resulted in slightly elevated $A\beta_{1-40}$ levels; hops was not toxic and resulted in increased $A\beta_{1-40}$ levels; and bugleweed was not toxic, yet resulted in decreased $A\beta_{1-40}$ levels. Thus, only bugleweed may have the potential to reduce $A\beta_{1-40}$ levels through its anti-inflammatory properties.

INTRODUCTION

Characterized by gradual memory loss and impairment of cognitive abilities, Alzheimer's disease (AD) is a type of dementia that affects more than 5.5 million Americans and

interferes with their daily lives [1-2]. Although there are no approved treatments for AD, it is known that amyloid-beta ($A\beta$) plaques and tau neurofibrillary tangles disrupt connections between neurons, leading to the neuronal loss that is responsible for memory [2-3].

This investigation focused on the neurotoxic $A\beta_{1-40}$ peptide, which accumulates between neurons in the hippocampus and forms amyloid plaques, one of the hallmarks of AD [3]. The sequential processing of amyloid precursor protein (APP) through the amyloidogenic pathway is significant in the production of cytotoxic $A\beta$ [4]. APP is a transmembrane protein that is processed in two distinct pathways: non-amyloidogenic and amyloidogenic (Figure 1). In the non-amyloidogenic pathway, APP is cleaved by α -secretase and γ -secretase. In contrast, in the amyloidogenic pathway, APP is cleaved by β -secretase and γ -secretase, releasing an $A\beta$ peptide. Due to its inclination to aggregate, $A\beta$ forms oligomers that are cytotoxic, disrupting cell function and leading to cell death [5]. Hence, inhibiting enzymes involved in amyloidogenic APP processing and promoting degradation of amyloid plaques are crucial goals among researchers looking to find treatments for AD [4]. For example, many clinical trials study inhibition of β -site amyloid precursor protein cleaving enzyme 1 (BACE1), which is a β -secretase enzyme that is thought to

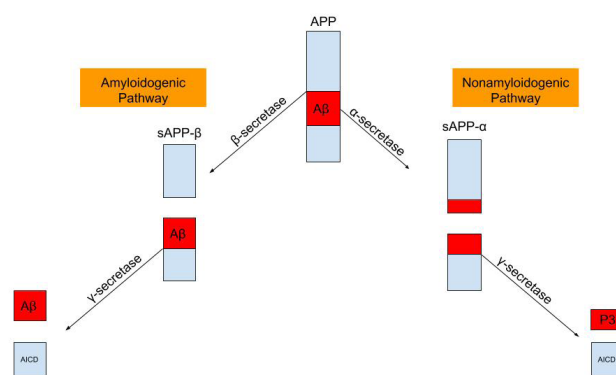


Figure 1. Amyloid precursor protein (APP) is a transmembrane protein that is processed in two distinct pathways: non-amyloidogenic (right) and amyloidogenic (left). In the non-amyloidogenic pathway, APP is sequentially cleaved by α -secretase and γ -secretase to form sAPP- α , $A\beta_{1-40/42}$ (P3) peptide, and APP intracellular domain (AICD) peptides. In contrast, in the amyloidogenic pathway, APP is cleaved by β -secretase and γ -secretase, creating sAPP- β , $A\beta$, and AICD peptides. This releases the cytotoxic $A\beta$ peptide that aggregates to form amyloid plaques, one of the major characteristics of Alzheimer's disease.

play a crucial role in the beginning stages of AD [6]. In theory, inhibition of this enzyme should prevent amyloidogenic APP processing and reduce A β plaque formation, but these clinical trials have met various challenges over the past years. In a study done in mice, BACE1 inhibition interfered with adult neurogenesis regulation in the hippocampus [7]. Despite reducing A β plaque formation, BACE1 inhibitors also caused side effects during chronic administration, including seizures, neurodegeneration, and hypomyelination [6]. Thus, more research into the appropriate level of BACE1 inhibitor needed for treatment and the stage of AD at which the inhibitor should be administered will be needed to attain optimal efficacy.

In our investigation, we wanted to screen the effects of various herbal extracts on A β_{1-40} peptide concentrations. Previous studies have shown that some herbs or herbal formulations can offer cognitive benefits in treating AD. For instance, there is evidence that ginseng's main active ingredient, panaxsaponin, can enhance psychomotor and cognitive performance in those with AD [8]. Another Japanese-Chinese traditional medicine, Kihito, has been shown in mice to ameliorate A β -induced impairments in memory and object recognition [9]. The extracts we used (bugleweed, hops, sassafras, and white camphor) were selected by virtue of availability, on the condition that they possessed anti-inflammatory properties. Past studies have shown that neuroinflammatory cytokines reduced the efflux transport of A β from the brain, resulting in increased A β concentrations [10]. Thus, compounds that reduce inflammation may, in theory, reduce A β levels. An immortalized line of human neuroblastoma cells (SH-SY5Y) was chosen for this experiment because they divide rapidly and give rise to neurons, which AD primarily affects. Cells were transfected to overexpress APP prior to the extract treatments so that measurable amounts of A β_{1-40} peptide would be present during the experiment. After treating our cells with the various herbal extracts, we measured changes in extracellular A β_{1-40} peptide concentrations. To ensure that decreases in A β_{1-40} concentration were not due to cell toxicity, we also used an MTT, 3-(4,5-dimethylthiazol-2-yl)-2,5-diphenyltetrazolium bromide, assay to measure the viability of the cells, because MTT can readily penetrate viable eukaryotic cells in comparison with compounds used in other cytotoxicity assays [11]. All the herbal extracts used in our study have anti-inflammatory properties, which are known to decrease A β_{1-40} peptide levels. Thus, we predicted that all treatment groups would have decreased A β_{1-40} levels, with the possible exception of white camphor, because even small doses of this extract are known to be highly cytotoxic [12].

RESULTS

We chose SH-SY5Y cells for this investigation because they are part of an immortalized cell line that can divide indefinitely and are often used as an *in vitro* model to study neurodegenerative diseases, as well as neuronal function and differentiation [13]. We engineered these neuroblastoma

cells to overexpress APP (see Methods and Materials). After incubating the cells overnight to allow for sufficient APP production, we exposed them to a 1% herbal extract solution. We retrieved the supernatants from these cell cultures and measured the extracellular A β_{1-40} peptide concentrations by a sandwich ELISA. We could determine the effects of each extract on the extracellular A β_{1-40} peptide concentrations using the ELISA, but a decrease in A β_{1-40} could be a result of an extract's cytotoxicity, destroying cellular metabolism. Thus, we also measured the cell's viability in the overnight treatment using an MTT assay.

Addition of the control solution (1% ethanol) resulted in an extracellular A β_{1-40} peptide concentration of 26.3 fmol/mL (Figure 2). A β_{1-40} levels were largely unaffected by sassafras (concentrations were 30.1 fmol/mL, or 114.45% of the concentration measured for the control). SH-SY5Y cells exposed to bugleweed and white camphor treatments had diminished A β_{1-40} peptide concentrations of 11.1 fmol/mL and 0.1 fmol/mL, or 42.21% and 0.38% of the control value, respectively. On the other hand, the hops extract drastically increased A β_{1-40} concentrations to 95.4 fmol/mL, 362.74% of the control value.

We set the MTT assay cell survival cutoff value to 50% of the control value; previous studies have also used this cutoff to define certain compounds as irritants that would prevent accurate data collection of A β_{1-40} peptide concentrations [14]. The cell viability rates of bugleweed, hops, sassafras, and white camphor were, respectively, 98.99%, 81.94%, 70.18%, and 11.48% of the control value. Therefore, only the white camphor treatment caused the cell survival rate to fall below the 50% cutoff (Figure 3).

Taken together, the results demonstrate that bugleweed had the greatest effect of lowering A β_{1-40} peptide levels, because while cell survival rates remained relatively similar

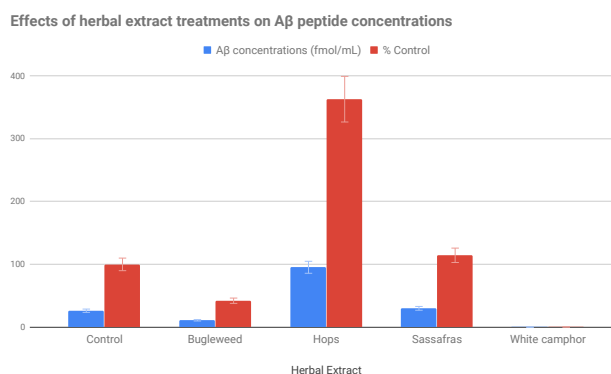


Figure 2. Comparing the effects of the various treatments on the A β_{1-40} peptide concentrations in fmol/mL and as a percent of control. The averages of the triplicate A β_{1-40} peptide concentrations in the control, bugleweed, hops, sassafras, and white camphor treatments were 26.3 fmol/mL, 11.1 fmol/mL, 95.4 fmol/mL, 30.1 fmol/mL, and 0.1 fmol/mL, respectively. As percentages of the control value, these levels were 42.21%, 362.74%, 114.45%, and 0.38%, respectively. The error bars represent 10% deviations from the measured results.

Effects of herbal extract treatments on cell viability

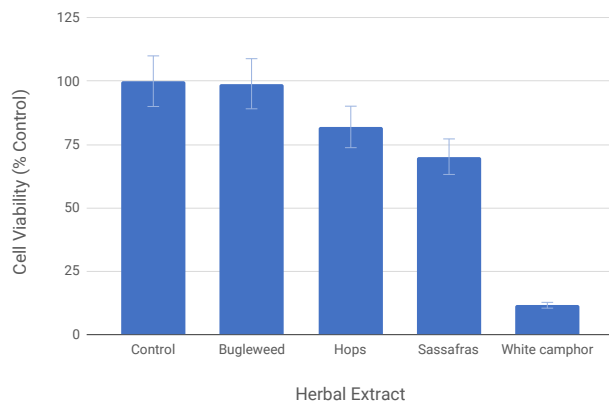


Figure 3. Comparing the effects of the various treatments on cell viability as a percent of control. The average survival rates of the triplicate bugleweed, hops, sassafras, and white camphor treatments were 98.99%, 81.94%, 70.18%, and 11.48%, respectively. The cutoff mark for cell toxicity was 50% cell survival, so only the white camphor extract was deemed toxic to the cells. The error bars represent 10% deviations from the measured results.

to those of the control (98.99%), bugleweed treatment caused $A\beta_{1-40}$ levels to decrease by 42.21%. Similarly, white camphor treatment caused $A\beta_{1-40}$ peptide levels to decrease by 0.38% (a 41.83% drop from the bugleweed treatment), but the cytotoxicity assay suggested that the decreased $A\beta_{1-40}$ peptide levels were due to cell toxicity, rather than a true effect on $A\beta$ peptide processing or degradation. White camphor's cytotoxicity limited our ability to assess the compound's effects on $A\beta$ processing or degradation due to inflammation. On the other hand, hops drastically increased $A\beta_{1-40}$ levels despite cell survival rates that decreased by 18.06% in comparison to the control. In fact, hops-treated cells showed a 322.51% increase in survival in comparison to bugleweed treatment. Furthermore, sassafras did not induce significant cell death, and $A\beta_{1-40}$ levels increased by 14.45% in comparison to control levels (a 72.24% increase compared to bugleweed treatment). While none of the effects observed in this experiment reached statistical significance, the dramatically different effects induced by each herbal compound tested was nevertheless striking. However, bugleweed's ability to greatly reduce $A\beta_{1-40}$ levels may be attributed to its anti-inflammatory property.

DISCUSSION

Excessive accumulation of $A\beta$ peptides leads to the characteristic amyloid plaques of AD. Thus, finding potential drug targets that lower these concentrations has been a major goal of various clinical trials. Although we observed changes in $A\beta_{1-40}$ peptide levels across different experimental groups, a mechanistic explanation for these effects is outside the scope of this study. Decreases may have been due to inhibition of secretases that cleave APP and release $A\beta$. We could test this hypothesis in the future by using a western blot

to compare the amounts of each protein fragment produced after the cleavage of APP with β -secretase and γ -secretase. Similarly, an increase in $A\beta_{1-40}$ levels could have resulted from over-stimulation of these secretases. Other ways these extracts could have decreased $A\beta_{1-40}$ levels are by degrading the peptide faster than normal or modulating the production of APP through mechanisms not explored in this experiment. Moreover, we measured $A\beta_{1-40}$ levels by the amounts of peptide found in the extracellular media. Future experiments could analyze intracellular peptide concentrations or the peptide aggregates that remain adhered to the cells when the media is removed. Comparing this data to that found in this experiment could offer further insight into the compound's effects and may help to determine whether these extracts also impact plaque formation. For example, increased $A\beta_{1-40}$ concentrations in media could result from the ready dissociation of peptides from the cell membranes, and changes due to extract treatments could represent potential drugs that prevent $A\beta$ peptide formations.

In this investigation, the only viable candidate for reducing amyloid plaques was bugleweed, because it was the sole compound that lowered $A\beta_{1-40}$ peptides levels without causing cell viability to fall lower than the 50% cutoff. Bugleweed is currently used as a thyrostatic, as it can reduce the symptoms of hyperthyroidism by blocking thyroid-stimulating hormone (TSH) production, inhibiting the binding of stimulating antibodies of Graves' disease to thyroid cells, and inhibiting iodine metabolism [15-16]. Several studies also indicate that bugleweed treats malaria, insomnia, and hypoglycemia [16-17]. In AD, microglial cells can become chronically activated to clear $A\beta$ peptides via phagocytosis. As a result, these cells release cytokines that result in inflammation [18]. Currently, any agents that can assuage neuro-inflammation are prime candidates for the treatment of AD. Although bugleweed has not been tested in clinical trials, it could be a potential drug, especially with its uses in treating other inflammatory disorders, including hepatitis, pneumonia, and bone disease [19]. Nonetheless, further *in vivo* experiments and clinical trials will be needed to determine the efficacy of bugleweed in both reducing $A\beta$ concentrations and reducing inflammation. For instance, because this experiment was performed on neuroblastoma cells, the experimental results do not necessarily translate to other cell models, such as neurons and glial cells, that are more directly related to AD. Going forward, experimentation on these cell lines will offer more definitive results on bugleweed's potential uses in AD treatment.

Further, the herbal extract packaging was not sterile or airtight, so the purity of each compound could not be ensured. However, alcohol-based extracts were used to minimize the chances of bacterial and fungal growth, and the precaution was taken to view the extracts under a microscope prior to treatment to ensure that there was no microscopic growth. Regardless, the extracts may still have contained other compounds or contaminants.

The differential growth of the cells in separate wells after overnight incubation may have also affected the $A\beta_{1-40}$ levels measured. The experiment assumed that the number of cells per well was the same, but this is likely not true due to the stochastic nature of cell culture. Higher counts of cells in certain wells would result in higher $A\beta_{1-40}$ production relative to that in other wells. To prevent large deviations in the data, variables, such as the amount of media and the sizes of the wells, were kept constant and each control and treatment group was cultured in triplicate. Additionally, future experiments can test the concentration of another protein, whose concentration is not expected to change. That value can then be normalized as a control for cell number to more accurately calibrate $A\beta_{1-40}$ production.

The MTT reagent used in the cytotoxicity assay is also slightly toxic to cells. To lessen the possible detrimental effects, the cells were only incubated with the reagent for two hours to prevent overexposure that would affect the cell survival.

While the herbal extracts chosen were not known to have properties that would decrease the amount of amyloid plaques, these tests simulate drug screening conducted in research laboratories and pharmaceutical companies. Because there is currently no approved treatment for AD, extensive research is being undertaken in order to discover the basis of neuronal loss that leads to cognitive decline and memory loss. Many clinical trials are focusing on drugs that will prevent the production and aggregation of $A\beta$, such as the inhibition of secretase enzymes that cleave APP. Others focus on removing $A\beta$ plaques post-formation through antibody targeting [20]. Unfortunately, these trials have failed to reduce the load of toxic plaques or improve cognition; however some recent studies with an $A\beta$ -targeted antibody therapy may show promise [21]. These unfavorable results may force researchers to explore new avenues to understand the molecular basis of the disease and find treatments for AD. Nonetheless, more information will be needed to produce appropriate drugs, and drug screenings similar to this experiment would be employed to determine the compounds' efficacy in treating AD.

MATERIALS AND METHODS

Transfection

For SH-SY5Y transfection, NanoJuice reagent (EMD Chemicals) was used according to the manufacturer's suggestions. A transfection enhancer with a DNA ratio of 2:1 was added to the media, and the cells were incubated for 72 hours prior to experimentation.

Cell culture

The SH-SY5Y neuroblastoma cells reached a state of confluency after being incubated at 37°C. In order to lift and seed these cells, the media was removed, and the cells were washed with 5 mL of phosphate buffered saline (PBS). After removing the PBS, 1 mL of trypsin was introduced into the

flask to break down the proteins that allow the cells to adhere to the flask. After incubating the cells with trypsin at 37°C for 5 minutes, 2 mL of media was added to dilute the trypsin solution. Then, the cells were gently pipetted up and down to break up cell clumps. Using a hemocytometer, an average of six cells was calculated per quadrant; after accounting for the trypan blue 1:2 dilution, the concentration of the cells was calculated as 5.75×10^5 cells/mL. The cells were diluted to a 4 mL cell to 11 mL media ratio, and 100 μ L per well of the cell suspension was plated in a 96 well plate to incubate overnight.

Herbal extract dilution

The herbal extracts were bought from Herb Pharm. Because they were alcohol-based to prevent bacterial and fungal growth, 1% dilutions were made to prevent the alcohol from killing the SH-SY5Y cells. After transferring 100 μ L of each compound into individual eppendorf tubes, the extracts were centrifuged to precipitate any debris. Next, the compounds were diluted in a 96 well plate by adding 198 μ L of media to 2 μ L of extract. The same was done for the control by adding 198 μ L of media to 2 μ L of ethanol.

Cell treatment

After overnight incubation of the SH-SY5Y cells, the media was aspirated without disturbing the cells. 100 μ L of the diluted extracts and control were added to the cells in triplicate wells and incubated overnight.

MTT assay

An MTT assay was used to assess cell viability after treatment. Because this assay involves a colorimetric reaction that can measure mitochondrial respiration, it indirectly assesses cellular energy capacity. All the media, which contains extracellular $A\beta_{1-40}$ peptide, was removed with a multichannel pipette and transferred to a blank 96 well plate (to be used in the ELISA). 100 μ L of MTT reagent diluted to a concentration of 0.25 mg/mL was added to each of the wells that contained the remaining cells. The plates were incubated at 37°C for two hours to prevent excessive toxicity. After two hours, the yellow tetrazole found within the MTT reagent was reduced by living cells to purple formazan crystals. Dimethyl sulfoxide (DMSO) was added to solubilize the formazan crystals and form a homogenous solution whose absorbance can be read with a spectrophotometer. Based on the wavelength absorbance, the survival rates of each of the treatments were measured as a percent of control. The cutoff mark for cell toxicity in the experiment was 50% cell survival.

Sandwich enzyme-linked immunosorbent assay (ELISA)

The wells were first coated with human $A\beta_{1-40}$ capture antibody. Human $A\beta_{1-40}$ 33.1.1 was diluted in PBS to 50 μ g/mL, and 100 μ L of the antibody was added to each well in the blank 96 well plate. The plate was then incubated overnight. After overnight incubation of the treated cells with capture

antibody, the capture antibody was discarded and 300 μ L of blocking solution (Block Ace) was added to block nonspecific binding sites. The plate was left at room temperature for 3 hours before blocking solution was discarded and wells were washed two times with 300 μ L of PBS. Afterwards, 80 μ L of electrical conductivity (EC) buffer and 20 μ L of the samples (set aside while performing the MTT assay) were added to each well for a total volume of 100 μ L in each well.

Next, a standard curve using A β ₄₀ (Thermo Fisher) was created using two-fold serial dilutions, the first one containing only EC buffer and the following having the concentrations of 3.125 fmol/mL, 6.25 fmol/mL, 12.5 fmol/mL, 25 fmol/mL, 50 fmol/mL, 100 fmol/mL, 200 fmol/mL, 400 fmol/mL, and 800 fmol/mL. 100 μ L of each standard was added in triplicate to wells that did not contain the samples. This plate was put in the refrigerator overnight to allow the samples and standards to bind to the capture antibody. After removing the samples and standards, the plates were washed two times with 300 μ L of PBS. The C-terminal A β ₄₀ 13.1.1 horseradish peroxidase (HRP) conjugated detection antibody was diluted at a 1 to 2000 ratio in Buffer C (Thermo Fisher). 100 μ L of the detection antibody was added to each well and incubated at room temperature for two hours.

After two hours, the detection antibody was removed by washing the wells two times with 300 μ L of PBS-Tween, and 100 μ L of a combination of TMB (3,3',5,5'-tetramethylbenzidine) substrate and HRP was added to each well. After 15 minutes, blue color changes in the wells were evident and analyzed under a spectrophotometer. Once the 800 fmol/mL standard reached an optical density (OD) of 2.0, 100 μ L of stop solution (sulfuric acid) was added. The solution turned yellow and the plate was read under the spectrophotometer again. This data was recorded, and the A β ₁₋₄₀ peptide levels were calculated as a percent of the control value.

Received: August 11, 2019

Accepted: February 24, 2020

Published: February 25, 2020

REFERENCES

1. National Institute on Aging, U.S. Department of Health and Human Services, "Alzheimer's Disease Fact Sheet." 2019, www.nia.nih.gov/health/alzheimers-disease-fact-sheet.
2. Alzheimer's Association, "What Is Alzheimer's?" *Alzheimer's Disease and Dementia*, 2019, www.alz.org/alzheimers-dementia/what-is-alzheimers.
3. National Institute on Aging, U.S. Department of Health and Human Services, "What Happens to the Brain in Alzheimer's Disease?" 2017, www.nia.nih.gov/health/what-happens-brain-alzheimers-disease.
4. O'Brien RJ, Wong PC. "Amyloid Precursor Protein Processing and Alzheimer's Disease." *Annual Review of Neuroscience* vol. 34, 2011, pp. 185-204. doi:10.1146/annurev-neuro-061010-113613
5. Hicks DA, et al. "Lipid Rafts and Alzheimer's Disease: Protein-Lipid Interactions and Perturbation of Signaling." *Frontiers in Physiology* vol. 3, 2012, pp. 189. doi:10.3389/fphys.2012.00189
6. Vassar R. "BACE1 Inhibitor Drugs in Clinical Trials for Alzheimer's Disease." *Biomedical Central* vol. 6, 2014, pp. 89. doi:10.1186/s13195-014-0089-7
7. European Pharmaceutical Review, "Why Are BACE1 Inhibitors Failing Clinical Trials?" 2018, <https://www.europeanpharmaceuticalreview.com/news/77751/bace-clinical-trials/>
8. Tian J, et al. "Herbal Therapy: a New Pathway for the Treatment of Alzheimer's Disease." *Alzheimer's Research & Therapy* vol. 2, 2010, pp. 30. doi:10.1186/alzrt54
9. Obulesu M, Rao DM. "Effect of Plant Extracts on Alzheimer's Disease: An Insight into Therapeutic Avenues." *Journal of Neurosciences in Rural Practice* vol. 2, 2011, pp. 56. doi:10.4103/0976-3147.80102
10. Alasmari F, et al. "Neuroinflammatory Cytokines Induce Amyloid Beta Neurotoxicity through Modulating Amyloid Precursor Protein Levels/Metabolism." *BioMed Research International* vol. 2018, 2018. doi:10.1155/2018/3087475
11. Riss TL, et al. "Cell Viability Assays." *Assay Guidance Manual*, 2016, <https://www.ncbi.nlm.nih.gov/books/NBK144065/>
12. Gunawardena D, et al. "Anti-Inflammatory Properties of Cinnamon Polyphenols and Their Monomeric Precursors." *Science Direct* vol. 1, 2014, pp.409-425. doi:10.1016/B978-0-12-398456-2.00030-X
13. Kovalevich, Jane, and Dianne Langford. "Considerations for the Use of SH-SY5Y Neuroblastoma Cells in Neurobiology." *Methods in Molecular Biology* vol. 1078, 2013, pp.9-21. doi:10.1007/978-1-62703-640-5_2
14. Tasic-Kostov M, et al. "Objective Skin Performance Evaluation: How Mild Are APGs to the Skin?" *Alkyl Polyglucosides*, 2014, pp. 135-161. doi:10.1533/9781908818775.135
15. "Botanical Medicine for Thyroid Regulation." *Mary Ann Liebert, Inc., Publishers* vol. 2, 2009, pp. 27. doi:10.1089/9780913113462.323
16. Yarnell E, Abascal K. "Botanical Medicine for Thyroid Regulation." *Research Gate* vol. 12, 2006, pp.107-112. doi:10.1089/act.2006.12.107
17. Toiu A, et al. "Phytochemical Composition, Antioxidant, Antimicrobial and in Vivo Anti-Inflammatory Activity of Traditionally Used Romanian Ajuga Laxmannii (Murray) Benth. ('Nobleman's Beard' – Barba Împăratului)." *Frontiers in Pharmacology* vol. 9, 2018, pp. 7. doi:10.3389/fphar.2018.00007
18. Wiart C. "Terpenes." *Lead Compounds from Medicinal Plants for the Treatment of Neurodegenerative Diseases*, 2014, pp. 189-284. doi:10.1016/B978-0-12-398373-2.00002-9
19. Viljoen A, et al. "Anti-Inflammatory Iridoids of Botanical

Origin." *Current Medicinal Chemistry* vol. 19, 2012, pp. 2104-2127. doi:10.2174/092986712800229005

20. Singh SK, *et al.* "Overview of Alzheimer's Disease and Some Therapeutic Approaches Targeting A β by Using Several Synthetic and Herbal Compounds." *Oxidative Medicine and Cellular Longevity* vol. 2016, 2015, pp. 1-22. doi:10.1155/2016/7361613
21. Rosenblum WI. "Why Alzheimer Trials Fail: Removing Soluble Oligomeric Beta Amyloid Is Essential, Inconsistent, and Difficult." *Neurobiology of Aging* vol. 35, 2013, pp.969-974. doi:10.1016/j.neurobiolaging.2013.10.085

Copyright: © 2020 Xu and Mitchell. All JEI articles are distributed under the attribution non-commercial, no derivative license (<http://creativecommons.org/licenses/by-nc-nd/3.0/>). This means that anyone is free to share, copy and distribute an unaltered article for non-commercial purposes provided the original author and source is credited.

Temperatures of 20°C produce increased net primary production in *Chlorella sp.*

Kiran Biddinger*, Emma Bradley*, Julie Seplaki

Milton Academy, Milton, Massachusetts

*Authors contributed equally

SUMMARY

Chlorella sp. are autotrophs that introduce stored energy into biological systems through photosynthesis. Net primary production (NPP) reflects the amount of energy converted to sugar bond energy in photosynthesis minus the amount of energy consumed by cellular respiration. Because carbon dioxide (CO₂) acidifies water, the net CO₂ production leads to a change in pH that reflects the NPP. Establishing a relationship between temperature and NPP could provide insights into maximizing the biological removal of CO₂ from the atmosphere. In this experiment, the effect of temperature on the NPP of *Chlorella sp.* was measured as a function of ΔpH, which was determined using a standard curve of buffers of known pH versus absorbance. The ΔpH increased as the incubation temperatures increased towards 20°C, and then as the temperatures increased after 20°C, the ΔpH decreased, indicating that the NPP of the *Chlorella sp.* was maximized around 20°C. Around 20°C, the enzymes involved in photosynthesis, such as rubisco, may approach their optimal temperatures and thus be maximally efficient. As global warming is caused by excess CO₂ in the atmosphere, *Chlorella* incubated at temperatures around 20°C would be maximally efficient at naturally removing CO₂ through photosynthesis and could provide useful insights for new technologies to fight climate change.

INTRODUCTION

Chlorella sp. are unicellular autotrophs that lives in freshwater, saltwater, and soil (1). *Chlorella sp.* were chosen as a model organism to study photosynthesis due to their relatively easy cultivation. Autotrophic organisms use light energy to drive the synthesis of adenosine triphosphate (ATP) and reduced nicotinamide adenine dinucleotide phosphate (NADPH), which then is used to reduce carbon dioxide (CO₂) to glucose. *Chlorella sp.* anabolically produce glucose through photosynthesis, given by the reaction $\text{Energy} + 6\text{CO}_2 + 6\text{H}_2\text{O} \rightarrow \text{C}_6\text{H}_{12}\text{O}_6 + 6\text{O}_2$, and then catabolically break it down through cellular respiration, given by the reaction $\text{C}_6\text{H}_{12}\text{O}_6 + 6\text{O}_2 \rightarrow 6\text{CO}_2 + 6\text{H}_2\text{O} + \text{ATP}$ (2). The process of photosynthesis is carried out by a series of enzymes; for example, enzymes prompt the transfer of energized electrons to NADP⁺ to form NADPH and attach CO₂ to ribulose biphosphate (RuBP), beginning the process of creating glucose (3). These enzymes are proteins that speed up different photosynthetic reactions by increasing the stress of the bonds of substrates

so that the bonds require less energy to be broken, lowering the activation energy (4). Enzymes have active sites where substrates fit in like puzzle pieces (4). These enzymes create microenvironments, which have unique optimal pH and temperatures in which the reaction is carried out (5). Thus, if the temperature of a *Chlorella sp.* solution is manipulated, the microenvironments of enzymes, such as NADP⁺ reductase and rubisco, will not be the optimal conditions for the enzyme, and thus, the *Chlorella sp.* will not photosynthesize as much. In addition to affecting the functionality of enzymes, increased temperature will also affect the *Chlorella sp.* by manipulating the physics of the solution: according to the kinetic-molecular theory, higher temperatures lead to faster movement of molecules and lower gas solubility (6). While these higher temperatures could cause more intermolecular collisions, they could also remove gas reactants for biochemical reactions, as higher temperatures decrease the solubilities of gases (7). For example, higher temperatures could cause CO₂ particles to come out of solution, leaving less substrate for photosynthesis.

The goal of this experiment was to determine the effect of temperature on net primary production (NPP) of *Chlorella sp.* as a function of ΔpH. Given that *Chlorella sp.* grow best in temperatures of 20-30°C (8), we hypothesized that temperatures similar to this environment, such as 20°C, would also maximally stabilize photosynthetic enzymes and produce the highest observed net primary production. Below or above these temperatures, enzymes will not function optimally, and thus pH will decrease steadily as a result of a decreased photosynthetic rate.

RESULTS

To determine the effect of temperature on NPP of *Chlorella sp.*, we incubated six *Chlorella sp.* balls in cuvettes at temperatures 2°C, 12°C, 20°C, 40°C, and 53°C and, after an 8 hour exposure to light, measured the pH change of the solution as a proxy for NPP (Figure 1). We used liquid cultures of *Chlorella sp.* for all the trials. In our experiment, all the CO₂ that the *Chlorella sp.* took in or expelled occurred in the liquid medium. When CO₂ is placed in water, carbonic acid (H₂CO₃) forms and then partially dissociates into a proton (H⁺) and bicarbonate (HCO₃⁻). Therefore, when cellular respiration is occurring more than photosynthesis, an expected increase in CO₂ will render the solution more acidic (-ΔpH), whereas a decrease in CO₂ as a result of photosynthesis will render the solution more basic (+ΔpH). Therefore, pH of the solution

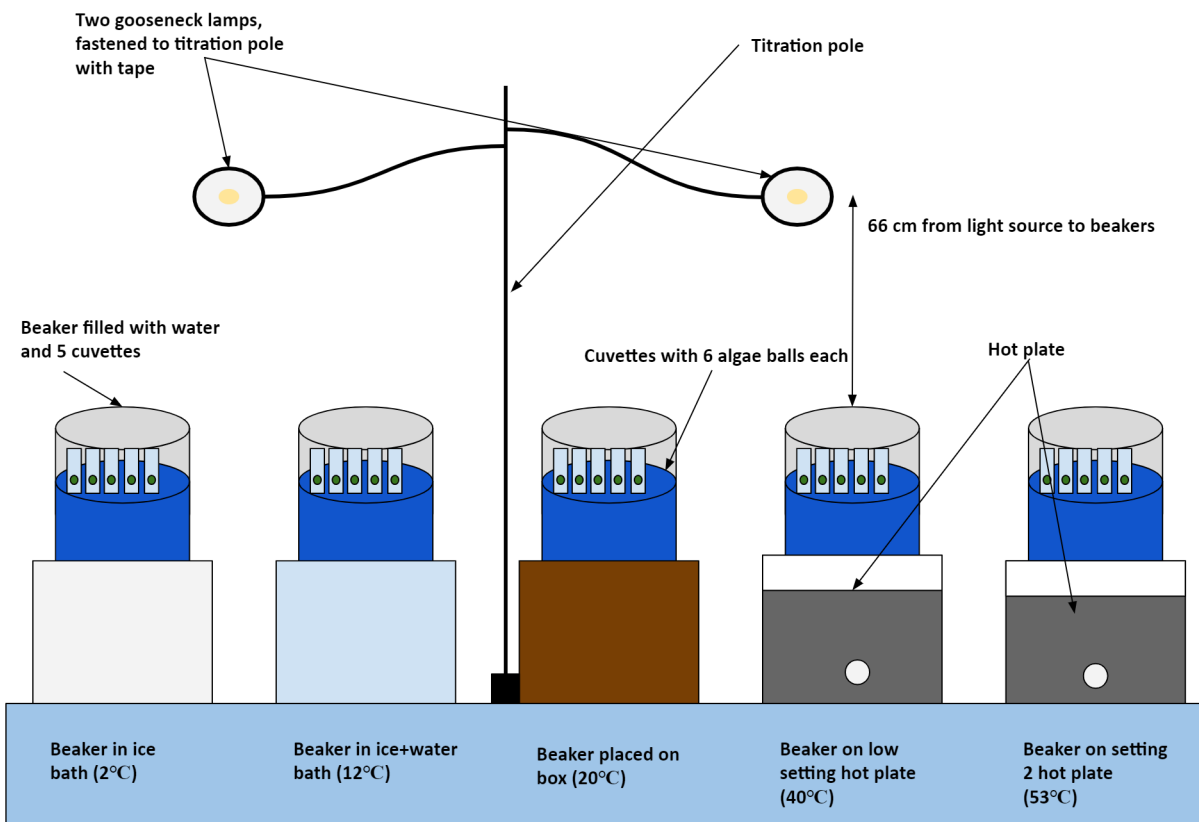


Figure 1: Experimental design setup. Pictured are the five water beakers (2°C, 12°C, 20°C, 40°C, and 53°C), each containing five cuvettes, thermometers used to take temperature readings, the light source, titration pole, ice baths, and hot plates.

would reflect the NPP of the *Chlorella sp.* pH of the cuvette solution was measured using a spectrometer to measure absorbance before and after 8 hours of exposure to a particular temperature. Since we added hydrogen carbonate indicator to the cuvettes and created a standard curve of known pH versus absorbance, the absorbance measures the pH of the solution, with a higher pH indicating that there is less CO₂ and more O₂—a greater NPP.

Room temperature cuvettes were used as a control to allow ΔpH to be more attributable to the changes in temperature rather than the presence of another variable. A blank control group (no *Chlorella sp.* balls) was placed in the grow tower for 8 hours in order to ensure that *Chlorella sp.* balls were producing the changes in color of hydrogen carbonate indicator observed. A t-test showed that pH of blank control after light exposure was not significantly different from pH of black control before light exposure ($p = 0.137$).

The ANOVA test for variance indicated that the experimental groups were significantly different from one another ($p < 0.0001$). A t-test showed that average pH change increased significantly from 0.334 to 0.764 ($p = 0.006$) as temperature increased from 2°C to 20°C, but then decreased significantly from 0.764 to -0.059 ($p = 5.74 \times 10^{-5}$) as temperature increased from 20°C to 53°C (Figure 2). Across the whole dataset, the highest average ΔpH was 0.764 at 20°C, and the lowest average pH change was -0.059 at 53°C.

The standard deviations (SD) for each temperature ranged from 0.01 for 40°C to 0.18 for 20°C. At 40°C and 53°C ΔpH falls to close to zero. Therefore, as the temperature increased towards 20°C, the ΔpH increased, but towards 40°C and 53°C, the ΔpH drastically decreased.

DISCUSSION

The hypothesis that photosynthesis would occur at greater rates in temperatures near *Chlorella sp.* environment, such as temperatures in the 20-30°C range, was supported by the data (Figure 2). A two-tailed t-test showed that the change in pH increased significantly between temperatures of 2°C and 20°C ($p = 0.006$), and then decreased significantly from 20°C to 40°C ($p = 5.72 \times 10^{-5}$). These data indicate that increasing the temperature towards 20°C approached the optimal temperature of the photosynthetic enzymes, such as rubisco. Temperatures around 20°C may have supported the optimal microenvironment for the enzymes involved in photosynthesis because the increased heat stressed the bonds of the substrate in order to require the least amount of energy for the reactions to take place without denaturing the enzyme. For example, the Calvin cycle requires rubisco in order to produce glucose from CO₂, and rubisco is most efficient around 22.5-30°C (9). When the temperature was increased to 40°C, the enzymes may have denatured, causing both the 40°C and 53°C replicates to have essentially no NPP (ΔpH = -0.055 and

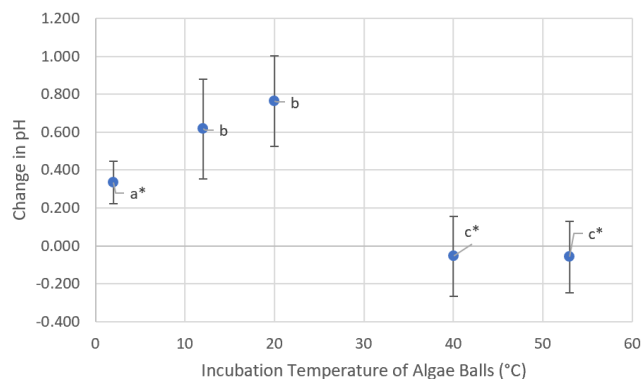


Figure 2: *Chlorella sp.* NPP, measured through change in pH, is optimized at 20°C. *Chlorella sp.* balls were incubated for 8 hours at cell density 3.57×10^5 cells/mm³. Data points indicate the average of 5 independent experiments, and error bars denote standard deviation. Letters denote significant groupings; runs that are not significantly different ($p > 0.05$) are annotated with the same letter. Asterisks indicate a significant difference ($p < 0.05$) from the control (20°C).

-0.059, respectively). Temperatures above 40°C may provide the energy required to break the hydrogen bonds important for the tertiary structure of the algal photosynthetic enzymes, thus denaturing them (10). Moreover, the *Chlorella sp.* likely photorespired at high temperatures (i.e. temperatures beyond 40°C) because they are C3 plants (11). At high temperatures, C3 plants exhibit photorespiration, a process similar to photosynthesis, but where O₂ enters the Calvin cycle instead of CO₂ and CO₂ is produced instead of glucose. Above 40°C, the *Chlorella sp.* may be producing, rather than consuming CO₂, thus producing the negative ΔpH values (Figure 2). However, even the photorespiration enzymes likely began to denature, accounting for the small magnitude of the ΔpH. For example, rubisco activase loses 50% efficiency after a 5-minute exposure to temperatures above 33°C (12). Additionally, because the temperature and movement speed of enzymes involved in reactions increased, there were more collisions between the enzymes and the corresponding substrates. As the temperature increased, a greater proportion of substrate molecules involved in photosynthesis may have had the necessary energy to overcome the activation barrier, collide with substrate molecules, and undergo a reaction, thus speeding up each reaction of photosynthesis and allowing the *Chlorella sp.* to photosynthesize more quickly. However, once the temperature exceeded 20°C, the likely denaturation of the enzymes inhibited this effect. Alternatively, at higher temperatures, gas molecules like CO₂ can break the intermolecular bonds of a solution (13). Thus, as the temperature increased, there could be less CO₂ reactants due to solubility to enter the Calvin cycle and be converted into glucose, causing lowered rates of photosynthesis.

NPP is important because it allows for natural CO₂ removal, which fights off the ever-present threat of climate change. Future projects could attempt to harness the photosynthesizing ability of *Chlorella sp.* and maximize activity in order to naturally remove CO₂ from the atmosphere.

While there are several factors that affect NPP, such as temperature, precipitation, and soil moisture (14), the findings of this experiment suggest that, to maximize *Chlorella sp.* NPP, the *Chlorella sp.* must be incubated at temperatures around 20°C. Additionally, because *Chlorella sp.* introduce glucose to the ecosystem through photosynthesis, these findings could also be used to maximize *Chlorella sp.* glucose production to be used as a food source.

The experiment had several potential pitfalls. First, when the 2.5 mL semi-micro cuvettes were placed into the beakers of heated or cooled water for incubation, the cuvettes tipped slightly. This tipping caused some of the *Chlorella sp.* balls to overlap, which meant that some of the *Chlorella sp.* balls were blocking others. Consequently, some *Chlorella sp.* balls were receiving more light than others and were likely photosynthesizing at a greater rate. Secondly, because the cuvettes float in water, the cuvettes were only partially submerged in the beakers. Thus, some cuvettes had more exposure to the room temperature air than others, causing slight variance in the internal temperatures of the cuvettes. Both of these uncertainties could have been eliminated by taping the cuvettes horizontally to the side of the beakers so that no *Chlorella sp.* balls were overlapping and so that the cuvettes were fully submerged. Thirdly, for the 2°C and 12°C baths, the ice may have begun to melt during the 8-hour incubation period. This would have resulted in the ice baths being colder in the beginning and the reported temperatures being inaccurately high. Though ice was replenished once after 4 hours, this inaccuracy could have been eliminated by replacing the ice baths every hour with new, fresh ones. In the ice baths, the temperature was observed to be constant over an hour during testing.

This study suggests that, in the presence of light, the optimal incubation temperature for maximizing NPP is around 20°C. However, future experiments could investigate the effect of temperatures in the 20°C to 40°C range in order to find the optimal temperature for producing the highest NPP. Though the graph peaks at 20°C, it appears that the peak is slightly shifted left, and slightly higher temperatures may more accurately represent the optimal temperature. Future experiments could also determine if this high ratio of photosynthesis to cellular respiration was due to an increase in photosynthesis or to a decrease in cellular respiration. This question could be answered by isolating the effects of temperature on cellular respiration by blocking photosynthesis by incubating the *Chlorella sp.* without light. Therefore, the same experiment would be performed, but with no light supplied to the *Chlorella sp.* balls as to prevent them from increasing the pH through photosynthesis.

In summary, as the incubation temperature nears 20°C, the ΔpH of a *Chlorella sp.* ball solution reaches its peak, suggesting that 20°C nears the optimal temperature for *Chlorella sp.* ball photosynthesis and that decreasing or increasing this temperature decreases the *Chlorella sp.*'s ratio of photosynthesis to cellular respiration.

METHODS

Creating the *Chlorella sp.* Balls

Chlorella sp. balls were created by mixing 5 mL bulked *Chlorella sp.* (Carolina Biological) with 5 mL 2% sodium alginate (Carolina Biological) in a graduated cylinder. Algae was bulked by allowing *Chlorella sp.* to separate in a beaker such that the densest algae were on the bottom. These dense *Chlorella sp.* were extracted using a pipette and used for the algae balls. Cell density was controlled by making *Chlorella sp.* balls from the same batch of bulked *Chlorella sp.*; cell density was standardized using a hemocytometer, with a density of 3.6×10^5 cells/mm³. A greater cell density would again allow for more cells to absorb photons and thus yielding a higher chance that CO₂ would be used up. This solution was then transferred to a 10 mL syringe, which was dripped into a beaker with 50 mL 2% CaCl₂ (Flinn Scientific). CaCl₂ was used to harden the outside of the algae into a ball formation. After all of the solution had dripped into the CaCl₂, the resulting solution was left for 5 minutes and then placed into a strainer to be rinsed thoroughly with distilled H₂O. *Chlorella sp.* balls were then placed into a beaker of 50 mL distilled water, covered with tin foil, and left in a lighted growth tower for storage.

Initial pH Measurement

25 glass cuvettes were prepared with 1 mL distilled water, 1 mL hydrogen carbonate indicator, and 6 *Chlorella sp.* balls each in order to test 5 temperatures, each with 5 replicates. The number of *Chlorella sp.* balls was also controlled by placing six equally sized *Chlorella sp.* balls into each cuvette. It was important to control for the number of *Chlorella sp.* balls because more *Chlorella sp.* balls would result in more photosystems to harness the energy of photons and thus a greater ability to use up CO₂, increasing the pH of the cuvette. A Vernier spectrophotometer was calibrated using a blank cuvette containing 1 mL of distilled water and 1 mL of hydrogen carbonate indicator. Once a cuvette was prepared, it was immediately placed under a sheet of tinfoil so as to not expose one cuvette to more light than the other. Each cuvette was then removed, one at a time, and the initial absorbance at 550.1 nm was taken using a spectrophotometer before placing it back under the tinfoil.

Set-up of temperature-controlled water and ice baths

Two hot plates were used to heat beakers of water to 40°C and 53°C, settings that preliminary testing revealed were the maximum settings before water in the cuvettes would begin to evaporate. Five beakers, each containing 300 mL of water, were filled and thermometers were placed inside. Two ice baths were then drawn, one containing 4000 grams ice (2°C) and the other containing 2000 grams ice and 2000 mL water (12°C). One 300 mL beaker was placed in the 4000 gram ice bucket (2°C), one was placed in the 2000 grams ice and 2000 mL water bucket (12°C), one was kept at room temperature (20°C), one was placed on the low-setting hotplate (40°C),

and one was placed on the high-setting hotplate (53°C). The ice buckets as well as the room temperature beaker were placed on boxes to be at even heights with the beakers on hot plates (**Figure 1**). The beakers were then left for 30 minutes to change temperature, which is the time it took for temperature changes to plateau in preliminary testing.

Chlorella sp. Cultivation

While the beakers were acclimating to the changing temperatures, two flexible gooseneck lamps were clipped and taped onto a titration tower at a height of 66 cm above the 5 beakers (**Figure 1**) to ensure stability and equal access to light. Boxes were used to level beakers with the height of the hot plates. A closer distance would decrease the distance photons had to travel, thus speeding up the rate of reaction. After beakers had been set up for 30 minutes, 5 capped cuvettes were floated in each beaker of distilled H₂O. Once the cuvettes were placed in beakers, a timer was started and was stopped after 8 hours, an interval that preliminary testing had indicated would yield some change in pH. The amount of time that each cuvette was exposed to light was also controlled because a greater exposure to light would mean more time for energy from photons to fuel the anabolic reaction of photosynthesis. Time of exposure was controlled by keeping cuvettes under tinfoil and only removing them to take preliminary absorbance readings. All cuvettes were placed into water beakers at the same time and removed at the same time. Beakers were left for four hours; after four hours, 1000 grams more of ice was added to the two ice baths to ensure consistently low temperatures (i.e. 2°C and 12°C) for four more hours.

Measuring post-incubation pH and calculating Δ pH

After four more hours, the temperature was recorded by reading the thermometer, yielding the temperatures of 2°C, 12°C, 20°C, 40°C, and 53°C. Each cuvette was removed, placed in the previously calibrated spectrophotometer, and the absorbance at 550.1 nm was recorded. A standard pH versus absorbance curve was used to calculate the pH of each cuvette before and after the incubation. This curve was previously determined by placing 1 mL buffer solution of known pH and 1 mL of hydrogen carbonate indicator, which changes color to indicate pH of the solution, inside a cuvette and obtaining the absorbance using a spectrophotometer. The pH was calculated according to the equation, $a = 0.4757 \times p - 3.721$, where p represents pH and a represents absorbance. Single-factor ANOVA was used to determine if the tested temperatures significantly altered the Δ pH of the solution. To further investigate the trends in the data, a t-test was performed between every combination of two temperatures from the five recorded in order to determine whether or not differences in Δ pH were statistically significant from one another.

ACKNOWLEDGEMENTS

The authors would first like to thank Michael Edgar and Joel Moore for their guidance in the writing of our report. The authors would also like to thank the entire Milton Academy Science Department for their assistance in providing the necessary materials and guidance for this experiment.

Received: September 18, 2019

Accepted: December 14, 2019

Published: February 25, 2020

REFERENCES

1. The Editors of Encyclopaedia Britannica. "Chlorella." *Encyclopædia Britannica*, Encyclopædia Britannica, Inc., 19 Jan. 2018, www.britannica.com/science/Chlorella.
2. Harwood, Jessica, *et al.* "Cellular Respiration and Photosynthesis." CK, CK-12 Foundation, 20 Nov. 2019, www.ck12.org/biology/cellular-respiration-and-photosynthesis/lesson/Connecting-Cellular-Respiration-and-Photosynthesis-MS-LS/.
3. Beck, Kevin. "Enzyme Activity in Photosynthesis." *Sciencing*, 23 Apr. 2019, sciencing.com/enzyme-activity-photosynthesis-12161.html.
4. "Enzymes and the Active Site (Article)." *Khan Academy*, Khan Academy, www.khanacademy.org/science/biology/energy-and-enzymes/introduction-to-enzymes/a/enzymes-and-the-active-site.
5. "Enzymes Review (Article) | Enzymes." *Khan Academy*, Khan Academy, www.khanacademy.org/science/high-school-biology/hs-energy-and-transport/hs-enzymes/a/hs-enzymes-review.
6. Key, Jessie A., and David W. Ball. "Kinetic Molecular Theory of Gases." *Introductory Chemistry 1st Canadian Edition*, BCcampus, 16 Sept. 2014, opentextbc.ca/introductorychemistry/chapter/kinetic-molecular-theory-of-gases-2/.
7. "Solubility." *Solubility*, www.chem.fsu.edu/chemlab/chm1046course/solubility.html.
8. Singh, S.p., and Priyanka Singh. "Effect of Temperature and Light on the Growth of Algae Species: A Review." *Renewable and Sustainable Energy Reviews*, vol. 50, 2015, pp. 431–444., doi:10.1016/j.rser.2015.05.024.
9. Feller, Urs, *et al.* Moderately High Temperatures Inhibit Ribulose-1,5-Bisphosphate Carboxylase/Oxygenase (Rubisco). *Whole Plant, Environmental, and Stress Physiology*, Feb. 1998
10. Holme, Thomas A. "Denaturation." *Denaturation, Chemistry Explained*, www.chemistryexplained.com/Co-Di/Denaturation.html.
11. Bekele, *et al.* "Easy Biology Class." *Easybiologyclass*, www.easybiologyclass.com/similarities-and-difference-between-c3-and-c4-plants-a-comparison-table/.
12. Eckardt, N A, and A R Portis. "Heat Denaturation Profiles of Ribulose-1,5-Bisphosphate Carboxylase/Oxygenase (Rubisco) and Rubisco Activase and the Inability of Rubisco Activase to Restore Activity of Heat-Denatured Rubisco." *Plant Physiology*, U.S. National Library of Medicine, Jan. 1997, www.ncbi.nlm.nih.gov/pmc/articles/PMC158136/.
13. "Temperature Effects on the Solubility of Gases." *Chemistry LibreTexts*, Libretexts, 11 May 2019, [https://chem.libretexts.org/Bookshelves/Physical_and_Theoretical_Chemistry_Textbook_Maps/Supplemental_Modules_\(Physical_and_Theoretical_Chemistry\)/Equilibria/Solubility/Temperature_Effects_on_the_Solubility_of_Gases](https://chem.libretexts.org/Bookshelves/Physical_and_Theoretical_Chemistry_Textbook_Maps/Supplemental_Modules_(Physical_and_Theoretical_Chemistry)/Equilibria/Solubility/Temperature_Effects_on_the_Solubility_of_Gases)
14. Yu, Bo, and Fang Chen. "The Global Impact Factors of Net Primary Production in Different Land Cover Types from 2005 to 2011." *SpringerPlus*, Springer International Publishing, 2 Aug. 2016, www.ncbi.nlm.nih.gov/pmc/articles/PMC4971002/.
15. Lee, Tse-Min, *et al.* "Characterization of a Heat-Tolerant Chlorella Sp. GD Mutant with Enhanced Photosynthetic CO₂ Fixation Efficiency and Its Implication as Lactic Acid Fermentation Feedstock." *Biotechnology for Biofuels*, BioMed Central, 12 Sept. 2017, www.ncbi.nlm.nih.gov/pmc/articles/PMC5596919/.

Copyright: © 2019 Biddinger, Bradley and Seplaki. All JEI articles are distributed under the attribution non-commercial, no derivative license (<http://creativecommons.org/licenses/by-nc-nd/3.0/>). This means that anyone is free to share, copy and distribute an unaltered article for non-commercial purposes provided the original author and source is credited.

Sponsorship



Editor's Circle

\$10,000+



Patron

\$5,000+



PORTFOLIOS
WITH PURPOSE®

Institutional Supporters



HARVARD
UNIVERSITY



HARVARD
MEDICAL SCHOOL



Tufts
UNIVERSITY

Charitable Contributions

We need your help to provide mentorship to young scientists everywhere.

JEI is supported by an entirely volunteer staff, and over 90% of our funds go towards providing educational experiences for students. Our costs include manuscript management fees, web hosting, creation of STEM education resources for teachers, and local outreach programs at our affiliate universities. We provide these services to students and teachers entirely free of any cost, and rely on generous benefactors to support our programs.

A donation of \$30 will sponsor one student's scientific mentorship, peer review and publication, a six month scientific experience that in one student's words, 're-energized my curiosity towards science', and 'gave me confidence that I could take an idea I had and turn it into something that I could put out into the world'. **If you would like to donate to JEI, please visit <https://emerginginvestigators.org/support>, or contact us at questions@emerginginvestigators.org.** Thank you for supporting the next generation of scientists!

'Journal of Emerging Investigators, Inc. is a Section 501(c)(3) public charity organization (EIN: 45-2206379). Your donation to JEI is tax-deductible.'



emerginginvestigators.org